Molecular Genetics of Axon Guidance in *Drosophila melanogaster*

Thesis by

Qi Sun

In Partial Fulfillment of the Requirements

for the Degree of

Doctor of Philosophy

California Institute of Technology

Pasadena, California

2000

(Submitted July 20th, 1999)

Acknowledgments

First of all, I would like to thank the two most important women in my life, my mother Yang, Min-Hua and my wife Hua, Jian. Their love is the source of my happiness and my strength. I might have lost faith in a lot of things in this world, but I will never lose my faith in both of them.

I would like to thank my advisor, Kai Zinn, for all his guidance and support through the past five years. I admire his personality, his brain power as well as his physical power. Most importantly, from Kai, I see a meaningful career and a meaningful life. I will always be his fan.

I have greatly benefited from the Caltech research community. I would like to thank many faculty memebers, especially Howard Lipshitz and my thesis committee, David Anderson, Bruce Hay, Elliot Meyerowitz and Paul Sternberg. I thank Elliot for letting me learn all the molecular techniques in his lab before I was admitted by Caltech. I still remember the first day of my rotation in Paul's lab. He spent half a day with me, making my first worm pick and introducing me to the commonly used genetic markers. I benefited so much from the Bi 218 that David taught. It is the best class I ever took in Caltech. I thank Howard for his guidance and encouragement, which gave me the self-confidence I desperately needed during my first year in Caltech. I thank Bruce, whose help is reflected in many parts of this thesis. My introduction to the molecular and genetics lab works was mainly through several former postdoctors and graduate students at Caltech, including Caren Chang, Tetus Saito, Michele Lamka, Richard Yip, Junho Lee and Chand Desai.

I would like to thank all my lab mates, who contributed significantly to my experience and knowledge. I owe much of my progress at Caltech to them.

I thank all my Chinese friends here in Caltech. I am at the border of two cultures. Their support is essential for me to survive the graduate school. Many of my happiest moments at Caltech were shared with them.

Chinese believe that there is a mysterious force called "Yuan" that brings people together. I was lucky to be put in such a wonderful school with a group of wonderful people. I would like to thank all these people, and may the force be with them.

Abstract

Understanding the cellular and molecular mechanisms governing axon guidance and synaptogenesis is a central issue in developmental neurobiology. The *Drosophila* embryonic central nervous system, with its simplicity and genetic accessibility, is an ideal model system to examine these problems.

One signaling mechanism by which growth cones respond to guidance factors is the control of tyrosine phosphorylation. Genetic studies in *Drosophila* have shown that neural receptor protein tyrosine phosphatases (RPTPs) are important regulators of motor axon guidance decisions. Chapters 2 and 3 of this thesis describe genetic studies of the RPTP gene DPTP10D. Removing DPTP10D and DPTP69D causes axon pathfinding errors at the midline and within the longitudinal tracts. These RPTPs genetically interact with genes involved in repulsion from the midline, including Slit, Roundabout and Commissureless. Slit is a midline repulsive signal, while Roundabout is the receptor for Slit. The phosphatases are likely to be components of signaling pathways downstream of Roundabout. DPTP10D is also involved in growth cone guidance decisions in the embryonic neuromuscular system. Phenotypic analyses of RPTP mutant combinations show that DPTP10D works together with other RPTPs to promote bifurcation of the SNa nerve and allow the ISNb nerve to separate from the common ISN pathway. DPTP10D, however, has a competitive relationship with the other RPTPs in controlling growth of the ISN. These results show that the functional relationships among the four neural RPTPs are complex. At individual choice points, RPTPs can have cooperative, collaborative, or antagonistic functions in controlling guidance.

In Chapter 4, I describe an overexpression/misexpression P element screen for new genes involved in axon guidance. This screen allows identification and rapid cloning of genes that cause axon guidance defects when they are overexpressed in all

neurons or all muscle fibers. One known axon guidance gene and several novel genes have already been identified in this screen, indicating that it may provide a powerful method to identify new genes that regulate axon guidance and synaptogenesis.

There are also three Appendices in the thesis. Two of these are reviews that I co-authored. The third Appendix describes a genetic analysis of the RPTP substrate protein gp150.

Table of Contents

Chapter 1

Genetic control of axon guidance –What have we learned from flies?

One of the most remarkable aspects of nervous system development is the specificity of neuronal connections. Despite decades of effort dedicated to studying the cellular and molecular mechanisms of axon guidance and synapse formation, how the billions of neurons in the human central (CNS) and peripheral (PNS) nervous systems are wired up into meaningful circuits remains poorly understood. Because molecular mechanisms underlying nervous system development are likely to be shared by modern invertebrate and vertebrate animals, many researchers have turned to genetically tractable invertebrate model systems, including the fruit fly *Drosophila melanogaster* and the nematode *Caenorhabditis elegans*. The genetic and biochemical studies of these model organisms have shown that signaling pathways that control developmental events are conserved throughout evolution. In the past decade, these multi-system approaches have proven fruitful in studying axon guidance.

Most elements of the fly and worm nervous systems are much simpler than the corresponding parts of vertebrate nervous systems. For example, the fly embryonic neuromuscular system consists of approximately 40 motoneurons and 30 muscle fibers per hemisegment. Each of these neurons and muscle fibers are individually specified; that is, an individual motoneuron displays a unique pattern of gene expression and always innervates a particular muscle fiber in every embryo examined. The motor axon patterns in abdominal segments A2 to A7 are highly stereotyped, and can be easily visualized with the monoclonal antibody (mAb) 1D4, which recognizes the cell-surface protein Fasciclin II (Van Vactor et al., 1993). Figure 1 is a diagram of the motor axon pattern in one abdominal hemisegment. Motor axons exit the CNS *via* the segmental nerve (SN) and intersegmental nerve (ISN) roots, and then extend peripherally in one of five nerve pathways. SNa and SNc emerge from the SN root, while ISNb (previously known as SNb), ISNd (previously known as SNd) and the ISN arise from the ISN root (Keshishian et al., 1996).

In the following sections I will review four aspects of fly axon guidance, focusing primarily on the neuromuscular system, and describe our current knowledge of how genetic mechanisms control the specificity of connections. (1) Axons extend along highly stereotyped pathways. How does a growth cone, the leading edge of an axon, make the right decision at each choice point? It is thought that growth cones recognize specific molecules on cells and in the extracellular matrix along their pathways, and use these to guide their navigation. Only a few such molecules have been identified thus far, however. (2) Pioneer axons must establish new pathways without navigating along existing axon tracts. Most axons, however, follow pre-existing axon bundles, at least for part of their trajectory. This process, called fasciculation, is highly specific; in the fly, a follower axon will always choose the same bundle to grow along. Genetic studies have identified many genes involved in selective axon fasciculation. Gain-of-function or loss-of-function mutants of these genes often lead to axon pathfinding errors, indicating that proper fasciculation is important for axon pathfinding; (3) Each motor axon forms synapses only on its target muscle fiber. How does the axon recognize its target? Recent studies have identified some factors determining synapse specificity in the fly neuromuscular system; (4) Growth cones respond to environmental cues using a variety of intracellular signaling pathways. Here I will discuss one of the mechanisms that link growth cone behavior to contact with guidance cues: control of tyrosine phosphorylation. This is directly relevant to my own work on receptor tyrosine phosphatase (RPTP) function. Appendix 2 is a review that I co-authored which also discusses tyrosine phosphorylation and axon guidance.

1. Choice points and guidance cues

The precision of axonal pathfinding is remarkable given the long distances that many axons must travel to reach their targets. It appears that the long trajectories of axons are broken down into numerous small segments to facilitate axon navigation. At the end of each segment of the pathway, a growth cone may often have the option to make one of several guidance decisions; such locations are called choice points. At the choice points, one can often identify specialized cells that express guidance cues.

Studies of the Ti1 sensory neurons in the grasshopper limb bud showed that Ti1 growth cones encounter a series of "guidepost cells" before reaching their final targets in the CNS. Ablation of guidepost cells causes Ti1 pathfinding errors (Bentley and O'Connor, 1992). However, the cues on guidepost cells and at other choice points have seldom been identified as specific molecules. Genetic screens carried out in flies for genes encoding guidance cues have not been very successful, probably due to genetic redundant pathways and/or to difficulties in visualization of subtle guidance phenotypes.

To date, the most extensively studied choice point in flies is the CNS midline. Most interneurons in the CNS send axons across the midline that form synapses on the contralateral side of the embryo. Other interneurons and some motoneurons extend axons along ipsilateral pathways that never cross the midline. Mechanisms must exist that allow only the appropriate axons to cross the midline, and also ensure that commissural axons that have crossed do not turn and recross.

The specialized midline glial cells at this choice point express both attractive (Netrin) and repulsive (Slit) factors (Kidd et al., 1999; Mitchell et al., 1996) that activate (or inactivate) their receptors on CNS growth cones. The attractive and repulsive signals may be balanced so that each axon maintains its appropriate distance from the midline.

Most or all CNS neurons appear to express Frazzled (Fra), the attractive Netrin receptor, suggesting that they have an intrinsic affinity for the midline. It is unknown why some Fra-expressing neurons choose to extend growth cones in commissural

pathways that contact the midline, while others choose longitudinal pathways.

When a commissural axon contacts the midline, a transmembrane protein called Commissureless (Comm) that is expressed on midline glia is transferred into the axon and growth cone by an unknown mechanism. Comm transfer causes downregulation or degradation of Roundabout (Robo), which is the receptor for the repulsive Slit signal. As a result of this, the attractive signals predominate and the growth cone grows to the midline. Repulsive signaling must then be re-activated in order to allow the growth cone to leave the midline and reach the contralateral side of the CNS, since in the absence of repulsion (no Slit function), axons grow to the midline and never leave. It is unknown how this re-activation of repulsion is accomplished.

In summary, results on the midline suggest that there are always attractive and repulsive forces acting on each growth cone, and the balance between these controls pathway choice. Whether a growth cone responds to a ligand by attraction or repulsion appears to depend on the cytoplasmic domain of the relevant receptor, and the strength of the attractive or repulsive response may be determined by the relative levels of these cytoplasmic domains. It has recently been shown that expression of a chimeric receptor where the extracellular domain is derived from Fra (binds Netrin) and the cytoplasmic domain is from Robo (mediates repulsion) shifts the balance so that all neurons are now repelled from the midline, producing a *commissureless* phenotype. The strength of this phenotype depends on the amount of the chimeric receptor that is expressed. Conversely, expression of a Robo-Fra chimeric receptor produces an attractive response to the repulsive Robo ligand Slit, and therefore produces a *slit*-like phenotype (all axons converge on the midline) whose strength is dependent on the expression level of the chimera (Bashaw and Goodman, 1999). For further information on midline guidance, see Appendix 1; this is a review article that I co-authored which discusses Slit-mediated repulsion in more detail.

Genetic control of guidance at other known choice points in the fly embryo, such as the exit points of the motor nerve roots and the branchpoints at which motor axon pathways diverge, is more poorly understood. There are few single mutants that alter guidance at these choice points, suggesting that redundant guidance cues may be located there. Embryos lacking multiple RPTPs can display strong guidance phenotypes at these choice points, suggesting that RPTPs are necessary for execution of pathfinding decisions at these sites (see Chapter 3). I have attempted to deal with the problem of redundancy by conducting a misexpression screen of guidance phenotypes; this is described in Chapter 4.

2. Selective fasciculation and guidance of follower axons

During nervous system development, the earliest developing axons, or the pioneer axons, navigate in an environment devoid of any other axons. Their growth cones rely exclusively on environmental cues for guidance. Many later developing axons, or the follower axons, travel along the preexisting axon tracts (or fascicles), switching from one fascicle to another at specific choice points. This "selective fasciculation" strategy simplifies the pathfinding task of the follower axons.

a. Follower axons depend on pre-existing axon tracts for pathfinding

The CNS of the *Drosophila* embryo consists of two longitudinal axon bundles that run through the length of the body to the brain. In each segment, two commissural axon bundles cross the midline and link the two longitudinal connectives. The longitudinal tracts of the embryonic CNS are pioneered by four neurons per hemisegment: MP1, dMP2, vMP2 and pCC (Hidalgo and Brand, 1997; Lin et al., 1994). At stage 12, axons of vMP2 and pCC fasciculate with each other and extend

anteriorly, while the MP1 and dMP2 axons fasciculate and extend posteriorly. The ascending vMP2/pCC fascicle encounters the descending axons of dMP2 and MP1 at stage 13. These two fascicles contact each other only briefly. At stage 14 they separate again, forming two pathways that make contact only at the segment boundary: an outer fascicle composed of the axons of MP1 and dMP2, and an inner one consisting of pCC and vMP2. These four axons form the first continuous longitudinal tracts throughout the whole embryo. During embryogenesis, the fascicles of the pioneer axons are dynamic. Between stage 14 and 15, these axons reassort and change partners. dMP2 defasciculates from MP1 and fasciculates with pCC, while vMP2 defasciculates from pCC and runs in a more ventral plane along the same longitudinal pathway (Hidalgo and Brand, 1997; Lin et al., 1994).

Neuronal ablation experiments performed by Hidalgo provide direct evidence that the existing pioneer axons are essential for guidance of the followers (Hidalgo and Brand, 1997). By using the GAL4 system to drive expression of the toxin ricin A in specific neurons, they were able to ablate the four pioneer neurons genetically. When one or two of the pioneer neurons were ablated, the follower axons could still find their correct pathways. If all four pioneer neurons were ablated, the pathfinding ability of the follower growth cones was severely disrupted. Ablation of the four pioneer neurons causes axon defasciculation, the loss or thinning of axon fascicles, breaks in the longitudinal axon bundles, fusion of axons into a single fascicle, and misrouting of axons across the midline. These findings suggest that the follower axons do not have the intrinsic pathfinding abilities like the pioneers. Instead, follower axons depend on the existing scaffold of axon tracts to reach their targets.

b. Cell adhesion molecules mediate axon fasciculation

Both *in vitro* and *in vivo* studies have shown that cell adhesion molecules (CAMs) play a critical role in axon fasciculation. These molecules include those of the Immunoglobulin (Ig) superfamily, leucine-rich repeat proteins, and Ca^{2+} dependent cadherins (Doherty and Walsh, 1994; Van Vactor, 1998).

Genetic analyses of several neuron specific *Drosophila* CAMs have been reported, including Fasciclin II (Fas II) (Lin et al., 1994; Lin and Goodman, 1994), Fas III (Chiba et al., 1995), Neurotactin (Speicher et al., 1998), Neuroglian (Hall and Bieber, 1997; Speicher et al., 1998), Neuromusculin (Kania et al., 1993), Connectin (Nose et al., 1997), Fas I (Elkins et al., 1990) and DN-cadherin (Iwai et al., 1997). Loss of function mutants of any one of these genes produces very subtle or no axon guidance phenotypes, possibly because of functional compensation by other CAMs. Another likely reason is that in these CAM mutants, only a subset of axons is affected. Most genetic analyses of the loss-of-function CAM mutants used general axon markers that were not able to detect specific phenotypes caused by these mutations. In fact, the defasciculation phenotype of *Fas II* was only detected at the electron microscopic level (Lin et al., 1994).

The first neural cell adhesion molecule isolated was N-CAM, which is a member of the Ig superfamily (reviewed by Doherty and Walsh, 1994). Fas II is a *Drosophila* homologue of N-CAM and can function *in vitro* as a homophilic cell adhesion molecule (Grenningloh et al., 1991). Fas II is expressed on all motor axons and on a subset of interneuronal axons. Fas II positive interneuronal axons fasciculate into three bundles within each longitudinal tract. In loss-of-function *Fas II* mutants, some of the early developing interneuronal axons, including pCC, MP1 and dMP2, are no longer tightly bundled together, indicating that Fas II is involved in axon fasciculation (Lin et al., 1994). However, the overall motor axon projection remains unaffected in the Fas II

mutant, suggesting that there might be multiple cell adhesion systems involved in axon fasciculation.

Overexpression of Fas II on motor axons gives rise to more striking axon guidance defects. Three classes of ISNb nerve abnormalities are observed: (1) "bypass" phenotypes, in which ISNbs fail to defasciculate from the common ISN pathway at the exit junction (EJ) and instead continue to extend along the ISN; (2) "detour" phenotypes, in which bypass ISNb growth cones leave the ISN distal to the normal exit junction and enter the target ventrolateral (VLM) muscle field at abnormal sites; (3) "stall" phenotypes, in which ISNb growth cones leave the common ISN pathway but then stop before reaching their targets (Lin and Goodman, 1994).

The axon guidance phenotypes produced by Fas II overexpression are consistent with the role of Fas II as a homophilic CAM, in that Fas II overexpression blocks defasciculation by increasing axon-axon adhesion. These results suggest that specific defasciculation may be achieved by down regulation of cell adhesion molecules at certain choice points.

Non-Ig superfamily CAMs are also involved in axon fasciculation. *Drosophila* N-type cadherin (DN-cadherin) is a member of large family of Ca^{2+}-dependent adhesion molecules called cadherins. It is broadly expressed in the nervous system and in the mesoderm. In the DN-cadherin loss-of-function mutant, the initial axon elongation of Fas II-expressing pioneer neurons is unaffected, but axonal patterns become deformed as follower axons join the pioneer tracts. At late stage 16, the mutant CNS displays discontinuous axon bundles, suggesting stalling or misorientation of growth cones (Iwai et al., 1997). These phenotypes may be caused by the failure of follower axons to fasciculate correctly with existing axon tracts.

Although most single CAM mutants do not exhibit severe phenotypes, some double mutant combinations removing two different CAMs (or a CAM and another

transmembrane protein) show strong defects, indicating functional overlap between these genes. Neurotactin, a member of the serine esterase superfamily, is widely expressed in fly embryonic CNS neurons. In the developing PNS of the pupa, Neurotactin is expressed by ocellar pioneer neurons. *neurotactin* loss-of-function mutations cause defasciculation of the ocellar pioneer nerve, indicating its role in axon-axon adhesion. However, embryos lacking Neurotactin only exhibit minor defects in the Fas II-positive axons (Speicher et al., 1998).

Neuroglian is a neural CAM related to the vertebrate CAM L1. Like Neurotactin, Neuroglian is also expressed by most CNS neurons, and the overall structure of the CNS is normal in a *Neuroglian* mutant (Hall and Bieber, 1997). In contrast to the single mutant phenotypes, embryos lacking both Neurotactin and Neuroglian display a strong synergistic CNS phenotype. The defects observed in the double mutant embryos include thinning and interruption of the longitudinal axon bundles and extensive misguidance of axons (Speicher et al., 1998). It is likely that the *neurotactin* and *neuroglian* single mutants have reduced axon-axon adhesion, but not enough to cause severe defasciculation. In the double mutant embryos, the absence of both Neurotactin and Neuroglian-mediated adhesion may cause growth cones to lose contact entirely with the correct fascicles, resulting in guidance defects.

While all the CAMs we discussed above have very broad expression pattern, other CAMs such as Fas I, Fas III and Connectin, are expressed in a more restricted subsets of axons. These CAMs may also be involved in selective fasciculation of these axon subsets. Genetic analyses of loss-of-function mutations eliminating their expression have not revealed any phenotypes (although double mutants in which both Fas I and the Abl tyrosine kinase are not expressed display a midline guidance phenotypes; Elkins et al., 1990). This may be due to genetic redundancy or because the

markers used for visualization did not allow detection of subtle guidance phenotypes affecting small subsets of axons.

c. Signaling molecules that regulate defasciculation

Although many CAMs have been shown to be able to mediate axon fasciculation, CAMs alone cannot determine the specificity and dynamic nature of the fasciculation process. Equally intriguing is the defasciculation process, or how growth cones exit the common pathways at specific choice points.

The phenotypes of loss-of-function and overexpression mutants of Fas II suggest that defasciculation might in part involve either the removal of the CAMs from the cell surface or the downregulation of their functions. For vertebrate NCAM, several cell autonomous mechanisms for decreasing the affinity of homophilic binding have been discovered (Rutishauser, 1993). For example, studies in the chick have implicated polysialic acid (PSA) as a key regulator of a general form of axon defasciculation. Some forms of NCAM contain large amounts of PSA, and these forms are associated with a loss of adhesion between axons expressing them. PSA may decrease NCAM-mediated axon-axon adhesion by increasing the distance between apposed cell surfaces, or may have a more specific role in disrupting adhesive CAM interactions.

In order for chick motor axons to reach target muscles in the embryonic limb, they must defasciculate from common exit pathways, explore the plexus region in which efferent pathways converge, and then join new target-specific fascicles as they leave the plexus. PSA levels are observed to increase as axons defasciculate, and enzymatic removal of PSA from motor axons leads to an increased frequency of projection errors. (Tang et al., 1992; Tang et al., 1994; Yang et al., 1992).

PSA has not been identified as a regulator of axon-axon adhesion in *Drosophila*. Genetic screens have, however, identified a few genes that appear to control

defasciculation. One of these genes is *beaten path* (*beat*) (Van Vactor et al., 1993). Beat encodes a secreted protein that is expressed by motoneurons. Mutations in *beat* produce phenotypes that resemble those of Fas II overexpression mutants. In embryos lacking *beat*, ISNbs always fail to separate from the ISNs, and extend along the ISN pathway. Similarly, SNc nerves do not separate from SNa nerves in the mutant. *beat* phenotypes can be suppressed by reduced expression of CAMs like Fas II or Connectin, indicating that Beat facilitates defasciculation by counteracting the adhesion mediated by CAMs (Fambrough and Goodman, 1996).

As described above, PSA may reduce axon-axon adhesion by physically blocking homophilic binding of NCAM and other CAMs. One simple model for Beat function is that it binds directly to Fas II and blocks the Fas II activity; however, efforts to demonstrate direct binding between Beat and Fas II have been unsuccessful (Fambrough and Goodman, 1996). Alternatively, Beat may not directly interact with Fas II, but may instead be a ligand for another receptor molecule whose interaction with Beat causes modulation of Fas II-mediated adhesion. Beat contains two amino-terminal Ig domains and a carboxy-terminal cysteine-knot domain (Bazan and Goodman, 1997; Mushegian, 1997). In some growth factors, the cysteine-knot domain can function as a molecular dimerizer. Thus, it is possible that Beat activates or inactivates its receptors by facilitating dimerization.

The existing results on Beat do not yet explain what signals trigger defasciculation. Beat protein by itself is not sufficient for the defasciculation process. Overexpression of *beat* in all neurons does not produce any axonal phenotypes (Fambrough and Goodman, 1996). The native Beat protein is highly enriched at choice point regions during the period of branch formation, although Beat mRNA is constantly present in most of the motoneurons. One possible model is that a localized guidance signal or signals at the choice points leads to the accumulation and release of the Beat

protein, which in turn causes the defasciculation of axons and enables specific growth cones to leave common pathways.

3. Combinatorial signals define synaptic specificity in the neuromuscular system

Correct pathfinding decisions bring the motor growth cones to their appropriate target region (muscle field). Within each target region, however, there are several muscle fibers within filopodial grasp of the growth cone. Muscle ablation and duplication experiments indicate that individual motor axons are able to select their appropriate muscle targets with great precision (Cash et al., 1992; Chiba et al., 1993). How do the axons determine which muscle is the correct target?

A lock-and-key model seems to be an easy and straightforward strategy to achieve synaptic specificity. In this model, each motor axon and its corresponding target would have unique and complementary molecular labels, so that a motor axon can only form connections with its matching target muscle. Recent results from the human genome project have shown that there is a family of neuronal cadherin molecules with a striking genomic organization similar to that of immunoglobulin and T-cell receptor gene clusters (Wu and Maniatis, 1999). Although nothing is known about functions of these genes, it is interesting to speculate that this special genomic arrangement enables each neuron to express a unique cadherin gene, thus providing a mechanism for synaptic specificity. However, so far there is no direct evidence implying the existence of a family of lock-and-key genes in fly neural development.

In an alternative model, each muscle target presents a unique combination of repulsive and attractive signals. Individual growth cones would respond to qualitative and quantitative molecular differences on neighboring targets, and then integrate multiple

signals to decide which muscle is the appropriate target. In this model, it is not a single unique molecular label, but the balance of several different signals that determines target decisions. Recent studies from several laboratories have demonstrated that this second model better represents the real situation (Rose and Chiba, 1999; Winberg et al., 1998).

a. Genes contributing to defining synaptic specificity

Several genes have been identified that are expressed in a subset of motor axons and/or muscle fibers, and thus are potential genes defining synaptic specificity. These include Netrin (Mitchell et al., 1996; Winberg et al., 1998), Toll (Rose and Chiba, 1999; Rose et al., 1997), Fas III (Chiba et al., 1995; Kose et al., 1997), Capricious (Shishido et al., 1998) and Connectin (Nose et al., 1994; Nose et al., 1997). The expression patterns and functions of these genes during fly embryonic neuromuscular development are summarized in Table 1. One might expect that additional genes with such temporally and spatially selective expression patterns will be identified in the future, and that combinations of the proteins encoded by such genes will uniquely label each muscle fiber. Note that the molecules listed in Table 1 belong to several different gene families, providing evidence against the simple idea that a single large family of molecules is responsible for synaptic specificity.

Genes that are not expressed by specific muscles or motoneurons, such as *Fas II* and *Semaphorin II (Sema II)* , can modulate the specificity of target selection even though they do not have a restricted expression pattern (Winberg et al., 1998). Fas II is a CAM expressed by all motoneurons and muscles, and it can promote synapse formation. Sema II is a secreted member of the semaphorin family expressed by all body wall embryonic muscles; it functions as a pan-muscle repellent for motor growth cones (Kolodkin et al., 1993). The repulsive activity of Sema II and the dynamic expression pattern of Fas II may act in combination to promote synapse specificity by inhibiting

promiscuous synaptogenesis. Prior to synapse formation, Fas II is expressed at low levels across the entire surface of the muscle, overcoming Sema II repulsion and making the muscle permissive for growth cone exploration. As the first synapse forms on a muscle, Fas II disappears from the muscle surface, except at the developing synapse (Davis et al., 1997). Sema II repulsion then dominates, preventing further innervation of the muscle.

b. A balance of repulsive and attractive forces regulates target selection

There are multiple signals present on each muscle fiber (e.g., Table 1). Growth cone apparently sense and measure these signals, then integrate their effects in order to determine whether this muscle is the appropriate target. The balance between these different forces determines synapse formation. This concept is illustrated by the behavior of the RP3 motoneuron growth cone when encountering different environments (Rose and Chiba, 1999).

RP3 normally innervates the cleft between muscles 6 and 7. As shown in Table 1, Fas III promotes, while Toll inhibits RP3 synaptic initiation. Overexpression of Fas III and of Toll in all muscles thus produce opposite RP3 phenotypes. Rose et al. (1999) genetically manipulated *Drosophila* embryos so that different levels of Fas III and Toll could be simultaneously expressed in all muscles. Their results showed that only when Fas III and Toll levels are balanced, can RP3 successfully form synapses with muscles 6/7. Excess levels of Fas III or Toll led to failure of 6/7 innervation (Rose et al. 1999).

The signals for RP3 innervation are reminiscent of the axon guidance signals at the midline. In both cases, growth cones are able to sense multiple extracellular signals, but make decisions based on the net result of these competing forces. What happens inside a growth cone in response to these signals from outside is still mysterious,

although it has been studied for years by many neurobiologists. In the next section, I discuss one such intracellular signaling system, showing how control of tyrosine phosphorylation inside growth cones plays a key role in modifying growth cone behaviors.

Phosphotyrosine signaling and growth cone behavior

As reviewed above, recent progress has identified a number of environmental factors that convey guidance information, as well as neuronal receptor molecules that receive these inputs (Tessier-Lavigne and Goodman, 1996; Zinn and Sun, 1999). However, we understand far less about the mechanisms that interpret this information and convert extracellular cues into directional growth cone motility.

One signaling mechanism by which growth cones respond to guidance factors is the control of tyrosine phosphorylation (Desai et al., 1997b). Phosphotyrosine is enriched in filopodia, the highly motile extensions that emanate from growth cones and probe the surrounding landscape (Wu and Goldberg, 1993). Pharmacological and genetic studies have provided direct evidence that many tyrosine kinases and phosphatases play key roles during growth cone navigation. Menon et al. showed that applying tyrosine kinase inhibitors herbimycin A (HA) or genistein (GNS) to the grasshopper embryo produces specific axonal pathfinding errors in the CNS (Menon and Zinn, 1998). For example, HA treatment causes many extra axons to cross the midline. The pCC interneuron normally extends its axon anteriorly; in HA treated embryos, pCC extends a collateral branch across the midline.

Midline crossing has been extensively studied in flies (see section 1 above and Appendix 1) (Kidd et al., 1999; Kidd et al., 1998a; Kidd et al., 1998b; Zinn and Sun, 1999). Robo, the fly receptor for the midline repellent signal molecule Slit, has potential

tyrosine phosphorylation sites that could interact with SH2-domain adapter proteins (Kidd et al., 1998a). Grasshopper CNS structure like that of the fly, and probably uses the same molecular mechanisms for axon guidance at the midline. It is possible that HA inhibits phosphorylation of Robo, weakening or blocking Robo's ability to transduce the midline repellent signal so that many growth cones are misrouted across the midline.

Genetic analyses have identified many axon guidance genes that encode protein tyrosine kinases or phosphatases. Mutations in *derailed*, the *Drosophila* homologue of the vertebrate receptor tyrosine kinase (RTK) Ryk, causes defasciculation of a subset of interneurons in the CNS (Callahan et al., 1995). Interestingly, derailed displays a strong synergistic genetic interaction with the neuronal adhesion molecule Neurotactin (Speicher et al., 1998). It is likely that the function of Derailed is to regulate fasciculation.

Five receptor protein tyrosine phosphatases (RPTPs) have been identified in *Drosophila*. Strikingly, four of these five (DLAR, DPTP10D, DPTP69D, and DPTP99A) are expressed only on CNS axons in the embryo (Tian et al., 1991; Yang et al., 1991). RPTPs have extracellular regions consisting of immunoglobulin-like (Ig) and/or fibronectin type III (FN3) domains. These are linked *via* a single transmembrane domain to a cytoplasmic region containing one or two phosphatase domains (Figure 2). Genetic analyses of the four neural RPTPs shows that they are involved in multiple axon guidance decisions, including midline crossing, selective fasciculation, specific defasciculation and synapse formation (Desai et al., 1996; Desai et al., 1997a; Krueger et al., 1996) (This thesis). In embryos lacking all four neuronal RPTP genes, the CNS axon pattern is severely disrupted. All the longitudinal axons are misrouted across the midline, suggesting a role for RPTPs in midline crossing decision (Chapter 2). In the neuromuscular system, most ISNbs in the quadruple mutants fail to defasciculate from ISN common pathways at the exit junctions. This phenotype is similar to that observed

in the *beat* mutant (see above), indicating that RPTPs are involved in controlling specific defasciculation at this choice point. As described in Chapter 3, the four neuronal RPTPs function at multiple motor axon choice points. They have complicated relationships with each other, being functionally redundant at some choice points and having antagonistic functions at others.

Interactions among kinase and phosphatase proteins play a key role in determining the growth cone behavior. It has recently been shown that entry of ISNb into the VLM field is controlled by antagonistic interactions between DLAR and the ABL tyrosine kinase. Removing one copy of the *Abl* gene suppresses the VLM bypass phenotype conferred by *Dlar* mutations, and ABL overexpression produces bypass phenotypes (Wills et al., 1999). These data, together with the observation that removing DPTP99A function also suppresses the *Dlar* bypass phenotype (Desai et al., 1997a), suggest that DLAR permits entry of ISNb axons into the VLM field by downregulating signaling by ABL and DPTP99A. ABL and its substrate ENA also bind directly to the D2 domain of DLAR and can serve as substrates for DLAR *in vitro* (Wills et al., 1999).

To some extent, a growth cone functions like a computer. It has a very complicated network of molecules calculating and responding to changing environments. Someday we might be able to establish quantitative models of the growth cones on computers, or design a computer with a growth cone as its CPU.

The development of the *Drosophila* embryonic nervous system is arguably the best understood among all nervous systems. In the past decade, we have accumulated a great deal of knowledge of molecular mediators of axon guidance in this system. However, the picture is still very fragmentary. We lack answers to many fundamental questions. For example, the midline crossing control is the best understood signaling

pathway. Even here, though, we do not have a clear understanding of why some axons choose to cross the midline, while others do not. As described in more detail in section 1 above, most or all axons appear to express receptors for both attractive (Netrin) and repulsive (Slit) cues. Only a subset of these axons, however, downregulate Robo and cross the midline. The key factors determining selective midline crossing are thus still unknown. The mechanisms involved in the other decisions that I have described are even more poorly understood. Maybe someday we will be able to describe in our textbooks how a complete nervous system is wired up. We still have a long way to go before reaching that point, however.

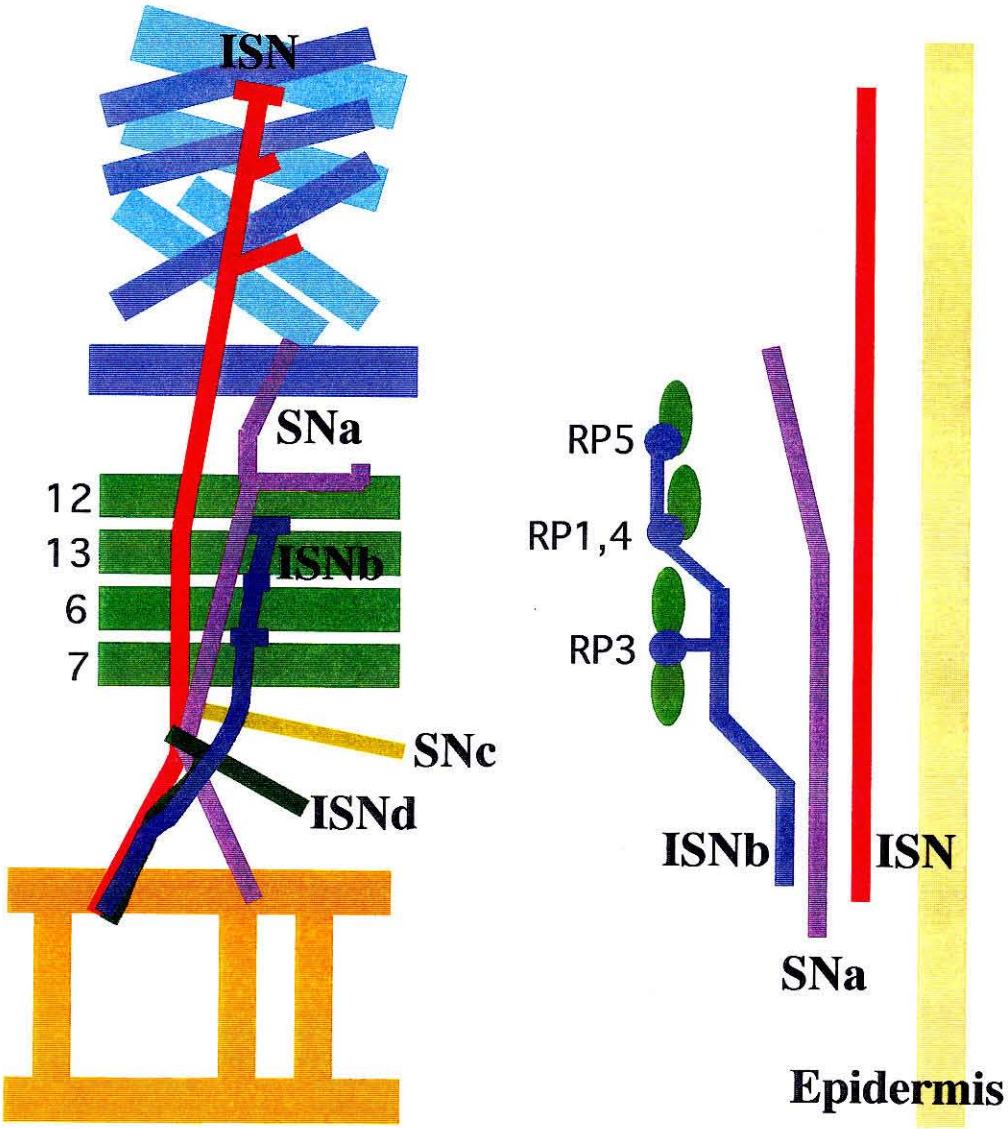

Figure 1. Schematics of motoneuron projections in the *Drosophila* embryo (One hemisegment from A2-A7 is shown here). The left panel is a dorsal view, the right panel shows a cross section. Each major nerve branch is shown in a different color: ISN (red), SNa (purple), ISNb (blue), SNc (brown) and ISNd (green). Four ISNb neurons (RP 1, 3, 4, 5, right panel) and their target muscles (6,7, 12, 13, left panel) are labeled.

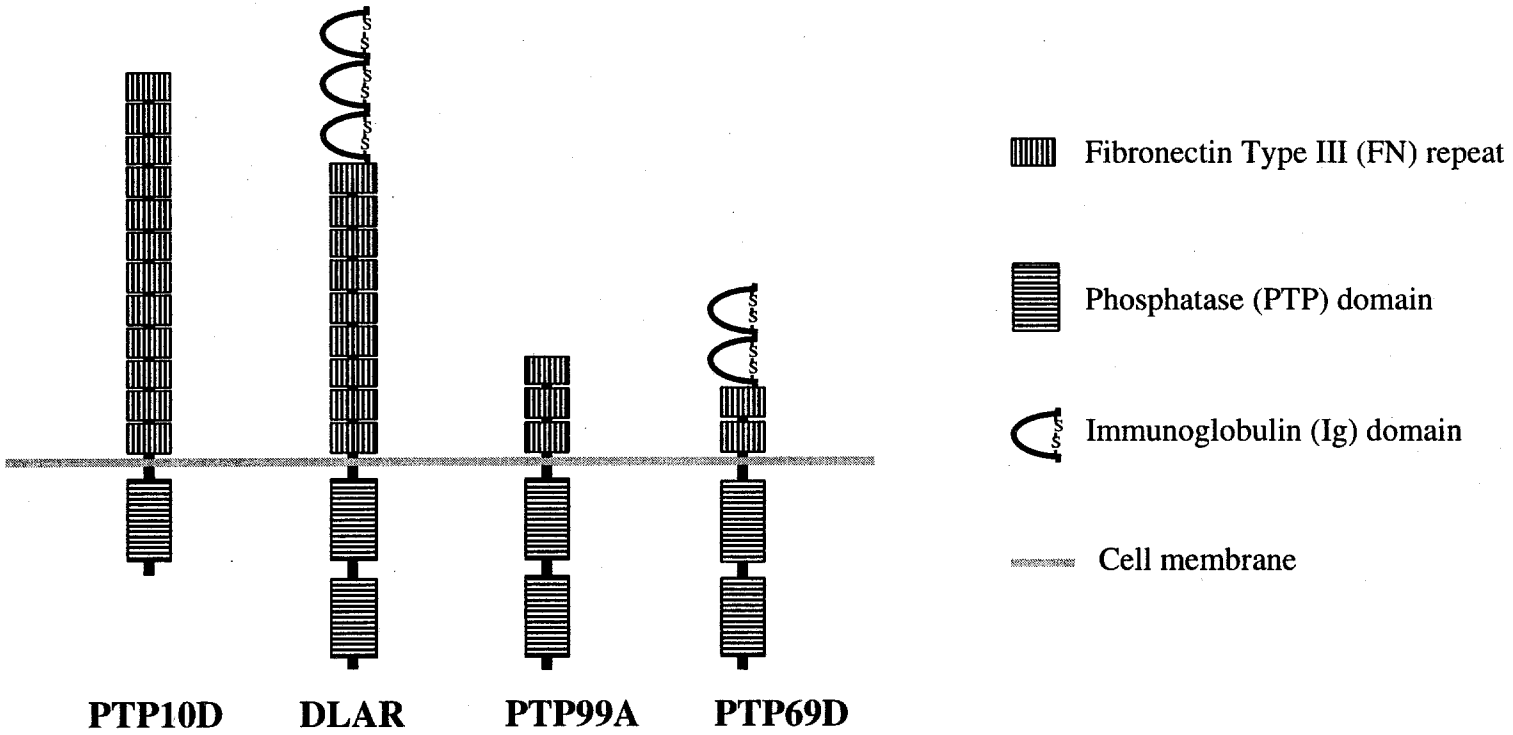

Figure 2. Molecular structures of the four *Drosophila* neural RPTPs.

Table 1. Molecules involved in neuromuscular synaptic specificity

	Molecular nature	Expression in the motor system	Loss of function phenotype	Misexpression phenotype	Function	Reference
Netrin	secreted protein with homology to laminin	Netrin A: muscles 1, 2, plus a dorsal lateral stripe in the epidermis. Netrin B: muscles 2, 6, 7.	Defects in projection of motor axons to the normally netrin positive muscles.	Misexpression of netrin in all muscles cause transverse nerves ectopically project to muscles 7, 6.	attractive	Mitchell et al., 1997 Winberg et al., 1998
Toll	leucine-rich-repeat transmembrane protein	Dynamic expression in the ventral half of embryonic musculature (high expression in muscles 7, 15, 16, 17, 28). Protein disappears in muscles 6/7 before ISNb innervation.	Ectopic innervation of RP3 axon (and possibly other ISNb axons) in the normally Toll positive ventral muscles.	Misexpression of Toll in all muscles prevents RPs growth cone from forming synapses at muscles 6/7.	repulsive	Rose et al., 1997 Rose et al., 1999
Fas III	immunoglobulin superfamily CAM	RP3 motoneuron and its target muscles (6 and 7). Motoneurons RP1 and RP4. Expression in 6 and 7 only after RP1 and RP4 pass through.	No phenotype observed.	Misexpression of Fas III in all muscles causes RP3 to incorrectly innervate neighboring non-target muscles.	homophilic adhesion	Chiba et al., 1995 Kose et al., 1997
Capricious	leucine-rich-repeat transmembrane protein	Muscles: four dorsal (1, 2, 9, 10) and six ventral (12, 14-17, 28). Motoneurons: aCC, RP2, RP5 U; all their targets are Caps positive muscles.	Overall normal CNS. RP5 sometimes forms extra synapse with muscle 13. (12 is the normal target.)	Misexpression of Caps in all muscles leads to similar phenotypes as loss of function.	possibly homophilic adhesion	Shishido et al., 1998
Connectin	GPI-linked cell surface protein of leucine rich repeat family	Muscles: six lateral muscles (21-24, 18, 5) and two ventral muscles (27, 29). Neurons: motoneurons projecting to these muscles, including SNa and SNc.	No phenotype observed.	Misexpression of Con in all muscles causes ectopic synapse formation by SNa axons.	homophilic adhesion	Nose et al., 1994 Nose et al., 1997

Chapter 2

Receptor tyrosine phosphatases regulate axon guidance across the midline of the *Drosophila* embryo

Qi Sun*, Sami Bahri#, Aloisia Schmid§, William Chia#, and Kai Zinn*

*Division of Biology, California Institute of Technology, Pasadena, CA 91125

#Institute of Molecular and Cell Biology, National University of Singapore, Singapore 117609

§Institute of Neuroscience and Institute of Molecular Biology, University of Oregon, Eugene, OR 97403

Summary

Neural receptor-linked tyrosine phosphatases (RPTPs) are essential for motor axon guidance in *Drosophila*, but have not been previously implicated in pathfinding by interneuronal growth cones within the central nervous system. Here we show that the DPTP10D and DPTP69D phosphatases are required for axon guidance at the midline and within the longitudinal tracts. Navigation across the midline is regulated by growth cone repulsion, which is triggered by interactions between neuronal Roundabout receptors and the midline ligand Slit. Interactions between the RPTP genes and genes involved in midline repulsion suggest that these phosphatases participate in Slit/Roundabout signaling. Repulsion is reduced in the absence of the RPTPs, indicating that they are positive regulators of this pathway.

Introduction

In the embryonic *Drosophila* central nervous system (CNS), axon guidance decisions are largely determined by genetic mechanisms. A small number of neuroblasts (NBs) arise in stereotyped positions within each segment, and each NB generates a unique lineage of neurons that extend growth cones along predetermined pathways to reach their synaptic targets. When visualized with antibody markers that stain all axons, the axonal array of the CNS appears to be a relatively simple ladder-like structure, with two commissural tracts that cross the midline in each segment and two longitudinal tracts that extend the length of the embryo. This simplicity is deceptive, however, because each tract includes many distinct and complex interneuronal pathways (Schmid et al., 1999; for review see Goodman and Doe, 1993).

Relatively little is known about the mechanisms by which individual axons navigate within the CNS, because it is usually very difficult to visualize single growth cones and observe the decisions they make. Many neurons, however, make a common decision to extend axons across the CNS midline that synapse with targets on the contralateral side of the embryo. Axon guidance at the midline has been intensively studied, and several of the key molecules controlling interactions between growth cones and the specialized midline cells have been identified.

In order to recruit growth cones into commissural pathways, midline glial cells produce attractive factors. These include the two Netrins, which are secreted proteins used in both vertebrates and invertebrates for control of guidance at the midline. In *Drosophila*, Netrins interact with the Frazzled receptor, an ortholog of vertebrate DCC which is expressed by most CNS neurons. Mutants lacking both Netrins or lacking Frazzled have reduced numbers of axons in commissural pathways (Harris et al., 1996; Kolodziej et al., 1996; Mitchell et al., 1996). Many axons still grow across the midline

in the absence of these proteins, however, suggesting that another attractive system may exist.

The midline also produces signals that repel growth cones. These are necessary to prevent longitudinal axons that express receptors for attractive factors from crossing the midline. In addition, repulsion may be required to allow the growth cones of commissural neurons to leave the midline and reach the contralateral side of the CNS. These growth cones must also be prevented from returning to the midline after crossing it once.

Recent studies have shown that repulsive signals are transduced *via* interactions between the Roundabout (Robo) receptor, which is expressed on neuronal growth cones, and the extracellular matrix protein Slit, which is produced by midline glial cells (Kidd et al., 1999). Slit binds directly to Robo and can mediate repulsion of Robo-expressing growth cones (Brose et al., 1999; Li et al., 1999; Nguyen Ba-Charvet et al., 1999; for review see Zinn and Sun, 1999). In *slit* mutants, all interneuronal axons converge on the midline and remain there, suggesting that repulsion has been eliminated. *robo* mutants, however, have a weaker phenotype in which longitudinal axons cross to the contralateral side of the embryo and then follow looping pathways that traverse the midline multiple times (Seeger et al., 1993; Kidd et al., 1998a,b). The difference between the *robo* and *slit* phenotypes is likely to be due to the existence of a second Robo protein, Robo2, which could mediate repulsion of some growth cones by Slit even when Robo is absent (Kidd et al., 1998a, 1999).

Another important component of the repulsive pathway is Commissureless (Comm), a transmembrane protein that is expressed by midline glia and transferred to commissural axons by an unknown mechanism (Tear et al., 1996). Transferred Comm causes downregulation of Robo, neutralizing the repulsive signal and allowing commissural axons to cross. In *comm* loss-of-function mutants, Robo fails to be

downregulated, and as a result all axons are repelled from the midline (Seeger et al., 1993; Kidd et al., 1998b).

Receptor-linked tyrosine phosphatases (RPTPs) are a large family of transmembrane signaling molecules that are conserved between vertebrates and invertebrates. They are essential for guidance of a subset of CNS axons in the *Drosophila* embryo, those of the motoneurons which innervate body wall muscle fibers (Desai et al., 1996, 1997a; Krueger et al., 1996). The four neural RPTPs (DPTP10D, DLAR, DPTP69D, and DPTP99A) are expressed on most or all CNS axons, including many interneuronal pathways (reviewed by Desai et al., 1997b). It has been difficult to assign functions to the RPTPs in controlling axon guidance within the CNS, however, because mutants lacking one or more of the three RPTPs that have been genetically characterized thus far do not display strong CNS phenotypes. Even a triple mutant lacking DLAR, DPTP69D, and DPTP99A has only subtle CNS defects (Desai et al., 1997a; Q.S. and K.Z., unpublished).

Here we report the isolation of mutations in the fourth neural *Rptp* gene, that encoding DPTP10D. *Ptp10D* single mutants are viable and fertile, and display no embryonic phenotypes. When DPTP69D is also removed, however, a striking CNS phenotype is observed in which many longitudinal axons are rerouted across the midline. Genetic interaction studies show that the RPTPs are likely to regulate pathfinding at the midline *via* modulation of the Robo/Slit/Comm repulsive signaling system. We also show that the absence of the RPTPs causes many other complex changes in the guidance of interneuronal axons.

Results

Isolation of mutations in the *Ptp10D* gene

To isolate *Ptp10D* mutations, we employed standard *P* element mutagenesis techniques. Several *P* element insertions have been mapped to the cytological location 10D. One of these, *EP1332*, is inserted less than 5 kb upstream of the translation start of *Ptp10D* (Figure 1; see Experimental Procedures). Embryos homozygous or hemizygous for *EP1332* express very low levels of DPTP10D protein as assayed by staining with monoclonal antibodies (mAbs) against DPTP10D (Tian et al., 1991). The phenotypic analysis described below indicates that the *EP1332* insertion is a hypomorphic *Ptp10D* mutation. In order to generate mutations that delete *Ptp10D* coding sequences, we mobilized *EP1332* and isolated five imprecise excision derivatives that delete the first coding exon of *Ptp10D*, which includes the ATG and the DNA encoding the signal sequence. The breakpoints of one of these deletions, $Ptp10D^{1}$, are indicated in Figure 1.

Another *P* element in the region, *P842*, was previously described by Bahri et al. (1997). *P842* is inserted 3' to *bifocal* (*bif*), the gene adjacent to *Ptp10D* (Figure 1). We carried out similar imprecise excision procedures for *P842* and isolated two deletion lines, *Df(1)59* and *Df(1)101*. *Df(1)59* completely removes the *Ptp10D* and *bif* genes, while *Df(1)101* deletes most of the *Ptp10D* coding sequence (but does not remove the first exon), and all of the *bif* coding sequence (Figure 1).

$Ptp10D^{1}$ deletes the ATG and signal sequence, and we were unable to detect any DPTP10D protein in $Ptp10D^{1}$ embryos. Thus, it is likely to be a null allele. $Ptp10D^{1}$, *Df(1)59* , *Df(1)101*, and a trans-heterozygous combination of $Ptp10D^{1}$ and *Df(1)101* all produced the same phenotypes when combined with *Ptp69D* (see below). $Ptp10D^{1}$ and *Df(1)101* do not overlap, so the only gene likely to be affected in these trans-heterozygotes is *Ptp10D*. Finally, the hypomorphic insertion *EP1332* is a *P* element containing multiple binding sites for the transcriptional activator GAL4 (Rorth, 1996), oriented in a manner which would direct GAL4-dependent transcription of *Ptp10D*.

When *EP1332* is crossed to *C155-GAL4* (Lin and Goodman, 1994), in which GAL4 is expressed in all postmitotic neurons, DPTP10D is expressed at high levels in neurons. This expression rescues the phenotype conferred by *EP1332* (see below). All of these data indicate that the phenotypes described below are due to the absence of the DPTP10D protein.

Ptp10D Ptp69D double mutant embryos display a synergistic midline crossing phenotype

Ptp10D^{1}, *Df(1)59*, and *Df(1)101* are all homozygous viable and fertile, and we were unable to detect any embryonic phenotypes conferred by these mutations. We focused our analysis on the nervous system, since DPTP10D is expressed only on CNS axons in the embryo (Tian et al., 1991; Yang et al., 1991). Figure 2B shows the CNS of a *Ptp10D*^{1} embryo stained with the 1D4 mAb, which recognizes the transmembrane form of Fasciclin II (Van Vactor et al., 1993). In late stage 16 and early stage 17 embryos, 1D4 stains three distinct axon bundles in each longitudinal connective of the CNS, but does not stain any commissural bundles. The pattern of 1D4-positive bundles seen in *Ptp10D*^{1} is identical to that observed in wild-type embryos (Figure 2A).

DLAR, DPTP69D, and DPTP99A have partially redundant functions in the control of motor axon guidance (Desai et al., 1996, 1997a; Krueger et al., 1996). A triple mutant lacking all three displays severe motor axon defects, but has a relatively normal pattern of 1D4-positive CNS axons (Desai et al., 1997a; Q.S. and K.Z., unpublished). This suggests that if these four neural RPTPs are involved in guidance within the CNS, expression of DPTP10D alone is sufficient to compensate for the absence of the other three. DPTP10D is not required when the other three are present, however, since *Ptp10D* mutants have no detectable CNS phenotypes.

To examine whether DPTP10D has a function in CNS axon guidance that is compensated for by another RPTP, we made double mutant combinations in which *Ptp10D* mutations were combined with mutations in each of the other three neural *Rptp* genes. Double mutants lacking DPTP10D and DPTP99A (Hamilton and Zinn, 1995) are viable and exhibit no detectable embryonic phenotypes. *Dlar* mutations are lethal and confer motor axon guidance phenotypes (Krueger et al., 1996; Desai et al., 1997a), but these are unchanged when DPTP10D is also absent. No CNS abnormalities are detectable by 1D4 staining in *Ptp10D Dlar* double mutants.

Ptp69D mutations are also lethal and cause motor axon phenotypes (Desai et al., 1996, 1997a). The pattern of 1D4-positive axons in the CNS of *Ptp69D* null mutants is identical to wild-type (data not shown). When null *Ptp10D* mutations (*$Ptp10D^{1}$/$Ptp10D^{1}$*, *$Ptp10D^{1}$/Df(1)101*, and others) are combined with null mutations in the *Ptp69D* gene (*$Ptp69D^{1}$/Df(3L)8ex25* and others; Desai et al., 1997a), a unique and highly penetrant CNS phenotype is observed in double mutant embryos stained with 1D4 (Figures 2D and 3). In these embryos, the longitudinal axon bundles are irregular and often fuse to each other, so that some segments have only one or two bundles instead of the usual three. The outer 1D4-positive bundle is usually missing or reduced to short, discontinuous stained regions, and breaks in the inner two bundles are also observed. Three or more 1D4-positive bundles are observed within the commissures of each segment; these are never seen in wild-type embryos.

We also examined embryos bearing null *Ptp69D* mutations combined with the hypomorphic *Ptp10D* insertion *EP1332*. DPTP10D protein is normally localized in these embryos, but is present at greatly reduced levels. This combination produces a much weaker phenotype, in which only the outer 1D4 bundle is strongly affected. Occasional fusions of the inner two bundles are also observed, and 1D4-positive bundles cross the commissures in a few segments of each embryo (Figure 2C). As

described above, this double mutant phenotype is rescued by driving high-level DPTP10D expression using a neuronal GAL4 source.

To examine the complete axonal array in double mutant embryos, we used the BP102 mAb, which recognizes an epitope present on all CNS axons (Seeger et al., 1993). Late stage 16 wild-type embryos stained with BP102 display a ladder-like pattern of axons, with two commissural tracts (anterior and posterior) in each segment, and bilaterally symmetric longitudinal connectives extending the length of the embryo. At this stage, the longitudinal tracts are thicker than the commissural tracts, especially in the neuropilar region between the anterior and posterior commissures (Figure 2F). *Ptp10D Ptp69D* double mutant embryos stained with BP102 have broader commissures than wild-type embryos, and the intercommissural space at the midline of the embryo is compressed along the A-P axis (arrow, Figure 2G). The longitudinal tracts are also somewhat reduced, especially in the intersegmental regions between the neuromeres (arrowhead, Figure 2G). The 1D4 and BP102 staining patterns are consistent with the hypothesis that some axons that would normally travel within the longitudinal tracts are rerouted across the midline in double mutant embryos.

We also examined double mutant phenotypes using mAb C1.427, which recognizes the Connectin protein (Meadows et al., 1994). In late stage 16 embryos, C1.427 stains two commissural bundles in each segment, as well as two longitudinal bundles, the SN motor axon tracts, and a small group of neuronal cell bodies (Figure 2I). In *Ptp10D Ptp69D* double mutant embryos, the C1.427-positive commissural bundles are much thicker, and the longitudinal bundles are irregular and sometimes broken (Figure 2J).

Although some longitudinal axons cross the commissures in *Ptp10D Ptp69D* double mutant embryos, many others remain within the longitudinal tracts. We wondered whether RPTPs might also be involved in defining these other longitudinal

pathways, since all four neural RPTPs are expressed on most or all CNS axons. Accordingly, we constructed and analyzed quadruple mutant embryos bearing null mutations in all four *Rptp* genes. When these embryos were stained with 1D4, a striking phenotype was observed in which most axons cross the midline and all longitudinal pathways are severely disrupted. Only short fragments of longitudinal tracts can be visualized in quadruple mutants (arrowhead, Figure 2E). Many bundles cross the midline in each segment, and these do not respect the normal boundaries of the commissures (arrows, Figure 2E). A comparison between Figures 2B and 2E reveals that removing all four RPTPs essentially converts all of the 1D4-positive longitudinal axons into commissural axons. Interestingly, although these longitudinal axons are rerouted to the midline, they do not remain there (as in *slit* mutants), nor do they appear to circle back to the midline after crossing (as in *robo* mutants; see below for further discussion).

Quadruple mutants stained with BP102 have fused anterior and posterior commissures, so that a single broad tract crossing the midline is observed in each segment. This phenotype is consistent with the hypothesis that more axons are rerouted across the midline than in double mutants (Figure 2H). We have also done a phenotypic analysis of all triple mutant combinations, in order to understand how each RPTP contributes to CNS and motor axon guidance, and this will be published elsewhere.

Longitudinal pioneer axons develop normally in *Ptp10D Ptp69D* double mutants

1D4-positive axons make a number of different axon guidance errors in *Ptp10D Ptp69D* double mutants. First, the three longitudinal bundles, which are normally separate, fuse with each other for short regions and then separate, and the outer bundle is usually missing. Thus, in the embryo of Figure 3A, a single longitudinal bundle is visible at the

upper left; in the middle region it separates into two bundles, and these bundles fuse again at the lower left (arrows). Second, the entire 1D4-positive longitudinal tract is sometimes rerouted across the midline within the domain that is demarcated by the anterior and posterior edges of the commissures (Figure 3B, arrows). The ectopic commissural tract does not appear to avoid the zone between the commissures, which is normally free of axons; this is reflected in the BP102 staining pattern, which shows expansion of the commissures into this zone (Figure 2G). Third, a longitudinal bundle occasionally wanders diagonally across the midline, traversing the intersegmental region between neuromeres where no axons normally grow (Figure 3C, arrow). Finally, longitudinal bundles often stop abruptly, causing breaks in the longitudinal tracts (Figure 3D, arrows).

Although these phenotypes indicate that 1D4-positive axons have been rerouted, they do not show what changes have occurred in the pathways taken by individual growth cones. This is because many axons are stained by 1D4 in stage 16 embryos, and staining appears to be primarily restricted to mature bundles rather than to growth cones. To analyze the behavior of individual growth cones, we examined 1D4-stained double mutant embryos at much earlier stages. During stage 12, the only neurons stained by 1D4 are the longitudinal pioneer neurons MP1, dMP2, vMP2, and pCC, in addition to the motoneuron aCC (Figure 4A; Seeger et al., 1993). In normal embryos, the vMP2 and pCC axons fasciculate with each other and extend anteriorly, while MP1 and dMP2 axons fasciculate and extend posteriorly. By stage 13, the ascending vMP2/pCC fascicle encounters the descending axons of dMP2 and MP1. These fascicles attach to each other briefly (Figure 4C), then separate again, so that by stage 14 they have pioneered two continuous longitudinal pathways. One of these becomes the inner 1D4-positive bundle, and the other comprises part of the middle bundle (Hidalgo and Brand, 1997).

The longitudinal pioneer growth cones follow abnormal pathways in *robo* and *slit* mutants, turning toward the midline rather than navigating within the longitudinal tracts (Seeger et al., 1993; Kidd et al., 1998a,b, 1999; Battye et al., 1999). When we examined *Ptp10D Ptp69D* double mutants at these early stages, however, we found that pioneer growth cone navigation and establishment of the longitudinal pathways occurred in a normal manner (Figures 4B, D). Similarly, early C1.427-positive growth cones follow normal pathways in the double mutants (data not shown). These data suggest that the axons that cross the midline in *Ptp10D Ptp69D* mutants are those of later neurons whose growth cones would normally follow established longitudinal pathways. We have been unable to find antibody or enhancer trap markers that allow selective visualization of these growth cones.

Lineage tracing experiments define growth cone guidance errors made by individual CNS neurons in *Ptp10D Ptp69D* mutants

To visualize individual axons and growth cones that are affected in *Ptp10D Ptp69D* mutants, we performed lineage tracing experiments in which the fluorescent dye DiI was used to label all of the progeny of a single neuroblast (NB) *in vivo*. NBs were labeled at stage 8, and the embryos allowed to develop until stage 17, after which the DiI-labeled axons and cell bodies of NB progeny were visualized by confocal microscopy (Schmid et al., 1999).

Analysis of a large number of NB lineages in the double mutants revealed that many CNS axonal pathways are altered in complex ways by the absence of DPTP10D and DPTP69D. A complete description of these changes will be published elsewhere. Here we describe the projection patterns of three sets of neurons that illustrate essential aspects of the phenotype: the progeny of NBs 3-1, 4-2, and 2-5. No alterations in

numbers or positions of cell bodies are observed for these lineages in *Ptp10D Ptp69D* embryos.

The NB 2-5 lineage generates 15-22 cells by stage 17, of which 8-16 are intersegmental interneurons. Some of these (4 to 8 neurons) extend axons across the midline in the anterior commissure; these axons then turn anteriorly in the contralateral longitudinal tract and grow all the way to the brain (up to 10 segments). The remaining intersegmental interneurons (4 to 8 neurons) extend axons anteriorly in the ipsilateral longitudinal tract that stop after projecting about half as far. There is also a single motoneuron which extends an axon in the ipsilateral ISNd pathway and innervates muscles 15-17 (Schmid et al., 1999; Figure 5E). In *Ptp10D Ptp69D* mutants (n=3), the contralaterally projecting interneuronal axons cross the midline and turn anteriorly in a normal manner, but then double back across the midline after about two segments and grow posteriorly in the ipsilateral longitudinal tract (Figure 5F). The axons of the ipsilateral intersegmental neurons grow anteriorly for a short distance and stop. The ISNd motoneuron extends an axon toward the midline that stalls and never enters the ISN root. This lineage illustrates that interneuronal axons abnormally cross the midline in the *Rptp* double mutant, and that a motor axon is deflected toward the midline.

The NB 4-2 lineage produces about 22 cells, including the well-characterized RP2 motoneuron, which extends its axon along the ISN pathway and innervates the dorsal muscle 2. It also generates the CoR motoneurons, whose axons comprise all of the SNc motor nerve. All of the interneurons are local; two or three of them extend axons across the anterior commissure that bifurcate in the contralateral connective (Schmid et al., 1999; Figure 5C). In *Ptp10D Ptp69D* double mutants (n=6), the RP2 axon stalls before reaching its target, and the CoR axons do not branch onto all of their target muscles. An ipsilateral longitudinal projection is formed that extends anteriorly from the clone and crosses the segment border; this is never observed in wild-type.

Finally, the local interneuronal projection splits after crossing the midline, so that two pathways form instead of one; this was observed in all lineages examined (Figure 5D). In summary, this lineage illustrates that abnormal longitudinal pathways are formed in mutant embryos and that pathway selection in the commissures is altered.

NB 3-1 produces the RP1, RP3, RP4, and RP5 motoneurons, which extend axons across the anterior commissure and into the ISNb nerve, eventually innervating the ventrolateral muscles. It also generates a variable number of interneurons, which cross the midline and project both posteriorly (intersegmental interneurons) and anteriorly (local interneurons) in the contralateral connective (Schmid et al., 1999; Figure 5A). In *Ptp10D Ptp69D* mutants (n=3), the RP neurons extend axons normally across the commissure and into the ISNb nerve, although they do not form normal synapses. The interneuronal projections, however, are radically altered. They still cross the midline, but do not form defined anterior and posterior projections in the contralateral connective. Instead, they grow anteriorly in a circular path around the neuropil, contacting the midline at the end of their trajectory (Figure 5B). Like the other lineages, 3-1 illustrates that longitudinal pathways cannot form normally. Both the anterior and posterior interneuronal projections are missing, and are replaced by a swirl of axons that grow to the midline. These kinds of pathway alterations could give rise to the connective breaks that are observed in mutant embryos.

Ptp10D Ptp69D interacts genetically with *comm*, *robo*, and *slit*

The interaction of Robo with Slit produces a repulsive signal that keeps longitudinal axons away from the midline and prevents commissural axons from recrossing. *robo* mutants have a phenotype in which the inner 1D4-positive longitudinal bundle crosses the midline and circles around it. The outer two bundles are less affected (Figure 6G).

Mutations in *slit* confer a more extreme phenotype in which most axons converge on the midline and do not leave (Figure 7E).

robo is likely to have a weaker phenotype than *slit* because Robo2, a second Slit ligand, can mediate repulsion of some axons when Robo is absent. Consistent with this, removal of one copy of*slit* , which would be expected to reduce repulsion through both Robo family proteins, produces a weak midline crossing phenotype when a copy of *robo* is also removed (*slit/+, robo/+*), and enhances the phenotype of *robo* homozygotes (*slit/+, robo/robo*) (Kidd et al., 1999). Removing one copy of *slit* in a wild-type background does not produce any phenotypes.

Another component of this system, the Comm protein, is transferred from midline glia to commissural axons and downregulates Robo, allowing commissural axons to cross the midline (Tear et al., 1996; Kidd et al., 1998b). In *comm* mutants, Robo is not downregulated, and all axons are repelled from the midline. This produces a striking phenotype in which no commissures form (Figure 6A). Because Comm acts through Robo, elimination of Robo suppresses the *comm* phenotype and allows axons to cross the midline; thus, *comm robo* double mutants have phenotypes like those of *robo* single mutants (Seeger et al., 1993).

To investigate the relationship between the Robo/Slit/Comm system and the midline crossing phenotype of the *Rptp* double mutant, we combined the *Ptp10D* and *Ptp69D* mutations with *comm*, *robo*, and *slit*. In a *comm Ptp10D Ptp69D* triple mutant, axons are able to cross the commissures. A thick commissural tract, visualized by BP102 (Figure 6B) or 1D4 (Figure 6D) staining, is observed in about half of the segments in these triple mutants. This suggests that Robo-mediated repulsion from the midline is reduced in the absence of the RPTPs.

When *Ptp10D Ptp69D* is combined with *robo*, a severe phenotype is produced in which most of the 1D4-positive axons converge on the midline (Figure 6H). Some

circles around the midline are still seen in these triple mutants (arrow), but many axons fasciculate into a single thick bundle that extends up and down the midline (arrowheads). Vestiges of the lateral longitudinal pathways are also present in some segments. The *robo Ptp10D Ptp69D* phenotype approaches the severity of the *slit* phenotype (Figure 7E) when visualized with 1D4, suggesting that most repulsion from the midline has been eliminated in these mutants. Interestingly, however, when the full complement of CNS axons is visualized with BP102, the triple mutant looks more like *robo* than like *slit* (Figures 6E-F; a *slit* mutant CNS stained with BP102 would be a single fused midline tract). Thus, the *Rptp* mutations seem to have a stronger effect on the subset of axons that are 1D4-positive. We also combined *robo* with each of the *Rptp* single mutants, and removed one copy of *robo* from the *Ptp10D Ptp69D* double mutant, but found that none of these combinations produced synergistic phenotypes.

To investigate the relationship between the RPTPs and Slit, we removed one copy of *slit* from the *Ptp10D Ptp69D* double mutant. As shown in Figure 7, this produces a significant enhancement of the phenotype. More 1D4-positive axons cross the midline, and the longitudinal tracts move closer together, so that the average width of the CNS axonal array decreases from 7.7 μm (+/- 0.5 μm) to 4.7 μm (+/- 0.5 μm; Figures 7A-B). In BP102-stained embryos, the axonal array is also compressed toward the midline when one copy of *slit* is removed, and more extensive commissural fusion is observed (Figures 7C-D). These results indicate that, like reducing or eliminating Robo expression, removal of the RPTPs sensitizes the embryo to a 50% reduction in the amount of Slit-mediated repulsion from the midline.

To examine the specificity of the interaction between the *Rptp* mutations and the Robo/Slit/Comm system, we also combined the *Ptp10D Ptp69D* double mutation with a deletion of both Netrin genes. The *Netrin* deletion alone produces a phenotype in which commissures are reduced but not eliminated (Harris et al., 1996; Mitchell et al., 1996),

and this phenotype is unaffected when the RPTPs are also removed (data not shown). Thus, the suppression of the *comm* phenotype by the *Rptp* double mutation is due to a selective effect on the repulsion system rather than to a generalized suppression of any phenotype that reduces midline crossing.

We also examined whether the *Rptp* phenotypes are affected by alterations in interaxonal adhesion. In one model, longitudinal bundle fusion and midline crossing might be explained by a decrease in interaxonal adhesion that would allow longitudinal axons to separate from their normal pathways and fasciculate with other longitudinal and commissural bundles. Conversely, fusion of longitudinal bundles might be produced by an *increase* in adhesion that would cause two normally separate bundles to adhere to each other.

In *PlexinA* mutants, which lack a Semaphorin receptor, the outer 1D4 (Fasciclin II)-positive bundle is discontinuous, as it is in *Ptp10D (hypomorph) Ptp69D* mutants. This phenotype is suppressed when one copy of the *FasciclinII (FasII)* gene is removed. Since *FasII* encodes a homophilic adhesion molecule expressed on these axons, this manipulation would be expected to decrease interaxonal adhesion within the 1D4-positive longitudinal bundles (Winberg et al., 1998). To examine whether this reduction in adhesion would affect *Rptp* phenotypes, we removed one copy of *FasII* from *Ptp10D Ptp69D* mutants. We observed no effect on the phenotype, however (data not shown).

Discussion

Four of the five known *Drosophila* RPTPs are selectively expressed on CNS axons and growth cones, suggesting that their major developmental roles are in guidance and synaptogenesis. In earlier studies, we and others have analyzed the phenotypes produced by removal of three of these neural RPTPs: DLAR, DPTP69D, and DPTP99A

(Desai et al., 1996, 1997a; Krueger et al. 1996; Garrity et al., 1999; Wills et al., 1999). These studies showed that many of the specific pathfinding decisions made by motor axon growth cones are dependent on RPTP function.

Most decisions are strongly affected only in double or triple mutants, indicating that the RPTPs have partially redundant functions. Competitive genetic relationships between RPTPs are also observed for certain decisions, however. For example, the ISNb guidance phenotype of *Dlar* mutants is suppressed by removing both copies of the *Ptp99A* gene (Desai et al., 1997a). Removal of one copy of the *Abl* tyrosine kinase gene also suppresses this phenotype. These results suggest that DLAR regulates ISNb guidance by antagonizing signaling through Abl and DPTP99A. DLAR also binds directly to Abl and to its substrate Ena (Wills et al., 1999).

RPTPs are also required for innervation of the larval optic lobe by photoreceptor axons. When R1-6 photoreceptor growth cones do not express DPTP69D, they fail to recognize a stop signal in their lamina target layer, and continue through into the medulla. Phosphatase activity and a portion of the extracellular domain are required for this recognition (Garrity et al., 1999). These results imply that ligands for DPTP69D may be present in the lamina, and that interaction with the ligands affects phosphorylation of substrates that control the changes in R1-6 growth cone morphology that occur at the target layer. These ligands and substrates have not been identified, however.

DPTP10D and DPTP69D regulate axon guidance across the CNS midline

Although the RPTPs are expressed on most or all interneuronal axons, genetic studies have not defined clear phenotypes within the CNS associated with removal of DLAR, DPTP69D, or DPTP99A. Even in a triple mutant lacking all three of these RPTPs, the overall structure of the CNS is unaltered and longitudinal axons follow relatively normal

pathways (Desai et al., 1997a; Q.S. and K.Z., unpublished results). In this paper, we describe the isolation of mutations in the gene encoding the fourth RPTP, DPTP10D, and show that this phosphatase is critical for control of interneuronal axon guidance. No phenotypes are observed in single mutant embryos lacking only DPTP10D. However, when DPTP10D and DPTP69D are both absent, a striking CNS phenotype is observed in which many longitudinal axons abnormally cross the midline.

We visualized ectopic midline crossing in *Ptp10D Ptp69D* double mutants by staining with mAbs 1D4, C1.427, and BP102 (Figures 2, 3), and by dye-filling lineages of neurons derived from specific NBs (Figure 5). These results indicate that longitudinal pioneer axons are not affected by the *Rptp* mutations (Figure 4), but many later axons cross the midline or follow abnormal pathways within the longitudinal tracts. The opposite situation is observed in mutant embryos lacking the Robo receptor, which transduces a midline repulsive signal. Here longitudinal pioneer axons in the medial 1D4-positive longitudinal bundle cross the midline and circle around it, while the later axons in the middle and lateral bundles appear to follow relatively normal pathways (Kidd et al., 1998a,b; Figure 6G). In triple mutants lacking Robo, DPTP10D, and DPTP69D, a very strong phenotype is observed in which all three longitudinal 1D4 bundles are severely affected. In some segments, only a single tract running along the midline is observed (Figure 6H).

This triple mutant phenotype does not necessarily indicate that Robo and the RPTPs are involved in the same pathways, since simply adding together the guidance errors seen in *robo* and in *Ptp10D Ptp69D* might be expected to generate a strong phenotype affecting all three 1D4-positive longitudinal bundles. Furthermore, the phosphatases are not required for Robo function in some axons, because the growth cones of longitudinal pioneer neurons are rerouted across the midline in *robo* mutants but are not affected in *Ptp10D Ptp69D* embryos (Figure 4). We showed that the RPTP

mutations do perturb repulsive signaling at the midline by examining their interactions with two other genes in the repulsive pathway, *comm* and *slit*.

Comm is a protein made by midline glia that is transferred to commissural axons and causes downregulation of Robo. The loss of Robo from these axons allows them to ignore the repulsive signal and cross the midline. When Comm is not expressed, Robo cannot be downregulated and no axons are able to cross (Figures 6A,C; Tear et al., 1996; Kidd et al., 1998b). Because Comm acts through Robo, in a *comm robo* double mutant the *comm* phenotype is suppressed and extra axons cross the midline (Seeger et al., 1993). We find that *Ptp10D Ptp69D* partially suppresses *comm*, indicating that removal of the RPTPs interferes with reception of the repulsive signal (Figures 6B,D).

The repulsive factor produced by midline cells is likely to be the extracellular matrix protein Slit. In the absence of Slit, all interneuronal axons converge on the midline and remain there (Figure 7E; Kidd et al., 1999; Battye et al., 1999; for review see Zinn and Sun, 1999). Robo and Slit proteins bind to each other (Brose et al., 1999; Li et al., 1999), and *robo* and *slit* also interact genetically. Removing one copy of *slit* , which produces no phenotype on its own, enhances the *robo* homozgyote phenotype and confers a weak phenotype on *robo*/+ heterozygotes (Kidd et al., 1999). Similarly, the *Ptp10D Ptp69D* phenotype is strengthened by removal of one copy of *slit* (Figures 7A-D).

Slit ligand is thought to interact with two Robo receptors: Robo and Robo2. Many axons follow normal longitudinal pathways in *robo* mutants, probably because repulsive signaling through Slit and Robo2 keeps them from converging on the midline. If Robo and Robo2 are the only receptors for Slit, removing both would be expected to eliminate repulsion, producing a *slit*-like phenotype (Kidd et al., 1999). We find that the *robo Ptp10D Ptp69D* triple mutant, when visualized with 1D4, has a phenotype which approaches that of *slit* (Figures 6H, 7E). This suggests that DPTP10D and

DPTP69D are required for signaling through Robo2 or other, as yet unidentified, Slit receptors. Our data, however, do not support a model in which the RPTPs are *only* involved in Robo2 signaling. If this were the case, one would not expect to observe a genetic interaction between the *Ptp10D Ptp69D* and *robo2* mutations. The *robo2 Ptp10D Ptp69D* triple mutant, however, has a very strong synergistic phenotype, favoring a model in which DPTP10D and DPTP69D function in repulsive signaling through both Robo receptors (Q.S., J. Simpson, T. Kidd, C.S. Goodman, and K.Z., unpublished results).

Although some longitudinal axons follow normal pathways in the absence of DPTP10D and DPTP69D, they apparently still require RPTP function to avoid the midline. In a quadruple mutant embryo lacking all four neural RPTPs, all 1D4-positive longitudinal axons are diverted into commissural pathways (Figure 2E). Interestingly, however, the quadruple mutant phenotype is quite different from that of *slit*, because these ectopic commissural axons are still able to leave the midline and cross to the contralateral side of the CNS. Thus, growth to the midline and midline crossing may be under separate genetic control in ways we do not yet understand.

The major features of the *Ptp10D Ptp69D* phenotype as visualized with 1D4 are midline crossing and fusion of longitudinal bundles. The bundle fusion indicates that selective fasciculation within the longitudinal tracts has been altered. It is possible that midline crossing could be influenced by these changes within the longitudinal tracts, because it has been shown that ablation of the longitudinal pioneer axons with which later axons fasciculate produces ectopic midline crossing (Hidalgo and Brand, 1997). In this scenario, crossing the midline would be a 'default' pathway that longitudinal axons select when they fail to adhere normally to their appropriate bundles. We were not able to alter the *Ptp10D Ptp69D* phenotype by reducing FasII-mediated homophilic adhesion (which does suppress a similar longitudinal bundle phenotype produced by the absence

of the PlexinA receptor for Semaphorins; Winberg et al., 1998), but it is possible that a different adhesion molecule is critical for the *Rptp* phenotype. It is unlikely, however, that alteration of fasciculation within the longitudinal tracts would lead to the observed suppression of the *comm* phenotype by *Ptp10D Ptp69D,* since the only known function of Comm is to neutralize repulsive signaling through Robo receptors.

What biochemical mechanisms are involved in facilitation of Robo2 and Robo signaling by the RPTPs? Fly, worm, and mammalian Robo family proteins (Robos) have conserved tyrosine-containing PYATT sequences in their cytoplasmic domains that could be targets for tyrosine kinases (Kidd et al., 1998a; Zallen et al., 1998). Furthermore, inhibition of tyrosine kinase activity in grasshopper embryos causes a *robo*-like phenotype in which the pCC axon crosses the midline and circles back to the ipsilateral side. This suggests that Robo signaling may involve a tyrosine kinase (Menon and Zinn, 1998).

A simple model would be that the PYATT motifs of Robos are phosphorylated by a tyrosine kinase and dephosphorylated by the RPTPs, and that the dephosphorylated forms are more active in signaling. This seems unlikely, however, since normally it is the phosphorylated form of a signaling module that binds to downstream adapters.

In a variant of this model, Robo family proteins might become phosphorylated on tyrosines after engagement of Slit, and DPTP10D or DPTP69D would be recruited into the signaling complex by their interactions with the phosphotyrosine motifs. The RPTPs might remain bound to these sites for a significant time period if they hydrolyze the phosphate-tyrosine bonds slowly. Most RPTPs, including DPTP69D, have two cytoplasmic phosphatase homology units. Membrane-proximal catalytic domains can have quite slow catalytic rates, at least for certain substrates, while membrane-distal domains often exhibit little catalytic activity but can still bind to phosphotyrosyl peptides (for example, see Lim et al., 1998). Furthermore, other interactions between Robos and

the RPTPs might prevent rapid dissociation even if the phosphate-tyrosine bond is hydrolyzed. In this model, the RPTPs themselves would serve as adapters, binding to downstream signaling proteins and recruiting them into a Slit/Robo/RPTP signaling complex.

Finally, the RPTPs might not interact directly with Robos at all, but could facilitate signal transduction through Robos by dephosphorylating other signaling proteins in their pathways. For example, the RPTP CD45 participates in T cell receptor signaling by removing an inhibitory phosphotyrosine from the tyrosine kinase Lck, thereby activating it and allowing it to phosphorylate the ζ chain of the receptor (Weiss and Littman, 1994). Distinguishing between these models will require biochemical studies of interactions between Robo, Robo2, Slit, the RPTPs, and other signaling proteins.

Growth cone guidance and RPTP function

Examination of *Rptp* loss-of-function phenotypes in the embryonic neuromuscular system, the embryonic CNS, and the larval optic lobes reveals that many different kinds of guidance defects can be caused by the absence of particular RPTPs. R1-6 photoreceptor axons extend past their normal optic lobe targets in *Ptp69D* mutants (Garrity et al., 1999. Conversely, some pathways in the neuromuscular system are truncated (the ISN and ISNb) or absent (ISNd) in embryos lacking one or more RPTPs (Krueger et al., 1996; Desai et al., 1997a). Within the CNS, the dye-filling experiments described here show that some longitudinal interneuronal pathways are truncated, while others extend past their normal termination points (Figure 5).

Rptp mutations often alter fasciculation patterns, so that axons fail to separate from common pathways at choice points, separate at abnormal sites, or join bundles that they would normally avoid. Loss of RPTP function in the neuromuscular system can

cause the ISNb nerve to fail to separate from the common ISN pathway at the exit junction (Desai et al., 1996, 1997a). In the CNS, 1D4-positive bundles in the longitudinal tracts become fused to each other in *Ptp10D Ptp69D* mutants (Figures 2 and 3). Longitudinal pathways formed by many NB lineages are defasciculated (unpublished results). A commissural bundle formed by the axons of NB 4-2 progeny splits into two after crossing the midline (Figure 5).

Guidance errors also occur in *Rptp* mutants that do not appear to directly correlate with fasciculation patterns. These include the midline crossing phenotypes described here, as well as many of the alterations visualized in the dye-filling experiments. For example, the NB 3-1 progeny axons grow in a swirling pattern around the neuropil rather than forming distinct anterior and posterior longitudinal projections (Figure 5). In the neuromuscular system of *Dlar* mutants, the ISNb leaves the ISN in a normal manner but then bypasses its muscle targets. This bypass phenotype does not involve defasciculation from another set of axons (Krueger et al., 1996).

It is difficult to find a common element that links all of these diverse phenotypes. Perhaps the most likely hypothesis is that RPTP signaling is necessary for rearrangements in the growth cone's cytoskeleton that are required for execution of several different kinds of pathfinding decisions.

Experimental Procedures

Genetics

The *Ptp10D* gene is contained within three cosmid clones: cos 1, cos 8 and cos F (Figure 1). *EP1332* (BDGP line EP(X)1172) was isolated by Rorth et al. (1998). A short segment of *EP1332* flanking sequence is available in Genbank (#AQ025398). The *EP1332* insertion was mapped by Southern DNA hybridization to a 5 kb EcoR1 fragment of cos 8 that is 5' to the breakpoint of *Df(1)59* (Bahri et al., 1997). Therefore *EP1332* is located about 5 kb upstream of the translation start of DPTP10D. Imprecise excision lines were generated as described by Hamilton and Zinn (1994). Since deletions in the *Ptp10D/bif* region are viable, we were able to screen for deletions by PCR analysis of genomic DNA from single adult flies (Gloor et al., 1993) with primer sets specific to sequence tags at various locations (Figure 1). The deletion in $Ptp10D^{1}$ starts from the *EP1332* insertion site and ends between primer sets 10D-1 and 10D-2. The P element line *P842* and deletion *Df(1)59* were previously described by Bahri et al. (1997). *Df(1)59* is a ~60kb deletion which removes the entire coding regions of *bif* and *Ptp10D*. *Df(1)101* was generated by mobilizing *P842* and selecting for lines missing the 10D-4 PCR fragment. One of the breakpoints of *Df(1)101* falls within a 14 kb region 3' to 10D-3. Because this region contains repetitive sequences, we were unable to map the precise location of this breakpoint by Southern hybridization. The other breakpoint of *Df(1)101* is 3' to the *P842* insertion site. Sequences of primers used for mapping are available on request.

Immunohistochemistry

Whole-mount antibody staining of staged fly embryo collections was performed essentially as described by Patel (1994). mAbs 1D4 (Van Vactor et al., 1993), 3F11 (anti-PTP69D (Desai et al., 1994)), 45E10 (anti-PTP10D (Tian et al., 1991)), and 8C9

(anti-DLAR; B. Burkemper and K.Z., unpublished) were used at a dilution of 1:5. BP102 (Seeger et al., 1993) was used at dilution of 1:10. For staining with anti-connectin mAb C1.427, embryos were fixed for 20 minutes in 4% formaldehyde/PEM buffer, and incubated with 1:3 dilution of the C1.427 supernatant (Meadows et al., 1994). mAb staining was visualized using HRP-conjugated secondary antibodies and DAB immunohistochemistry. Mutant embryos were identified by the absence of staining with particular anti-RPTP mAbs, sorted, and restained with 1D4, BP102, or C1.427. Dissected embryos were photographed on a Zeiss Axioplan microscope using DIC optics.

DiI labeling, neuroblast identification and clonal analysis

We delivered DiI (1,1'-dioctadecyl-3,3,3',3'-tetramethylindocarbocyanine perchlorate; Molecular Probes, Inc.) to neuroectodermal cells by the method of Bossing and Technau (1994), with modifications described elsewhere (Schmid et al, 1999). Embryos were labeled at stage 8. After 10 hours at 16^{o}C, embryos developed to stage 11; at this stage, the parasegmental groove, the segmental groove and the midline are used as morphological landmarks for NB identification and GFP-marked balancers are used to distinguish homozygous embryos. By 37 hours AEL at 16^{o}C, the embryo is well advanced into stage 17. Dissected stage 17 embryos were imaged on a Biorad 1024 microscope, using a Leitz 50X water immersion lens, as 1.5 μm step *z*-series. Data were collected at 568 nm excitation (for DiI), and each *z*-series was immediately rescanned using Nomarski optics to determine cellular positions within the CNS and identify motoneuronal target muscle(s). Cell and axon measurements were done with Biorad software calibrated to a stage micrometer. Biorad software was used to project each *z*-series to form 2 dimensional images, which were assembled into figures using Photoshop (v 5.0) and Freehand (v 7.02) software.

Acknowledgements

We thank the members of the Zinn group for discussions and comments on the manuscript, and Tom Kidd, Julie Simpson, and Corey Goodman for communication of results before publication. This work was supported by a Human Frontiers Science Project grant, RG0122/1997-B.

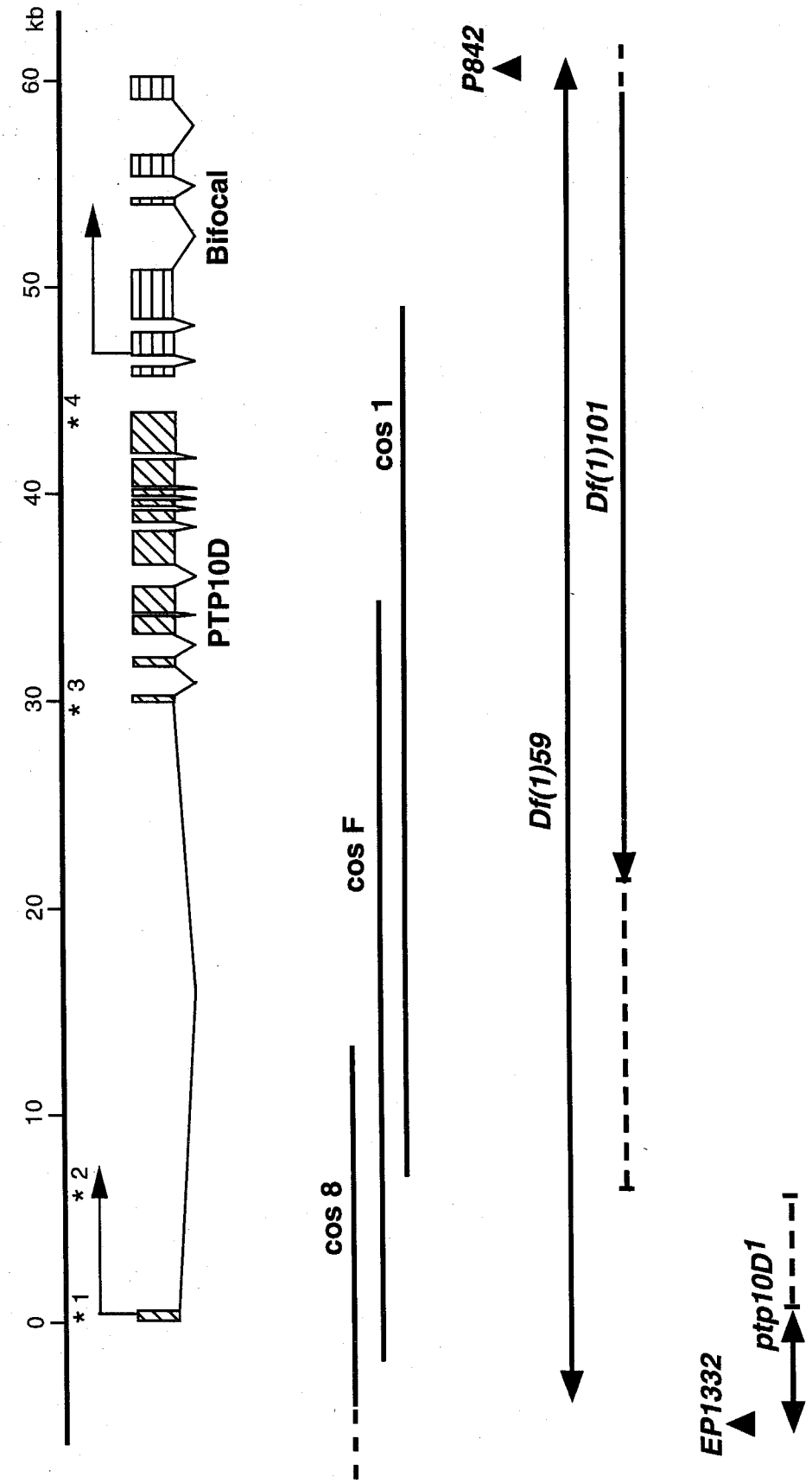
kb
0
10
20
30
40
50
60
*1
*2
*3
*4
PTP10D
Bifocal
cos 8
cos F
cos 1
Df(1)59
Df(1)101
P842
EP1332
ptp10D1

Figure 1. A molecular map of the *Ptp10D* region.

The exons of the *Ptp10D* and *bifocal* genes are indicated by boxes. Arrows above these boxes indicate the direction of transcription. Asterisks indicate the locations of primers used for mapping deletion breakpoints. Three overlapping cosmid clones (cos 1, cos 8 and cos F) that span the *Ptp10D* gene are indicated by lines below the gene map. The insertion sites of two *P* elements (*EP1332* and *P842*) used to generate deletion mutations are indicated by triangles. DNA removed by three deletions generated by imprecise excision of the two P elements, denoted *Df(1)59*, *Df(1)101*, and $Ptp10D^{1}$, is indicated by lines with arrows. Uncertainties in the deletion break points are indicated by dotted lines. $Ptp10D^{1}$ removes the entire first exon of *Ptp10D*.

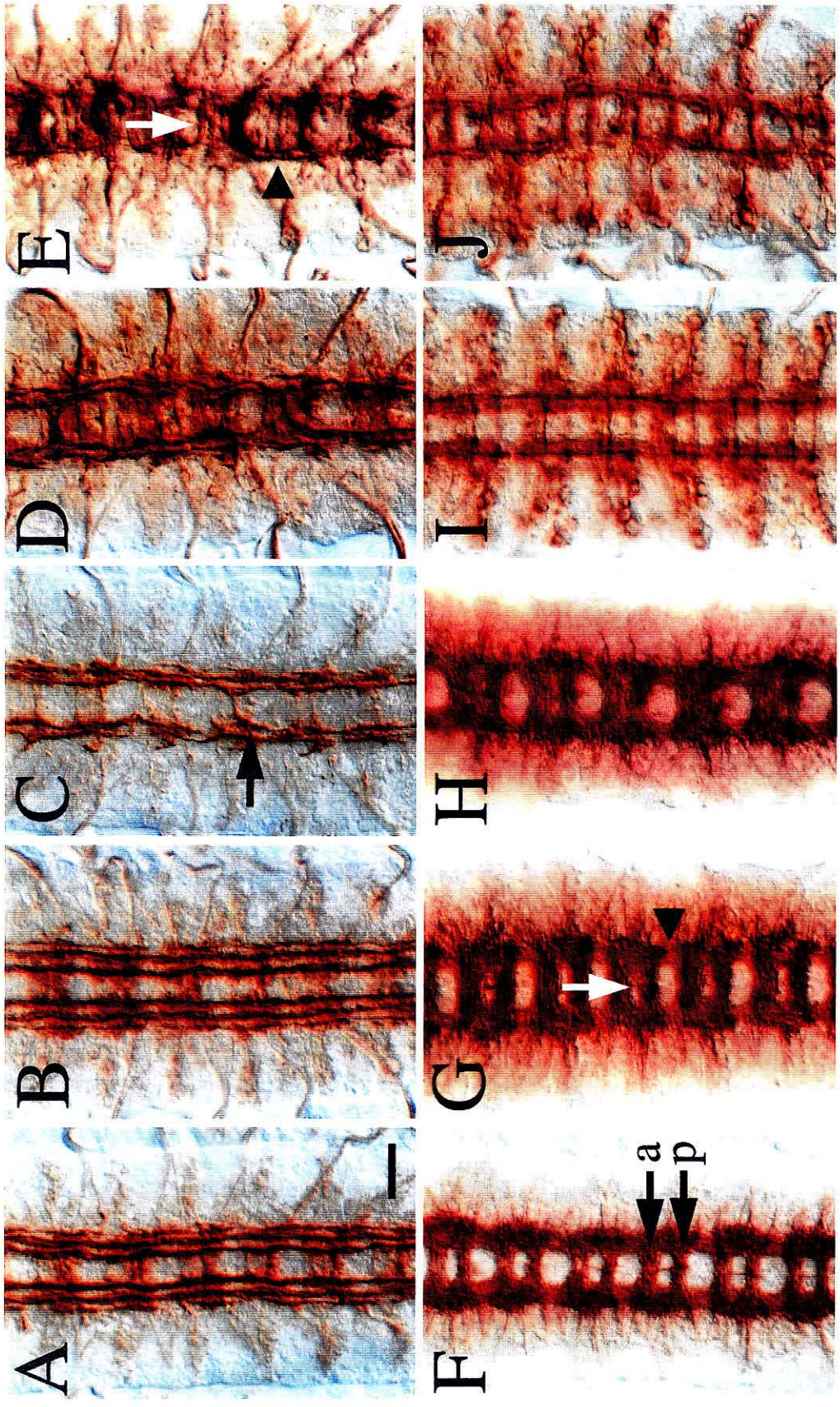
A
B
C
D
E
F
G
H
I
J
a
p

Figure 2. CNS phenotypes of *Rptp* mutants.

Each panel shows a DIC photomicrograph of several segments of the CNS in dissected late stage 16 embryos stained with mAbs 1D4 (A-E), BP102 (F-H) or C1.427 (I and J), using horseradish peroxidase (HRP) immunohistochemistry for visualization. (A) Wild-type. Note the three distinct axon bundles in each longitudinal connective; the outer bundle is still slightly discontinuous at this stage. There are no darkly staining commissural bundles in late stage 16 embryos, although light staining of axons and cell bodies is visible between the longitudinal tracts. (B) *Ptp10D*^{1} . The 1D4 staining pattern of *Ptp10D*^{1} embryos is identical to that observed in wild-type. (C) *EP1332*; *Ptp69D*^{1}/ *Df(3L)8ex25*. The 1D4 positive axon bundles are fused or interrupted in some segments, and the outer bundle never forms. One axon bundle is misrouted across the midline (arrow). (D) *Ptp10D*^{1} ; *Ptp69D*^{1}/ *Df(3L)8ex25* . Multiple axon bundles cross the midline in each segment, and extensive fusion of longitudinal bundles is observed. (E) *Ptp10D*^{1} ; *Dlar*$^{13.2}$/*Dlar* $^{5.5}$; *Ptp69D*^{1}, *Df(3R)R3/Df(3L)8ex25, Ptp99A*^{1}. In these quadruple mutant embyros the longitudinal tracts are fragmented (arrowhead), and most 1D4 staining is now on commissural bundles. The bundles that cross the midline do not respect the normal boundaries of the commissures (white arrow). (F) Wild-type. In each segment, axons cross the midline within the anterior (a) and posterior (p) commissures (arrows). (G) *Ptp10D*^{1} ; *Ptp69D*^{1}/ *Df(3L)8ex25* . The commissures are broader than in wild-type embryos and separated by a smaller space (white arrow). The longitudinal tracts are reduced in the intersegmental regions between the neuromeres (arrowhead). (H) *Ptp10D*^{1} ; *Dlar*$^{13.2}$/*Dlar* $^{5.5}$; *Ptp69D*^{1}, *Df(3R)R3/Df(3L)8ex25, Ptp99A*^{1}. Commissures are completely fused in quadruple mutants. (I) Wild-type. Two commissural bundles and two longitudinal bundles (one is out of focus) are stained by this mAb. (J) *Ptp10D*^{1} ; *Ptp69D*^{1}/ *Df(3L)8ex25* . The commissural bundles are thicker

than in wild-type, and longitudinal bundles are irregular and sometimes broken. Scale bar, 5 μm.

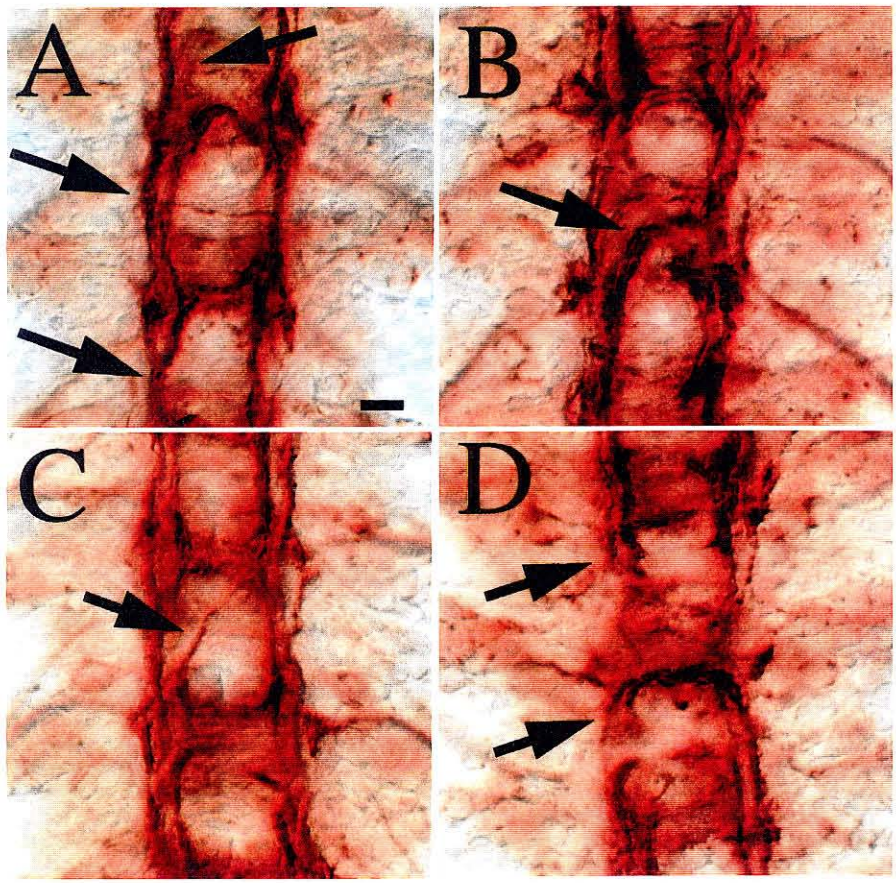
A
B
C
D

Figure 3. Axon guidance errors in *Ptp10D Ptp69D* double mutants.

All four panels show the CNS in late stage 16*Ptp10D*^{1}; *Ptp69D*^{1}/ *Df(3L)8ex25* embryos stained with 1D4. (A) Longitudinal bundle separation and fusion (arrows). (B) Rerouting of the longitudinal tract across the midline (arrow). (C) Diagonal midline crossing (arrow). (D) Broken longitudinal tracts (arrows). Scale bar, 2 μm.

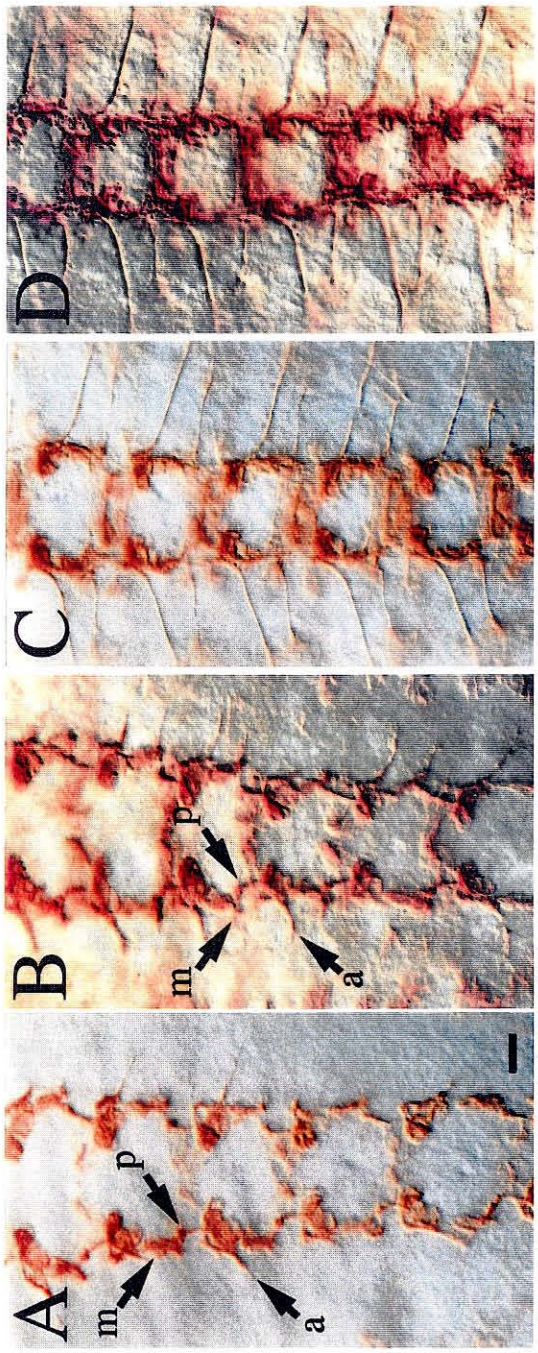
A
m
p
a
B
m
p
a
C
D

Figure 4. Establishment of early longitudinal pathways is unaffected in *Ptp10D Ptp69D* double mutants.

The CNS of late stage 12 (A and B) and stage 13 (C and D) embryos, stained with 1D4. (A and C) Wild-type. (B and D) *Df(1)59; Ptp69D^{1}/ Df(3L)8ex25* . Axonal patterns are indistinguishable from wild-type at these stages. Arrows indicate three pioneer axons: aCC (a), pCC (p) and MP1 (m). Scale bar, 2 μm.

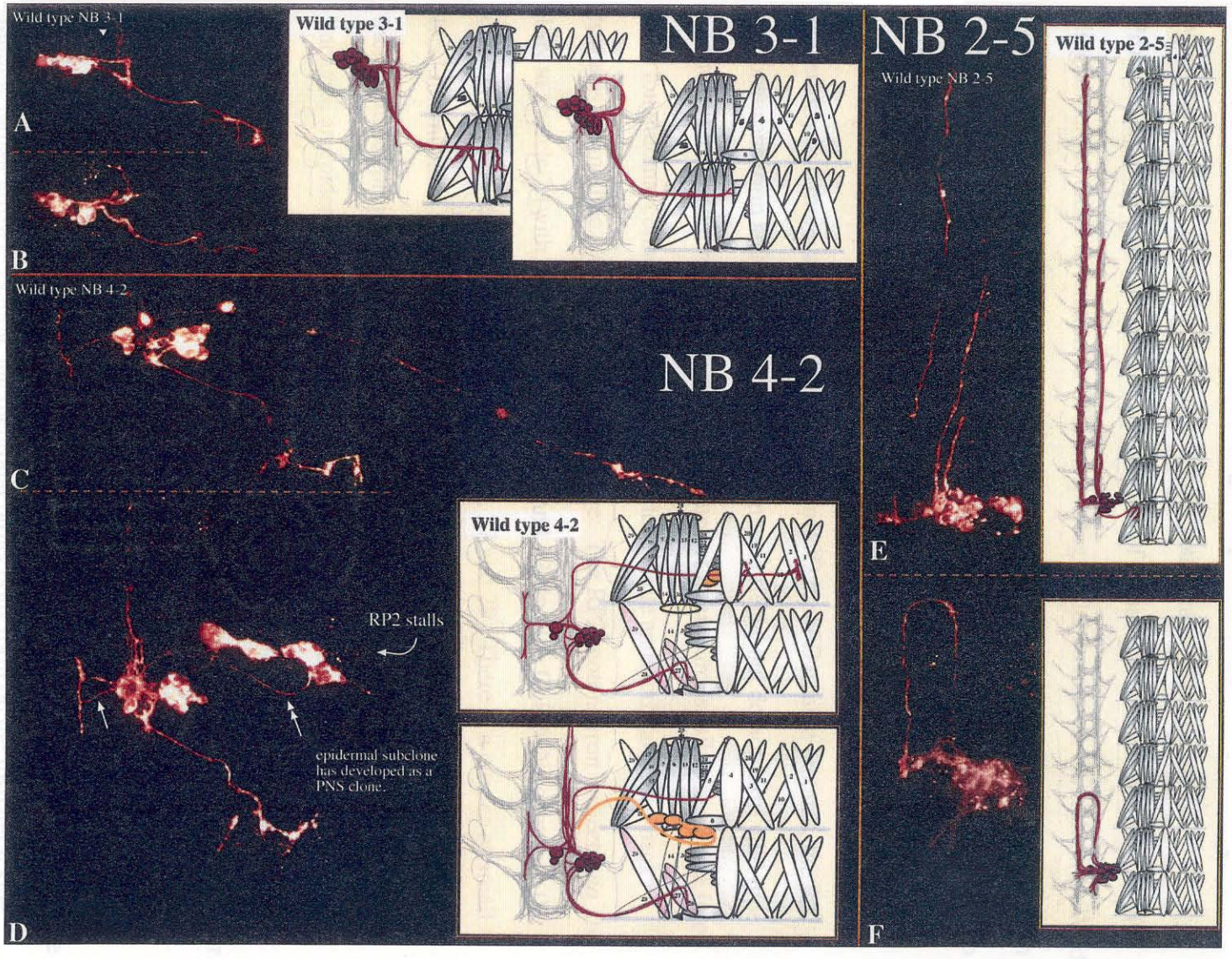
Wild type NB 3-1
A
B
Wild type 3-1
NB 3-1
NB 2-5
Wild type NB 2-5
Wild type 2-5
E
Wild type NB 4-2
NB 4-2
C
Wild type 4-2
RP2 stalls
epidermal subclone has developed as a PNS clone.
D
F

Figure 5. DiI labeled lineages in wild-type and *Ptp10D Ptp69D* mutant embryos. Neurectodermal cells were labeled with single droplets of DiI at embryonic stage 8 and were examined by confocal microscopy at embryonic stage 17 (Experimental Procedures). Each panel consists of a projection of a confocal *z*-series on the left and a diagram of the clone in relation to CNS morphological landmarks on the right. (A) Wild type 3-1 lineage: RPs (1,3,4,5) project across the midline to ISNb, forming endings on ventral muscles 6, 7, 12, 13, 14, 28 and 30 (in the abdomen). Interneuronal axons also cross the midline, and fall into two classes: local interneurons project anteriorly in a medial fascicle of the longitudinal connective, and intersegmental interneurons project posteriorly in a more lateral fascicle. (B) In *Ptp10D Ptp69D* double mutants, the RP motoneurons form and project to their target muscle fields, but do not form wild type endings at individual muscle fibers. Both groups of interneurons fail to segregate into their longitudinal connective pathways and instead circle anteriorly and then back towards the midline. (C) Wild type 4-2 lineage: The RP2 motoneuron projects *via* the ISN to muscle 2 (with branches at muscles 3 and 19) and the CoR MNs comprise the entirety of SNc, sending axons to muscles 26, 27 and 29. There is a cluster of small local interneurons that project across the midline as a tightly fasciculated axon bundle; these neurites project to segmental borders anteriorly and posteriorly. In 25% of 4-2 lineages, an epidermal subclone forms along the RP2 trajectory (yellow cells in diagram). (D) In *Ptp10D Ptp69D* double mutants, RP2 always projects to the ISN, but in 5/6 cases, stalls around muscle 3. The CoRs always form correctly and grow to their appropriate targets, although their synapses have an abnormal appearance. The projection of local interneurons across the midline in the anterior commissure appears wild type, except that the axons always defasciculate into two bundles after crossing the midline (small arrow). Ectopic interneuronal projections form on the ipsilateral side, and project across segmental boundaries in the anterior direction; these axons never form

in the wild type. In the lineage shown here, the epidermal subclone developed as a PNS subclone and sent an axon back towards the CNS (double arrow). (E) Wild type 2-5 lineage: 4-8 intersegmental interneurons send axons anteriorly toward the brain on both the ipsilateral and contralateral sides; these axons are the most substantial fibers in the longitudinal connectives. The lineage also consists of a MN innervating muscles 15, 16 and 17 via ISNd, local interneurons, a segmental nerve glial cell, and a frequent epidermal subclone. (F) In *Ptp10D Ptp69D* double mutants, contralateral intersegmental interneurons project anteriorly for two segments before crossing the midline and turning back towards the segment of origin. Ipsilateral projections begin to extend anteriorly but do not cross segmental boundaries. The motoneuron fails to exit the CNS via its normal ISNd route.

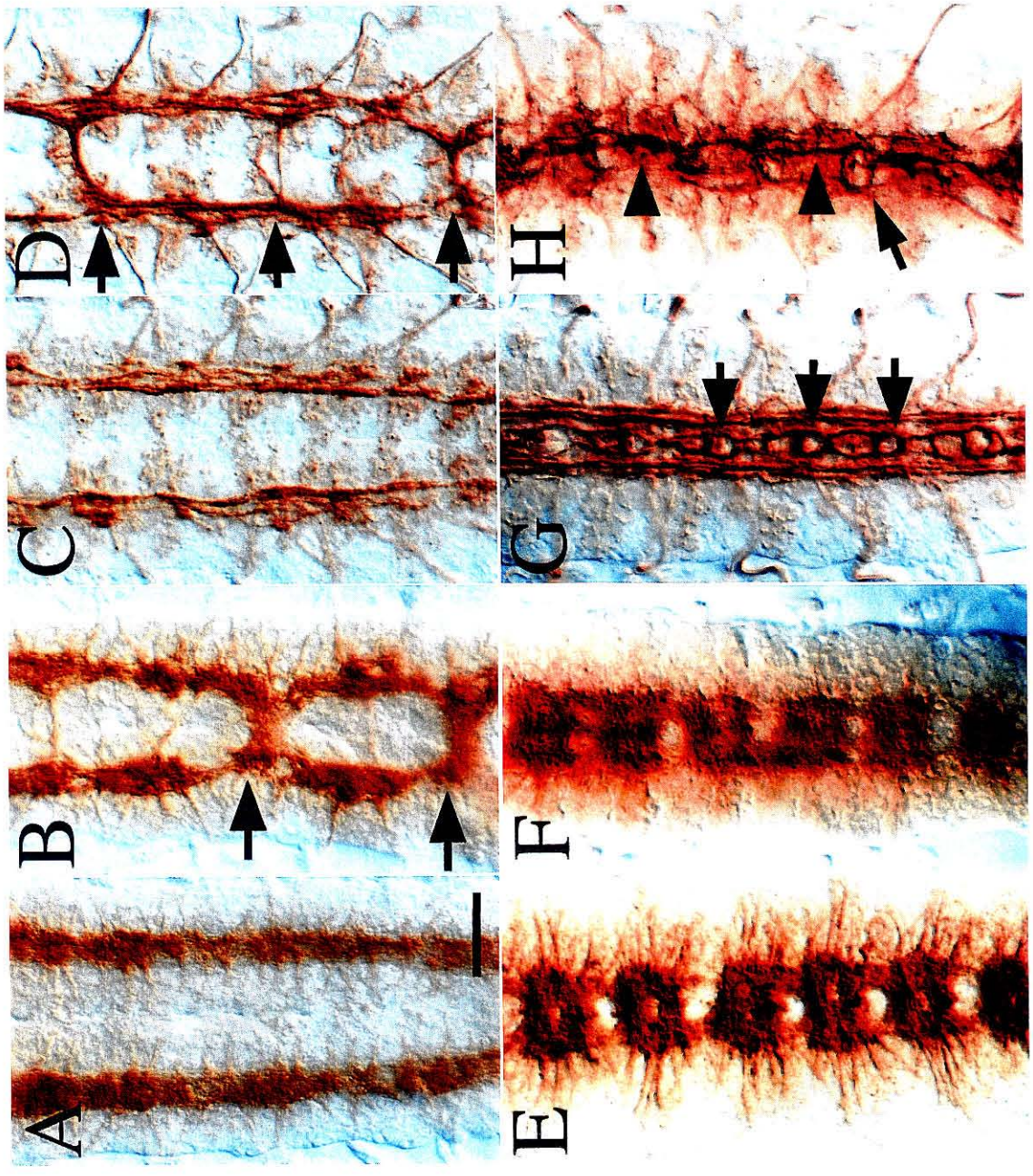
A
B
C
D
E
F
G
H

Figure 6. Genetic interactions between *Ptp10D Ptp69D*, *comm*, and *robo*.
All panels show the CNS in late stage 16 embryos stained with BP102 (A, B, E, F) or 1D4 (C, D, G, H). (A and C) *comm*. There are no commissural axons in the *comm* mutant (compare to Figure 2F). (B and D) *Ptp10D*^{1} ; *comm*^{e39} *Ptp69D*^{1}/ *comm*^{e39} *Df(3L)8ex25*. Commissural tracts are observed in about every other segment, and some of these are as thick as in wild-type (arrows). Also note that the 1D4-positive axons seen in (D) would not normally cross the midline. (E and G) *robo*^{1}. The commissures are broad and partially fused, and longitudinals are reduced (E); the inner 1D4 bundle circles around the midline (G; arrows). (F and H) *Ptp10D*^{1}; *robo*^{1}/*robo*^{1}; *Ptp69D*^{1}/ *Df(3L)8ex25* . The triple mutant phenotype visualized with BP102 (F) is somewhat stronger (more commissure fusion, and thinner longitudinals) than that of the *robo* single mutant (E). The triple mutant phenotype visualized with 1D4 (H) is much stronger than that of *robo* mutants. Many axons fasciculate into a single thick bundle that extends along the midline (arrowheads). Circles around the midline like those in *robo* are still seen in triple mutants (arrow). Scale bar 5 μm.

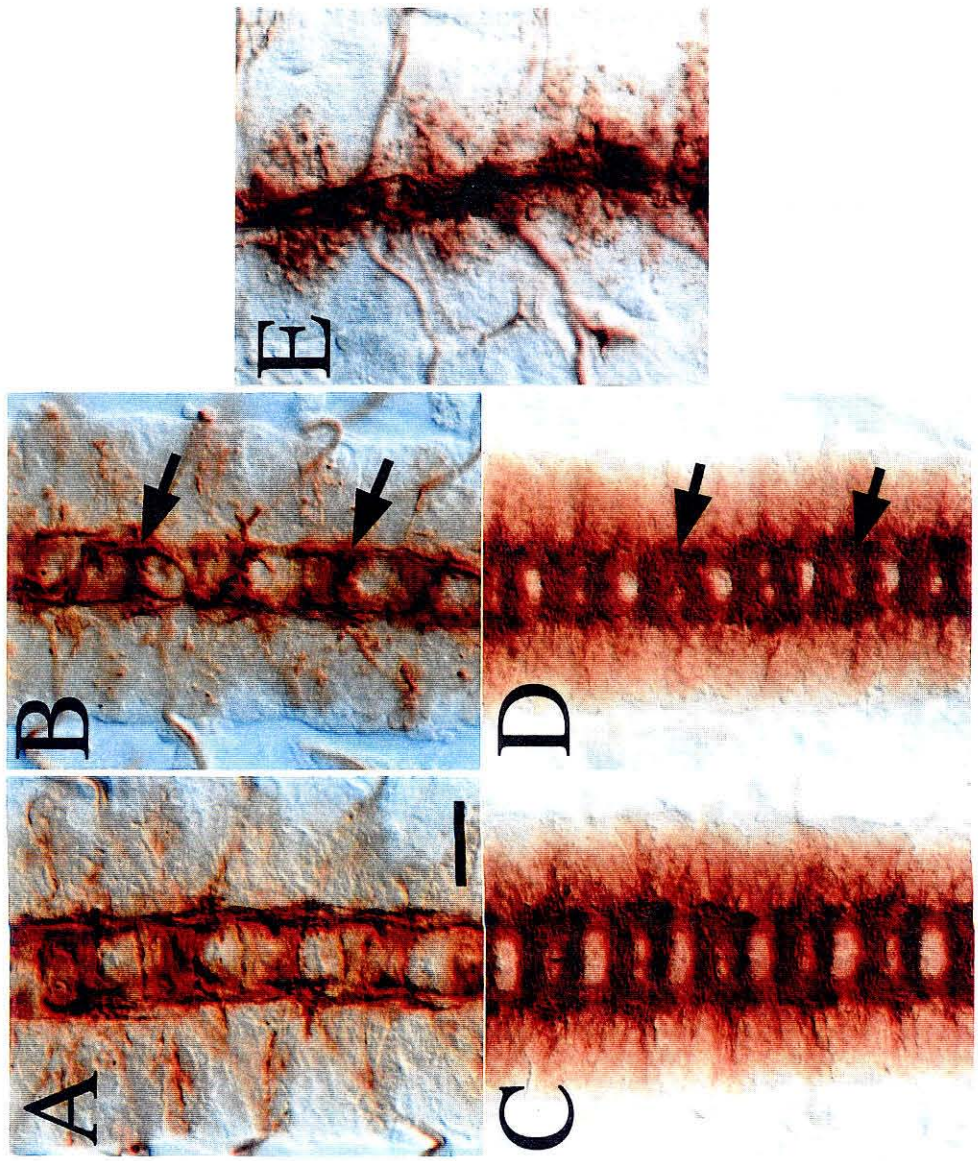
E
B
D
A
C

Figure 7. Genetic interactions between *Ptp10D Ptp69D* and *slit*.

All panels show the CNS in late stage 16 embryos stained with BP102 (C, D) or 1D4 (A, B, E). (A and C) *Ptp10D*^{1} ; *Ptp69D*^{1}*/ Df(3L)8ex25* , (B and D) *Ptp10D*^{1}*; slit*^{2}/+; *Ptp69D*^{1}*/ Df(3L)8ex25* , (E) *slit*^{1}*/slit*^{2}. The CNS becomes narrower, so that the separation between longitudinal tracts is reduced, when one copy of *slit* is removed from *Ptp10D Ptp69D* (compare B to A, and D to C). Bundles crossing the midline become thicker and more irregular (B, arrows), and commissure fusion is increased (D, arrows). Removal of one copy of *slit* from wild-type produces no phenotype. (E) All CNS axons converge on the midline in *slit*^{1}*/slit*^{2} embryos. Scale bar 5μm.

Chapter 3

Interactions between DPTP10D and other receptor tyrosine phosphatases control motoneuron growth cone guidance in the *Drosophila* embryos

Qi Sun and Kai Zinn

ABSTRACT

The neural receptor tyrosine phosphatase DPTP10D is involved in growth cone guidance decisions at multiple choice points in the embryonic neuromuscular system. There are four neural RPTPs. Their roles can only be understood through detailed examination of the phenotypes of all single and multiple *Rptp* mutants. Phenotypic analyses of these mutant combinations show that DPTP10D works together with other RPTPs to promote bifurcation of the SNa nerve and allow the ISNb nerve to separate from the common ISN pathway. DPTP10D, however, has a competitive relationship with the other RPTPs in controlling growth of the ISN past intermediate targets. These results show that the functional relationships among the four neural RPTPs are complex. At individual choice points, RPTPs can have cooperative, collaborative, or antagonistic functions in controlling guidance.

INTRODUCTION

During embryonic development, growth cones, which form the leading edges of neuronal processes, sample the environment and make pathfinding decisions. Contacts between growth cone surface receptors and attractive or repulsive guidance cues on surrounding cells and in the extracellular matrix affect signal transduction cascades within the growth cones. These signaling events change the growth cone's cytoskeleton, altering its morphology and direction of movement. In insect systems, axonal trajectories are often very similar or identical among individuals and among different segments of the same individual. This suggests that these axons reach their targets by interacting with highly localized guidance cues, rather than by following long-range gradients of attractive or repulsive molecules.

One signaling mechanism by which growth cones respond to guidance factors is the control of tyrosine phosphorylation. Phosphotyrosine is enriched in filopodia, the highly motile extensions that emanate from growth cones and probe the surrounding landscape (Wu and Goldberg, 1993). Pharmacological inhibition of tyrosine kinase activity can alter axonal pathfinding *in vivo* (Menon and Zinn, 1998; Worley and Holt, 1996).

Phosphotyrosine levels within the growth cone are regulated by engagement of surface receptors. These include the Eph and Derailed receptor tyrosine kinases, as well as neural adhesion molecules that interact with cytoplasmic tyrosine kinases. Another class of neuronal growth cone receptors that control tyrosine phosphorylation are receptor tyrosine phosphatases (RPTPs). RPTPs often have extracellular regions consisting of immunoglobulin-like (Ig) and/or fibronectin type III (FN3) domains. These are linked *via* a single transmembrane domain to a cytoplasmic region containing

one or two phosphatase domains. In *Drosophila*, five such RPTPs have been identified. Strikingly, four of these five (DLAR, DPTP10D, DPTP69D, and DPTP99A) are expressed only on central nervous system (CNS) axons in the embryo. RPTPs are also localized to axons and growth cones in vertebrate systems (Ledig et al., 1999; Stoker and Dutta, 1998).

Genetic studies in *Drosophila* have shown that three of the neural RPTPs are important regulators of motor axon guidance decisions. In the fly embryo, the 30 body wall muscle fibers in each abdominal hemisegment are innervated by about 40 motoneurons in a highly stereotyped manner (for review see Keshishian et al., 96). *Dlar* and *Ptp69D* mutations perturb specific guidance decisions made by axons of the ISNb and ISNd (also known as SNb and SNd) motor nerves (Desai et al., 1996; Krueger et al., 1996). *Ptp99A* mutations have no phenotypes on their own, but modify the phenotypes of *Dlar* and *Ptp69D* mutations (Desai et al., 1996; Desai et al., 1997; Hamilton et al., 1995). Analysis of double and triple mutant combinations showed that several of the guidance decisions made by ISN, ISNb, and ISNd axons are dependent on RPTP function. In the absence of all three RPTPs, the ISN is unable to progress beyond intermediate targets, the ISNd is missing, and the ISNb is unable to enter its target ventrolateral muscle (VLM) field. These studies also showed that the relationships between the RPTPs are not always cooperative; DLAR and DPTP99A have opposing functions in controlling ISNb entry into the muscle field (Desai et al., 1997).

In the larva, DPTP69D regulates innervation of the lamina of the optic lobe by photoreceptor neurons. When DPTP69D is not expressed on the photoreceptor (R) axons, the growth cones of R1-6 photoreceptors fail to stop at their lamina targets and continue into the medulla, which is the normal target for R7 and R8 photoreceptors. Phosphatase activity and extracellular domain sequences are both required for DPTP69D function in lamina targeting (Garrity et al., 1999).

What mechanisms are involved in regulation of growth cone guidance decisions by the RPTPs, and why does each of the individual RPTPs control only a specific subset of decisions, given that all of the RPTPs are expressed on every motor axon? It is attractive to speculate that RPTP activity or localization within the growth cone is regulated by engagement of RPTP ligands localized to specific cells along the pathways of the motor nerves. Unfortunately, however, *in vivo* ligands for RPTPs have not yet been identified in any system, although LAR can interact with a laminin-nidogen complex (O'Grady et al., 1998) and RPTPβ/ζ binds to the neural adhesion molecule contactin (Peles et al., 1995).

The signaling pathways downstream of RPTPs are also poorly understood. It has recently been shown, however, that entry into the VLM field is controlled by antagonistic interactions between DLAR and the ABL tyrosine kinase. Removing one copy of the *Abl* gene suppresses the VLM bypass phenotype conferred by *Dlar* mutations, and ABL overexpression produces bypass phenotypes (Wills et al., 1999). These data, together with the observation that removing DPTP99A function also suppresses the *Dlar* bypass phenotype (Desai et al., 1997), suggest that DLAR permits entry of ISNb axons into the VLM field by downregulating signaling by ABL and DPTP99A. ABL and its substrate ENA also bind directly to the D2 domain of DLAR and can serve as substrates for DLAR *in vitro* (Wills et al., 1999).

In this paper, we show that the fourth neural RPTP, DPTP10D, also regulates motor axon guidance and optic lobe innervation. DPTP10D has both cooperative and competitive interactions with the other RPTPs in controlling growth cone guidance along the motor pathways. Analysis of *Ptp10D* mutations also shows that the RPTPs are central to axon guidance within the CNS. This had not been apparent before now because *Dlar*, *Ptp69D*, and *Ptp99A* mutations do not have strong CNS phenotypes alone or in combination. In another paper, we demonstrated that DPTP10D and DPTP69D

cooperate in regulating axon guidance across the midline of the embryo. The *Ptp10D/Ptp69D* mutant combination interacts with *roundabout (robo)*, *commissureless (comm)*, and *slit*, a set of mutations defining a repulsive pathway that prevents longitudinal axons from crossing the midline (Sun et al., 99; for review see Zinn and Sun, 99). Here we further define the roles of all four neural RPTPs in CNS axon guidance by analyzing the phenotypes of triple and quadruple mutants.

MATERIALS AND METHODS

All the alleles used in this study were previously described. To get comparable results, we used the same *Rptp* alleles in different mutant combinations. For *ptp10D*, we used *ptp10D*^{1}. For *ptp69D*, we used *ptp69D1*/Df(3L)^{8ex25}. For *dlar*, *dlar5.5/dlar13.2* was used. For *ptp99A*, *ptp99A*^{1}/Df(3R)^{R3} was used. Because all the alleles used in this study except *ptp10D*^{1} are homozygous lethal, embryos were collected from crosses between heterozygous flies. Mutant embryos were identified based on absence of staining with monoclonal antibodies (mAbs) specific for each RPTP. The mAbs used for each RPTP are: 45E10, 3F11, 3A6 and 8C9 for PTP10D, PTP69D, PTP99A and DLAR respectively (Desai et al., 1994; Tian et al., 1991; B. Burkemper and K. Zinn, unpublished). The mutant embryos were then restained with either MAb 1D4 or BP102, and dissected. Whole mount antibody staining of fly embryos and larval eye discs was performed as described (Patel, 1994; Van Vactor et al., 1991).

RESULTS

DPTP10D regulates fasciculation of photoreceptor axons

We and others have previously described embryonic motor axon guidance phenotypes conferred by single, double, and triple mutations in three neural RPTP genes: *Ptp69D*, *Ptp99A*, and *Dlar* (Desai et al., 1996; Desai et al., 1997; Krueger et al., 1996). The fourth neural RPTP, DPTP10D, is also selectively expressed on CNS axons in the embryo (Tian et al., 1991; Yang et al., 1991). *Ptp10D* null mutants are viable and fertile and have no detectable embryonic phenotypes. *Ptp10D Ptp69D* double mutant embryos, however, display a unique CNS phenotype in which axon guidance at the midline and within the longitudinal tracts is radically altered (Sun et al., 99).

Although *Ptp69D* single mutants have weak embryonic motor axon phenotypes (Desai et al., 1997), they display a strong phenotype during larval optic lobe development. In these mutants, R1-6 axons fail to stop in the lamina and grow through it into the medulla (Garrity et al., 1999). To evaluate whether DPTP10D might also be involved in optic lobe innervation, we first examined expression of the protein in third instar larval brain/eye-antennal disc complexes. As shown in Fig. 1A, DPTP10D is expressed on photoreceptor axons, but is not localized to specific axon pathways within the brain.

We visualized photoreceptor axons in wild-type and *Ptp10D* mutant larvae by staining with the R-cell specific mAb 24B10 (Zipursky et al., 84). In homozygous *ptp10D*^{1}, we observed a variable phenotype in which R1-6 axons do not spread out normally within the lamina layer, but remain fasciculated into clumps (Fig. 1C). This abnormal fasciculation produces gaps within the lamina, The R axon fasciculation phenotype is rather weak, and only 20% of brain hemispheres displayed phenotypes as strong as that shown in Fig. 1C. These data indicate that DPTP10D has a role in regulating fasciculation of R1-6 axons, but in the absence of this RPTP these axons can still usually separate and spread out normally within the lamina.

Removal of DPTP10D reveals roles for all four neural RPTPs in control of CNS axon guidance

To study the roles of DPTP10D in regulating axon guidance in the embryo, we generated and analyzed double, triple, and quadruple mutant embryos lacking DPTP10D and one or more of the other three neural RPTPs. For *Ptp69D*, *Ptp99A*, and *Dlar*, we used null transheterozygous mutant combinations previously employed by Desai et al., 97 to define the roles of these three RPTPs in motor axon guidance (see Materials and Methods for details). For DPTP10D, we used the null allele $Ptp10D^{1}$, which is homozygous viable and fertile and affects only the DPTP10D gene (Sun et al., 99).

All four neural RPTP proteins appear to be expressed on most or all embryonic CNS axons, beginning at the earliest stages of axon outgrowth. An individual RPTP, however, might be most important for axon guidance in a specific set of neurons, since each mRNA is expressed at highest levels in a different subset of CNS cells (Tian et al., 91; Yang et al., 91; Hariharan et al., 91; Desai et al., 94). To examine CNS axon guidance in *Rptp* mutant embryos, and in particular to determine whether longitudinal axons abnormally cross the midline, we stained embryos with mAb 1D4, which recognizes three longitudinal bundles in late stage 16 and early stage 17 embryos (Van Vactor et al., 1993). There is little commissural 1D4 staining at these stages (Fig. 2A).

With the exception of *Ptp10D Ptp69D* embryos, single or double mutants lacking any of the RPTPs display no CNS abnormalities visible by 1D4 staining (Sun 99). Remarkably, triple mutants lacking DPTP69D, DPTP99A, and DLAR, although they have very severe motor axon defects (Desai et al., 1997), also do not display strong CNS phenotypes that are detectable with this marker. Like wild-type embryos, they have three distinct longitudinal 1D4-positive bundles and little commissural staining. The outer bundle, however, is usually discontinuous in this genotype (Fig. 2B). Thus,

the CNS axon array can develop in a relatively normal manner when only one neural RPTP, DPTP10D, is expressed.

To examine in detail how DPTP10D contributes to CNS axon guidance, we analyzed the phenotypes of all triple mutant genotypes. When DPTP10D, DLAR, and DPTP99A are all absent, a relatively weak CNS phenotype is observed in which there are occasional fusions of longitudinal bundles, and extra axons cross the midline in one or a few segments of each embryo (Fig. 2C). Removal of DPTP10D, DPTP69D, and DPTP99A produces a phenotype similar to, but more severe than, that of *Ptp10D Ptp69D* (Sun et al., 99), in which the three longitudinal bundles are fused into one and many extra axons cross the midline (Fig. 2D). Thus, removal of DPTP99A strengthens the basic phenotype produced by the absence of DPTP10D and DPTP69D.

The *Ptp10D Dlar Ptp69D* triple mutant also has a strong phenotype involving ectopic midline crossing and longitudinal bundle fusion (Fig. 2E). It differs from the *Ptp10D Ptp69D Ptp99A* phenotype, however, in that the axons that abnormally cross the midline in these embryos often grow diagonally to the other side without respecting the normal borders of the anterior and posterior commissures. In many cases, all of the 1D4-positive connective axons appear to be rerouted across the midline, producing complete connective breaks (Fig. 2E, arrow).

Finally, when all four RPTPs are absent, a very severe CNS phenotype is observed in which most of the 1D4-stained axons are switched from longitudinal to commissural pathways. Longitudinal bundles are almost absent, and several distinct 1D4-positive fascicles cross the midline in each segment. These ectopic bundles do not respect the normal borders of the commissures (Fig. 2F; see also Sun et al., 99).

We also examined mutant embryos with mAb BP102, which stains all CNS axons. In wild-type late stage 16 embryos (Fig. 2G), clearly separated anterior and

posterior commissures are visible in each segment. These are somewhat thinner than the longitudinal tracts at this stage. In *Ptp10D Ptp69D* embryos the commissures are thicker, but are always still separated by a region lacking axons (Fig. 2H; Sun et al., 99). In quadruple mutants, however, the commissures are fused together, so that a single wide tract crosses the embryos in each segment. The longitudinal tracts appear to be somewhat depleted of axons (Fig. 2I).

The Roundabout (Robo) receptor, which controls midline crossing, is restricted to longitudinal tracts in late embryos as a result of its downregulation on the commissural tracts through the action of Commissureless (Comm) protein (Kidd et al., 1998). Interestingly, two of the RPTPs implicated in midline crossing have a similar expression pattern. While at early stages they are expressed on all axons, by late stage 16 DPTP10D and DLAR are selectively localized to the longitudinal tracts and almost absent from commissures (Figs. 2J-K; compare to Fig. 2G). This localization is not Comm-dependent, because high-level expression of Comm by all CNS neurons, which greatly decreases Robo expression, does not affect expression of these RPTPs (data not shown). DPTP69D and DPTP99A are never selectively localized to longitudinal tracts. Their expression pattern always resembles that of the mAb BP102 epitope(s) (Fig. 2G).

In summary, our phenotypic analysis of *Rptp* mutants indicates that DPTP10D has a primary role in regulating guidance of longitudinal axons in the CNS, because expression of this RPTP alone is sufficient for relatively normal development of 1D4-positive longitudinal pathways. When DPTP10D is absent, however, removal of DPTP69D, but not of DLAR or DPTP99A, generates a strong phenotype in which ectopic axons cross the midline (Sun et al., 99). If DPTP10D and DPTP69D are both lacking, removal of DLAR, but not of DPTP99A, causes axons to lose the ability to recognize commissural borders. Finally, removal of DPTP99A from a genotype lacking the other three RPTPs generates a phenotype in which most or all 1D4-positive

longitudinal axons now grow across the midline without respecting the normal boundaries of the commissures.

Loss of DPTP10D function partially suppresses the ISN truncation phenotypes of *Dlar Ptp69D Ptp99A* triple mutants.

As described by Desai et al. (Desai et al., 1997), the ISN passes two major lateral branchpoints, denoted FB and SB, before reaching its termination point (T) at the proximal edge of muscle 1 (Figs. 3A-B). In *Dlar Ptp69D* double mutants, about 50% of ISNs terminate at the SB position (SB phenotype; Fig. 3D, purple bars in Figs. 3F-N). The remainder of ISNs either terminate before reaching T (SB+ phenotype; Fig. 3C), or make an abnormally small terminal arbor (all axons passing SB (SB+ and T) are indicated in one bicolored blue bar, labeled 2+, in Figs. 3F-N). In *Dlar Ptp69D Ptp99A* triple mutants, about 50% of ISNs terminate at the FB position (FB phenotype; Fig. 3E, red bars in Figs. 3F-N), and most of the remainder stop at SB.

These earlier results indicated that: 1) DLAR is central to ISN guidance, because ISN truncations are seldom observed in any genotype in which *Dlar* is wild-type; 2) a hierarchy of RPTPs may control ISN progression past branchpoints. Expression of any of the three RPTPs DLAR, DPTP69D, or DPTP99A is sufficient to allow growth past FB, while expression of DLAR or DPTP69D, but not of DPTP99A, is sufficient for growth past SB. Expression of DLAR is uniquely required for formation of a normal terminal arbor (Desai et al., 1997).

To examine the roles of DPTP10D in ISN guidance, we analyzed the phenotypes of *Ptp10D* mutations combined with other *Rptp* mutations in all possible double, triple, and quadruple mutant combinations. None of these combinations produce muscle or peripheral nervous system (PNS) abnormalities (data not shown), consistent with the

observation that no expression of any of the four RPTPs can be detected on muscles or sensory neurons (Desai et al., 1996; Krueger et al., 1996; Fig. 4B).

Our analysis shows that the absence of DPTP10D function does not adversely affect ISN guidance, because the phenotypes of *Rptp* mutant combinations are not significantly strengthened by removing DPTP10D. First, multiply mutant genotypes that do not include mutant *Dlar* have weak ISN phenotypes whether or not *Ptp10D* is mutant. For example, <10% of ISNs prematurely terminate (3% SB, 6% SB+) in *Ptp10D Ptp69D Ptp99A* triple mutants (Fig. 3N). Second, the phenotypes of embryos in which *Dlar* is mutant are not worsened by inclusion of mutant *Ptp10D*. For example, 75% of ISNs prematurely terminate in *Dlar Ptp69D* (27% SB+, 45% SB), and 78% in *Ptp10D Dlar Ptp69D* (38% SB+, 38% SB; Figs. 3F-G, Table 1). 65% of ISNs prematurely terminate in *Dlar Ptp99A* (39% SB+, 21+ SB; Desai et al., 97), and 52% in *Ptp10D Dlar Ptp99A* (30% SB+, 21% SB; Fig. 3M, Table 1).

DPTP10D actually functions in opposition to the other RPTPs in regulating ISN growth past the FB and SB branchpoints. This is shown most clearly by a comparison of the phenotypes of *Dlar Ptp69D Ptp99A* triple mutants and *Ptp10D Dlar Ptp69D Ptp99A* quadruple mutants. In the triple mutant embryos, 52% of ISNs stop at FB, and only 11% grow past SB. In quadruple mutants, however, 15% of ISNs stop at FB and 31% extend beyond SB (Fig. 3H-I, Table 1). Thus, the distribution of ISN lengths is shifted toward wild-type by removal of DPTP10D function from a triple mutant. This result is formally similar to, but less dramatic than, our earlier finding that removal of DPTP99A function suppresses the ISNb parallel bypass phenotype of *Dlar* (31% partial or complete parallel bypass in *Dlar vs.* 1% in *Dlar Ptp99A*; Desai et al., 97).

DPTP10D regulates bifurcation of the SNa nerve

The SNa nerve has a characteristic bifurcated morphology. The bifurcation occurs at a specific choice point located between muscles 22 and 23. The posterior (or lateral) branch of SNa innervates muscles 5 and 8, and the dorsal (or anterior) branch innervates muscles 21-24 (Figs. 4A, C; N (normal) SNa phenotype indicated by green bars in Figs. 4H-N). SNa development is unaffected in all single *Rptp* mutants.

When we examined *Ptp10D Ptp69D* double mutant embryos, we observed that in >40% of hemisegments SNa fails to bifurcate. The mutant SNa nerves either stall at the bifurcation point, or, more commonly, have only one branch extending beyond this point (B phenotype; Figs. 4D, E, purple bar in Fig. 4M; Table 2). We have not observed any correlation between genotype and the identity of the missing branch; either the posterior or dorsal branch is absent with approximately equal frequency in all genotypes in which the B phenotype is observed. In most cases the remaining branch appears to target the correct muscles, suggesting that it contains its normal complement of SNa axons. Since there are no markers that label subsets of SNa axons, we do not know whether the axons that would normally form the missing branch stalled before the bifurcation point or bypassed their targets by following the remaining branch. It is interesting that the only motor axon phenotype observed in any double mutant lacking DPTP10D is the SNa bifurcation phenotype, because DPTP10D is expressed at higher levels on SNa axons and growth cones than on other motor pathways (Fig. 4B).

Analysis of all double, triple and quadruple mutant phenotypes shows that SNa bifurcation exhibits a complex dependence on RPTP function. Bifurcation failures (B phenotype) are observed at a lower frequency (25%) in another double mutant genotype, *Dlar Ptp69D* , but are not seen in *Ptp10D Dlar* . Removing one of the two remaining RPTPs from *Ptp10D Dlar*, however, now causes 46-58% of SNa nerves to fail to bifurcate (Figs. 4H-N). These data indicate that all four of the RPTPs can facilitate SNa bifurcation (see Discussion).

All four RPTPs are also involved in facilitation of SNa outgrowth to the bifurcation point. In quadruple mutant embryos, 55% of SNa nerves either do not reach the bifurcation point at all or are very thin and wandering (ST (short/thin) phenotype; Figs. 4F,G, red bar in Fig. 4L; Table 2). These phenotypes suggest that some SNa axons may not enter the nerve at all, and that the remaining axons are impaired in their outgrowth.

Defective SNa outgrowth (ST phenotype) is not observed in any double mutant, and is also very rare in any triple mutant in which *Dlar* or *Ptp69D* are wild-type (Figs. 4H, J, M, N). If *Dlar* and *Ptp69D* are both mutant, removal of DPTP99A or DPTP10D results in defective outgrowth of about 40% of SNa nerves, and removal of both produces the 55% penetrance seen in the quadruple mutant (Figs. 4I,K,L,N; Table 2). Thus, expression of DLAR alone, DPTP69D alone, or DPTP10D *plus* DPTP99A is sufficient to allow outgrowth of SNa axons to the bifurcation point in >95% of hemisegments. It is important to emphasize that we do not know that the same axons are always affected when a thin SNa morphology is observed using mAb 1D4. It is possible that a different subset of SNa axons fails to extend in different *Rptp* genotypes, but this cannot be analyzed at present because of the lack of antibody markers that can distinguish between these axons.

DPTP10D acts together with the other three RPTPs to facilitate ISNb defasciculation at the exit junction

The axons of the ISNb (SNb) nerve innervate the ventrolateral muscles (VLMs). ISNb growth cones extend out the ISN root and defasciculate from the common ISN pathway at the exit junction (EJ; Figs. 5A, F, G). ISNd (SNd) axons also leave the ISN at the exit junction, and follow the pathway laid down by the earlier ISNb axons

until they reach a nearby second junction where ISNd separates from ISNb (Figs. 5A, G). In *Dlar* embryos (and in all mutant combinations in which *Dlar* is mutant), ISNd is almost always missing (Krueger et al., 1996). Since they cannot be visualized separately from ISN and ISNb axons, it is unknown whether mutant ISNd axons follow one of the other ISN branches or fail to even reach the exit junction.

Our previous results showed that DLAR, DPTP69D, and DPTP99A are all involved in ISNb navigation at the exit junction (Desai et al., 97). In triple mutant embryos lacking all three of these RPTPs, about 30% of ISNb nerves fail to leave the ISN at the exit junction and continue to grow out along the common ISN pathway (bypass phenotype). In most of these bypass hemisegments, only one ISN branch is visible, and it is usually thicker than normal (Figs. 5B, H). We interpret this "fusion bypass" (FB) phenotype as indicating that the ISNb axons grew out along the common ISN pathway.

In quadruple mutant embryos, the frequency of bypass phenotypes is increased to 76%, indicating that DPTP10D also contributes to the decision of ISNb axons to leave at the exit junction (bicolored red/gold BP bar in Fig. 5L; Table 3). [Note that in some triple and quadruple mutant hemisegments (17% in the quadruple mutant collection; red bar section in Fig. 5L; Table 3) a small gap between the ISN and ISNb bundles is visible at the exit junction, but the bundles fuse together again after a short distance. We think that these also represent failures of the ISNb to leave correctly at the exit junction, since the axons quickly return to the ISN. Nevertheless, lacking a quantitative way to distinguish them from the "parallel bypass" (PB) phenotype seen in *Dlar* embryos, we have also classified these as PB. In *Dlar* embryos, however, bypassing ISNb axons usually grow out all the way past the VLMs as a separate pathway before returning to the ISN (Krueger et al., 1996, Desai et al., 1997; see

diagram in Fig. 5J), suggesting that they have successfully left the ISN and then made a separate decision to bypass the VLM field.]

In the remaining 24% of quadruple mutant hemisegments, some or all ISNb axons appear to leave the ISN but immediately stall (Figs. 5C, I), or extend short abnormal branches (Figs. 5D-E show two focal planes of a hemisegment in which a small branch grew out on the wrong (internal) face of the muscles). No axons are ever observed to enter the VLM field. We have classified all such hemisegments as S (stall) phenotypes (purple bar in Fig. 5J). Accurate classification of ISNb phenotypes in quadruple mutants is difficult, however, because axonal morphologies around the exit junction are very distorted and it is impossible to determine whether short projections from the ISN actually contain ISNb axons.

Phenotypic analysis of double and triple mutants suggests that DPTP10D does not contribute strongly to the other decisions made by ISNb axons (entry into the VLM field, navigation among the VLMs, and synaptogenesis). Removal of DPTP10D function does not enhance or suppress *Dlar* or *Ptp69D* single mutant phenotypes (data not shown). Combining the *Ptp10D* mutation with *Dlar Ptp69D* or with *Ptp69D Ptp99A* produces small increases in the frequencies of stall (S) phenotypes (Figs. 5K, M, O; Table 3; Desai et al., 1997).

DISCUSSION

Four of the five known *Drosophila* RPTPs, denoted DLAR, DPTP69D, DPTP99A, and DPTP10D, are selectively expressed on CNS axons. Three of these neural RPTPs have already been shown to control motor axon guidance and optic lobe innervation. The work described here shows that the fourth RPTP, DPTP10D, is also involved in regulation of specific guidance events in embryos and larvae.

RPTPs have very complex roles in controlling growth cone navigation. Each pathfinding decision that we have studied requires expression of at least one RPTP for its proper execution, but each has a different dependence on the functions of individual RPTPs. Most embryonic decisions are unaffected by mutations in any single *Rptp* gene, so it has been necessary to analyze double, triple, and quadruple mutant combinations in order to define how the RPTPs facilitate pathfinding. This analysis has shown that, for most decisions, the RPTPs have partially redundant (overlapping) activities. For example, extension of the ISN past the first branchpoint requires expression of either DLAR, DPTP69D, or DPTP99A (Desai et al., 1997). In other cases, two RPTPs have "collaborative" relationships. For example, outgrowth of the SNa nerve to its bifurcation point, or of the ISNb nerve to the muscle entry site, can be facilitated by DLAR or DPTP69D, but not by DPTP10D or DPTP99A. DPTP10D *plus* DPTP99A can allow normal outgrowth, however (Figs. 4,5). Finally, for three decisions the RPTPs display antagonistic interactions. Entry of the ISNb into the VLM field is regulated by competition between DLAR and DPTP99A (Desai et al., 97), while DPTP10D has an antagonistic relationship with the other RPTPs in controlling ISN extension past the first (FB) and second (SB) lateral branchpoints (Fig. 3).

Ptp10D null mutants are viable and fertile. The only phenotype we have been able to define thus far in single mutants is a defect in defasciculation of R1-6 photoreceptor axons in the lamina. In the absence of DPTP10D, R1-6 axons sometimes do not separate normally to form an even distribution of synapses among the columns of lamina neurons. Instead, the R1-6 terminals remain clumped together in an uneven array (Fig. 1). These data suggest that DPTP10D activity facilitates separation of R1-6 growth cones from each other when they reach their targets.

RPTPs and the logic of axon guidance decisions.

To describe more clearly how DPTP10D and the other RPTPs control motor and CNS axon guidance decisions, we use a different format in which, rather than discussing the penetrance of the defects produced by mutant combinations, we begin by asking what percent of axons can execute the first decision along a pathway in a quadruple mutant lacking any neural RPTP function. We then "add back" each RPTP and calculate what percent of the axons can now make the correct decision. For subsequent decisions along the pathway, we consider only the subpopulation of quadruple mutant nerves for which the previous decision was made normally, and then ask how adding back RPTPs influences the ability to make the next decision. "Flow charts" of this process are shown in Fig. 6.

We first discuss progression of the ISN past the FB and SB branchpoints. In a quadruple mutant, 84% of ISNs extend past FB. Adding back DLAR, DPTP69D, or DPTP99A increases this percentage to >95%, but adding back DPTP10D *decreases* the percentage of correct decisions to 48%. Adding one of the other three RPTPs to the triple mutant background expressing DPTP10D restores the ability to extend past FB in >95% of cases (Fig. 6A). For progression past SB, DLAR, DPTP69D, and DPTP99A now differ in their abilities to facilitate the correct decision. DLAR completely rescues (from 37% to >95%), while DPTP99A is relatively ineffective (to 60%), and DPTP69D is intermediate (79%). Again, adding DPTP10D decreases the percentage of successful extension, to 23%. When DLAR, DPTP69D, or DPTP99A are added to the triple mutant in which DPTP10D is expressed, their relative effectiveness at restoring growth past SB is the same as for addition to the quadruple mutant. These data suggest a competitive relationship between DPTP10D and the other RPTPs, especially DPTP99A; in the *Dlar Ptp69D Ptp99A* triple mutant, there is excess DPTP10D activity (in a formal genetic sense), and this favors truncation at FB or SB. When DPTP10D is removed,

the percentage of successful extension is increased at both branchpoints. The results also refine the model proposed in Desai et al. 97, in which DLAR or DPTP69D or DPTP99A are sufficient for extension past FB but only DLAR or DPTP69D can facilitate extension past SB. Here we see that extension past SB can be facilitated to some extent by any of the three, but there is a hierarchy of effectiveness, with DLAR fully restoring the normal decision and DPTP99A being relatively ineffective.

For SNa guidance, the flow charts reveal a different and more complex dependence on RPTP function. Extension to the bifurcation point can be completely restored by adding DLAR or DPTP69D to the quadruple mutant (45%-->95%), but only partially restored by DPTP10D or DPTP99A (to 60%; Fig. 6C). Addition of both DPTP10D and DPTP99A restores extension to >95%, however. Bifurcation into dorsal and posterior branches almost never occurs in a quadruple mutant (1%); it can be partially restored by DLAR or DPTP69D (to 53%), but DPTP10D is less effective (20%) and DPTP99A is ineffective (7%). DPTP99A also cannot restore the correct decision when added to triple mutants expressing only DLAR (53%-->57%). However, DPTP99A is quite effective when added to triple mutants expressing DPTP10D (20%-->75%) or DPTP69D (53%-->96%; Fig. 6D). These results suggest a "collaborative" relationship at this decision point between DPTP99A and DPTP10D, and to a lesser extent between DPTP99A and DPTP69D. DPTP99A cannot facilitate SNa bifurcation when expressed in the absence of DPTP69D and DPTP10D, but if one of these other RPTPs is expressed, DPTP99A can now collaborate with it to allow the nerve to bifurcate normally.

ISNb defasciculation from the common ISN pathway at the exit junction can be facilitated by expression of any of the four RPTPs, but DPTP69D, DLAR, and DPTP99A are more effective than DPTP10D (41%-->95% for the first three *vs.* 79% for DPTP10D; Fig. 6E). Extension of the ISNb from the exit junction to the muscle

entry site is more complex. ISNd axons normally separate from the ISNb shortly after it leaves the ISN, but it is likely that these axons are not yet present during the time at which ISNb is pioneering this section of its pathway. Thus, the ISNb "stall" phenotype is probably produced by a failure of ISNb extension rather than by a failure to separate from ISNd axons. A further piece of evidence supporting this is that ISNd fails to separate from ISNb (or does not extend at all) in *Dlar* single mutants (Krueger et al., 96), but ISNb does not stall in this genotype (Desai et al., 97). The ISNb never successfully enters the VLMs in quadruple mutants (that is, all quadruple mutant ISNbs that manage to defasciculate from the ISN stall before the muscle entry site). DPTP69D, and to a lesser extent DLAR, can restore successful entry into the muscle field (0%-->89% and 71%, respectively). DPTP10D and DPTP99A, however, are quite ineffective (to 11% and 18%, respectively). Interestingly, however, when one of this pair of RPTPs is present, addition of the other can now effectively restore extension (to 72%; Fig. 6F). These results, like those described above for SNa, suggest a collaborative relationship between DPTP10D and DPTP99A in which the two RPTPs can only function as a pair at this decision point.

Finally, we can also construct a qualitative flow chart for CNS axon guidance, although we cannot describe CNS guidance data in a quantitative manner because individual hemisegments cannot be considered independently. In the absence of all four neural RPTPs, all 1D4-positive longitudinal pathways become commissural and cross the midline at random positions. Adding back DPTP99A restores a longitudinal bundle on each side. The axons that abnormally cross the midline still do not respect the normal borders of the commissural tracts. Adding back DLAR to the resulting triple mutant (*Ptp10D Dlar PTP69D*) now rescues the ability to recognize commissural borders, because the axons that cross now do so within established commissural tracts. Finally, adding back DPTP10D or DPTP69D to create a single mutant restores the CNS to a

wild-type morphology, in which there are three distinct longitudinal bundles and no 1D4 axons crossing the midline. This wild-type morphology can also be restored by adding only DPTP10D to the quadruple mutant; when stained with 1D4, the resulting *Dlar Ptp69D Ptp99A* triple mutant differs from wild-type only in that the outer longitudinal bundle is discontinuous (Fig. 2).

The molecular mechanisms involved in these three types of relationships (partially redundant, collaborative, and competitive) among the RPTPs are unknown. One possibility that could explain both collaboration and competition is formation of RPTP heterodimers. For example, if a DPTP10D/DPTP99A heterodimer could function at a particular choice point but the DPTP10D and DPTP99A monomers were inactive in signaling, one could explain a genetic requirement for DPTP10D *plus* DPTP99A in facilitating guidance at this choice point.

Competition could be mediated by formation of inactive RPTP heterodimers from active monomers. For example, DLAR might suppress DPTP99A activity at the muscle entry site by forming a heterodimer with it in which DPTP99A was inactive (Desai et al., 97). An RPTPα crystal structure shows that the D1 domain can form a dimer in which a small helical region denoted as the 'wedge', which is conserved in many RPTPs, inserts into the active site of its partner in the dimer. This structure predicts that the RPTPα dimer would be catalytically inactive because the wedge would occlude access to the active site (Bilwes et al., 96). Consistent with this finding, introduction of mutations into the wedge region of the CD45 RPTP blocks inhibition of CD45 function caused by homodimerization of a CD45 chimera (Majeti et al., 98). There is as yet no evidence that wedge interactions are important *in vivo*, however, and the structures of other RPTP D1 domains have failed to reveal similar dimers. For DPTP69D, wedge mutants fully rescue the optic lobe phenotype, although they rescue lethality only poorly (Garrity et al., 99).

We have thus far been unable to obtain evidence showing that RPTP homodimers or heterodimers can form in heterologous cells (B. Burkemper, S. Fashena, K.Zinn, unpublished). The fact that the genetic relationships among the RPTPs differ at each choice point, however, suggests that if dimers do exist their formation might require contact with ligands localized to specific choice point regions. Determination of whether dimer formation, interactions between downstream signaling pathways, or both determine genetic relationships among the RPTPs is likely to require identification of the ligands and substrates that they recognize *in vivo*.

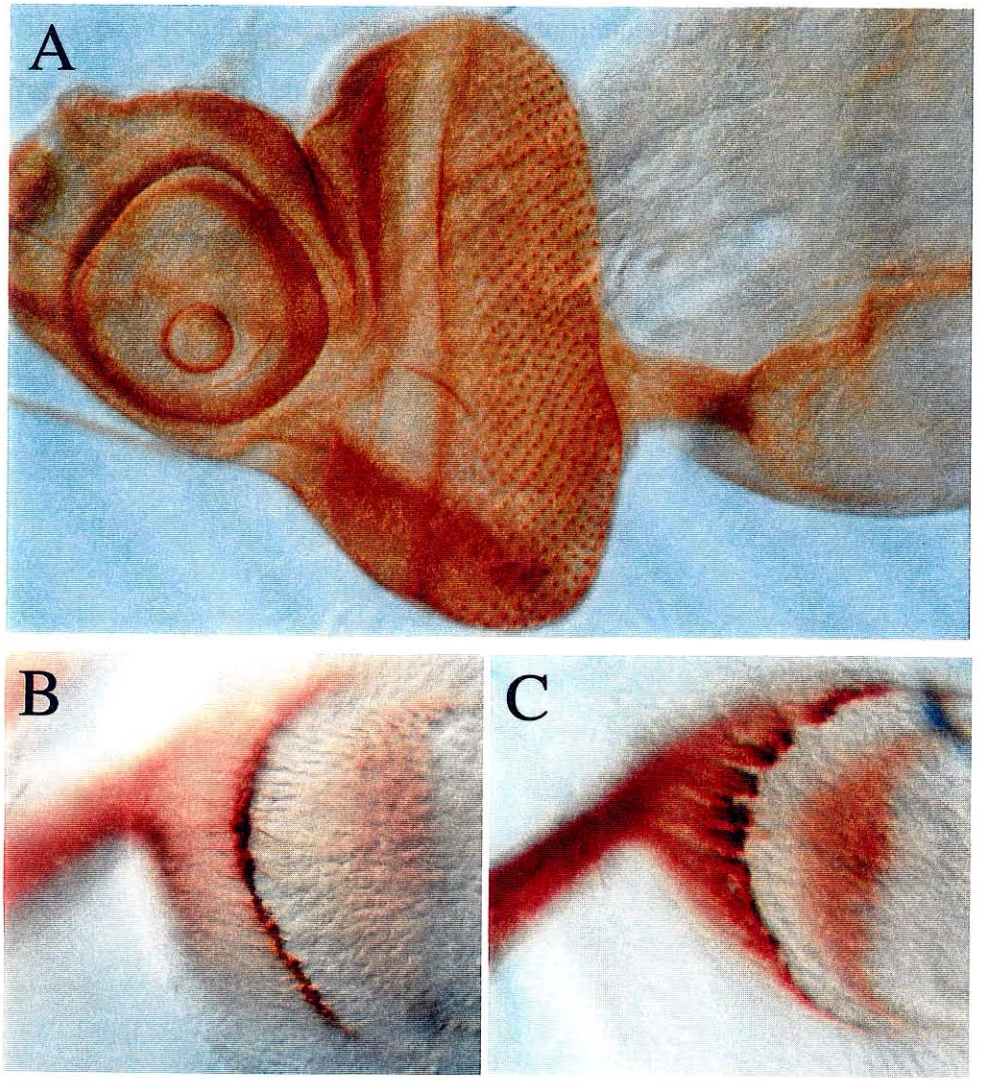
A
B
C

Figure 1. Retinal axon phenotypes in *Ptp10D* mutant.

(A) A whole-mount preparation of larval eye-brain complex stained with mAb 8B2. DPTP10D is expressed in all photoreceptor axons in the developing larval eye disc. (B and C) Photoreceptor cell projections in the lamina layer visualized with mAb 24B10. (B) Wild-type. Note the even plexus of R cell terminals in the lamina. (C) *Ptp10D*^{1}. There are many gaps and clumps in the R cell projections.

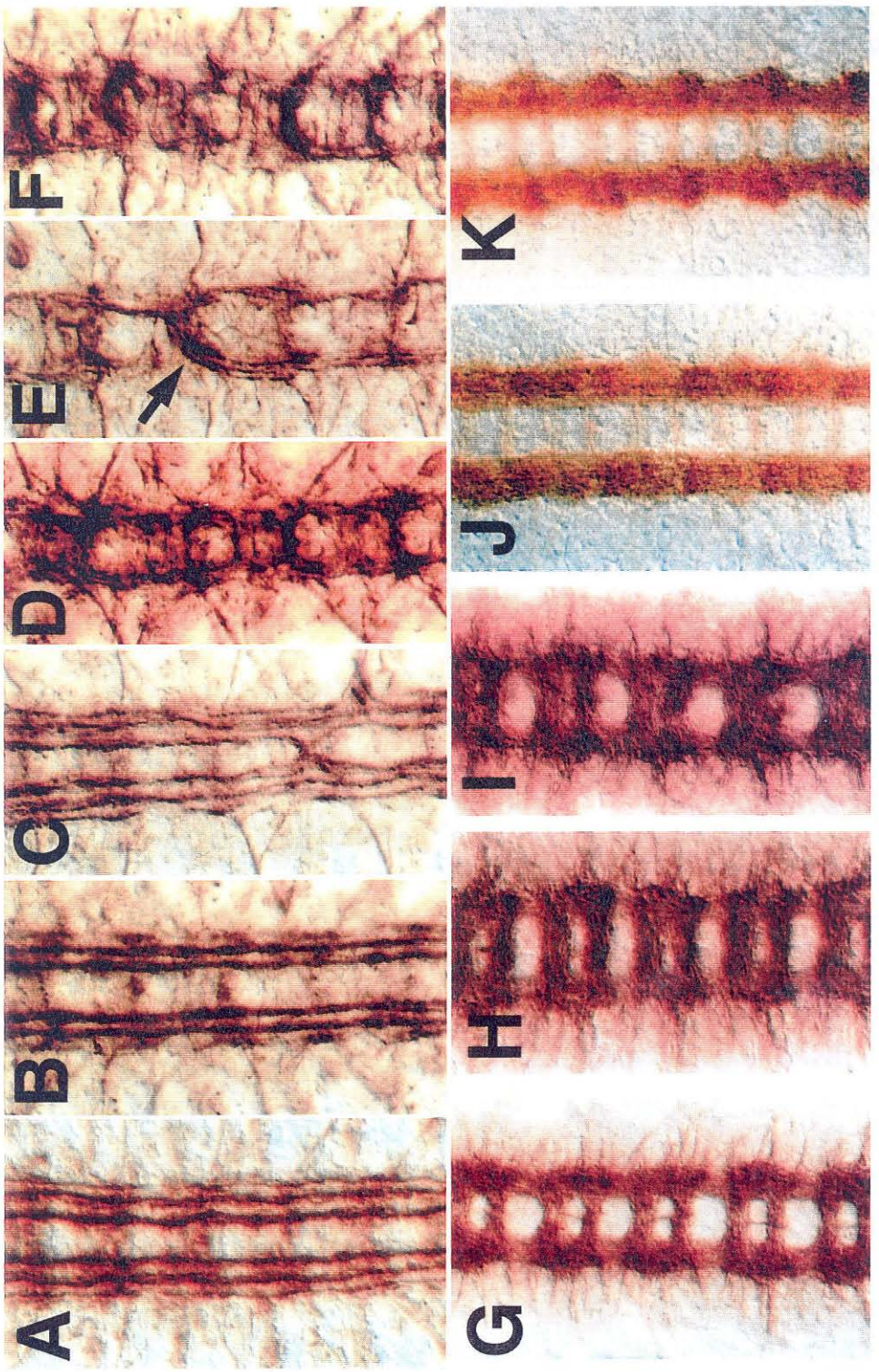
A
B
C
D
E
F
G
H
I
J
K

Figure 2. CNS phenotypes in *RPTP* mutant embryos.

(A - F) CNS of late stage 16/early stage 17 embryos stained with mAb 1D4. (A) Wild-type. (B) *Dlar*; *Ptp69D Ptp99A*. (C) *Ptp10D*; *Dlar*; *Ptp99A*. (D) *Ptp10D*; *Ptp69D Ptp99A*. (E) *Ptp10D*; *Dlar*; *Ptp69D*. (F) *Ptp10D*; *Dlar*; *Ptp69D Ptp99A*. (G-I) Wildtype and mutant embryos stained with mAb BP102. (G) Wild-type. (H) *Ptp10D*; *Ptp69D*. (I) *Ptp10D*; *Dlar*; *Ptp69D Ptp99A*. (J) Wild-type embryo stained with mAb specific for DLAR (8C9). (K) Wild-type embryo stained with mAb specific for DPTP10D (45E10).

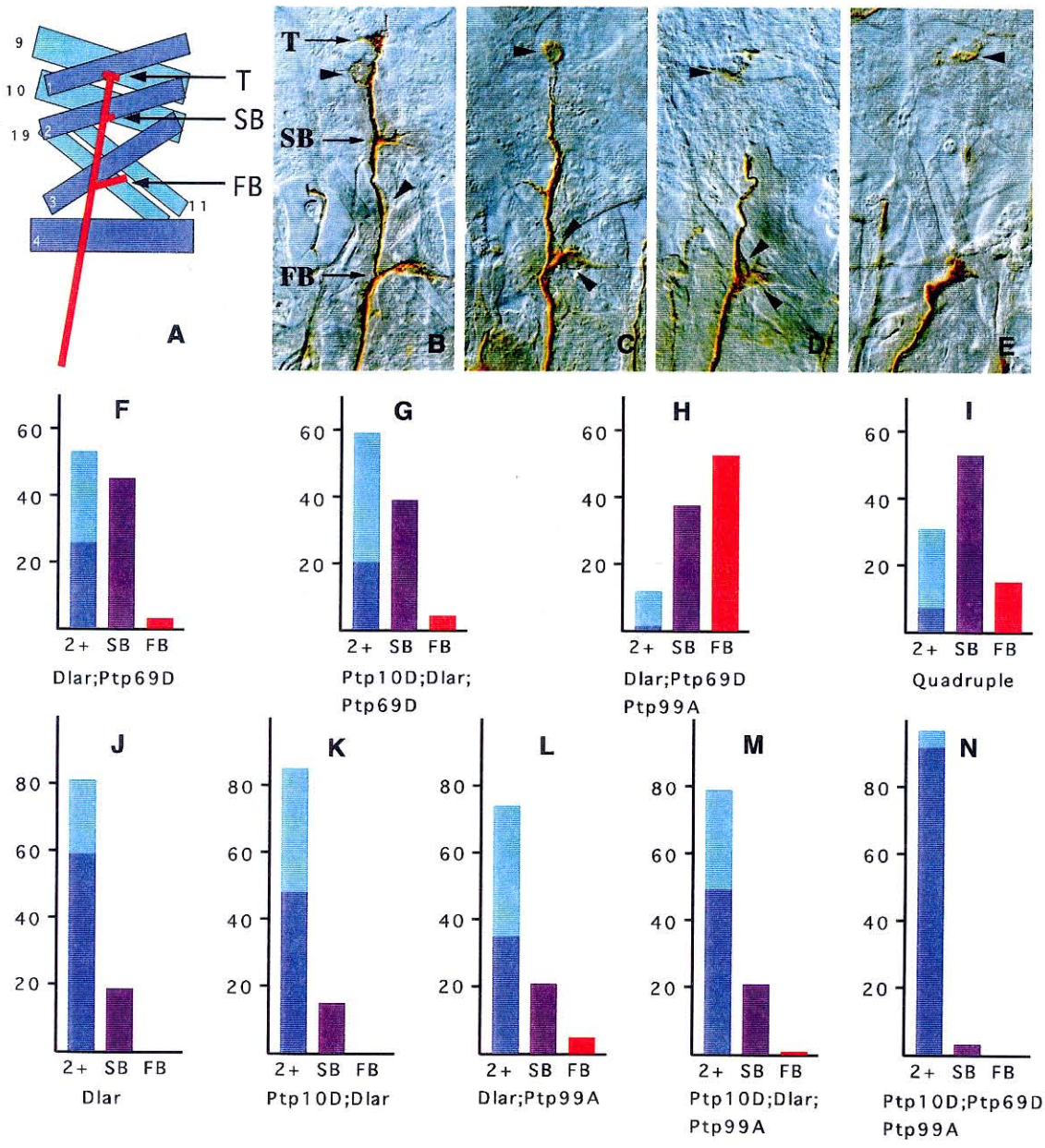
9
10
19
2
3
4
11
T
SB
FB
A
T
SB
FB
B
C
D
E
F
60
40
20
2+ SB FB
Dlar;Ptp69D
G
60
40
20
2+ SB FB
Ptp10D;Dlar;
Ptp69D
H
60
40
20
2+ SB FB
Dlar;Ptp69D
Ptp99A
I
60
40
20
2+ SB FB
Quadruple
J
80
60
40
20
2+ SB FB
Dlar
K
80
60
40
20
2+ SB FB
Ptp10D;Dlar
L
80
60
40
20
2+ SB FB
Dlar;Ptp99A
M
80
60
40
20
2+ SB FB
Ptp10D;Dlar;
Ptp99A
N
80
60
40
20
2+ SB FB
Ptp10D;Ptp69D
Ptp99A

Figure 3. ISN phenotypes in *rptp* mutant embryos.

(A) Schematic diagram of late stage 16 ISN. Some of the ISN target muscles are labeled. The first (FB), second (SB) branching points and the terminal arbor (T) are indicated. (B-E) Each panel shows an ISN stained with MAb 1D4. Three different kinds of phenotypes are represented. Abbreviations of each phenotype are described in the text. (B) Wildtype. (C) An SB+ ISN from a *dlar* embryo. (D) An SB ISN from a *dlar*; *ptp69D* embryo. (E) An FB ISN from a *dlar*; *ptp69D ptp99A* embryo. (F-N) Bar graphs showing ISN phenotypes of different *rptp* mutants. The ordinates represent the penetrances (in %) of the various phenotypes. The T (blue bars) and SB+ (light blue bars) categories are combined into one column labeled as 2+, meaning that these ISNs extend past SB. The arrowheads indicate the PT cells.

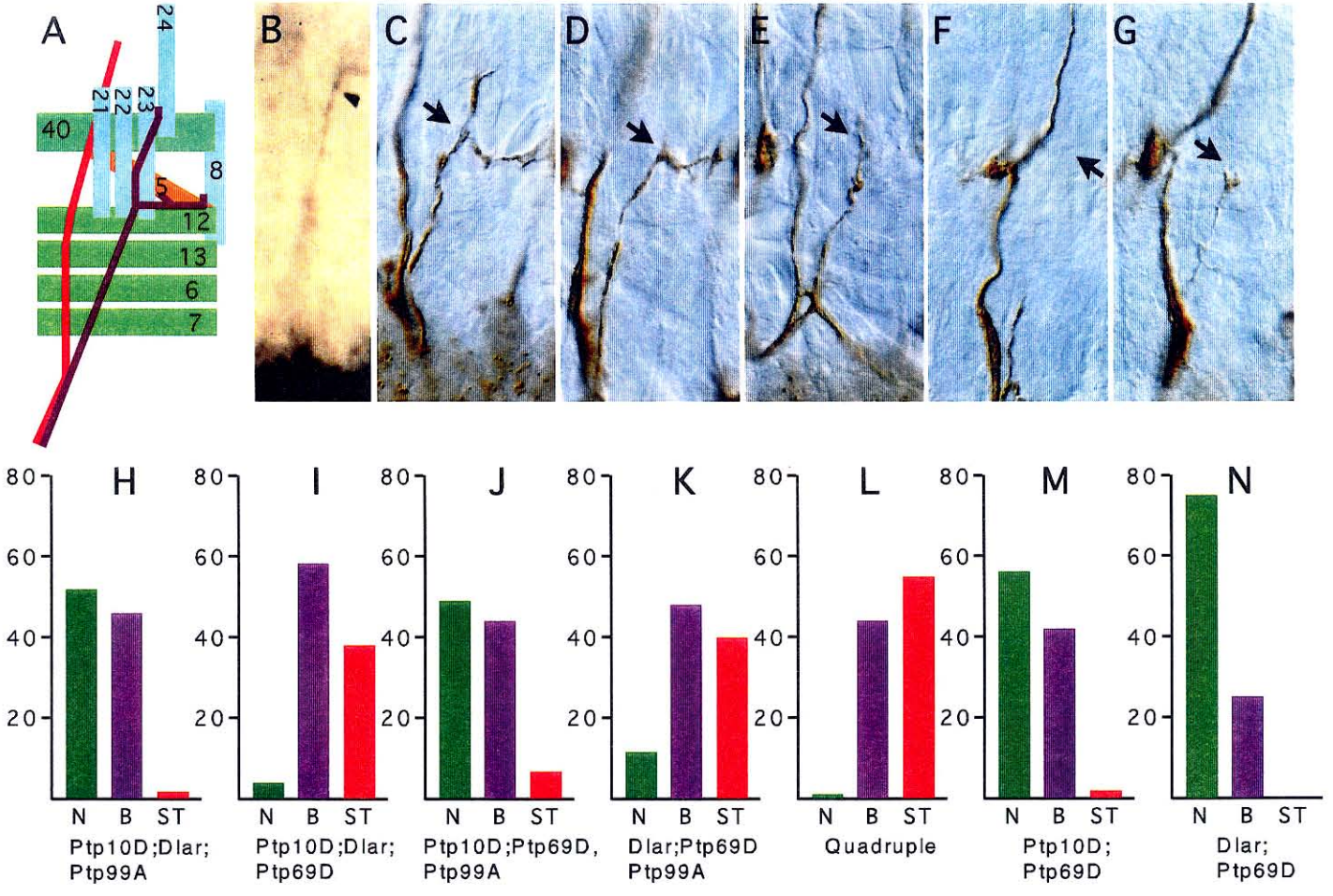
A
24
21
22
23
40
8
5
12
13
6
7
B
C
D
E
F
G
H
I
J
K
L
M
N
80
60
40
20
N B ST
Ptp10D;Dlar;
Ptp99A
Ptp10D;Dlar;
Ptp69D
Ptp10D;Ptp69D,
Ptp99A
Dlar;Ptp69D
Ptp99A
Quadruple
Ptp10D;
Ptp69D
Dlar;
Ptp69D

Figure 4. SNa phenotypes in *rptp* mutant embryos. (A) Schematic diagram of SNa (late stage 16 embryo). SNa branch is shown in purple, the ISN branch is shown in red. Note the SNa bifurcating point between muscle 22 and 23. (B) MAb for DPTP10D stains the SNa nerve branches (arrowheads). (C-G) Each panel shows an SNa stained with MAb 1D4. Arrows mark the bifurcating points. (C) Wildtype. (D) The anterior branch missing from this SNa of a *ptp10D*; *ptp69D* embryo. (E) This SNa does not have the posterior branch. Its anterior branch is abnormally short. (F) Abnormally short SNa. (G) Very thin SNa. (F) and (G) are from quadruple mutant embryos. (H-N) Bar graphs showing SNa phenotype of different mutants. The ordinates represent the penetrances (in %) of the various phenotypes. N (green bars): normal SNa. B (purple bars): SNa reaches the bifurcating points, but has no anterior, posterior or both branches. ST: SNa is either very short or very thin.

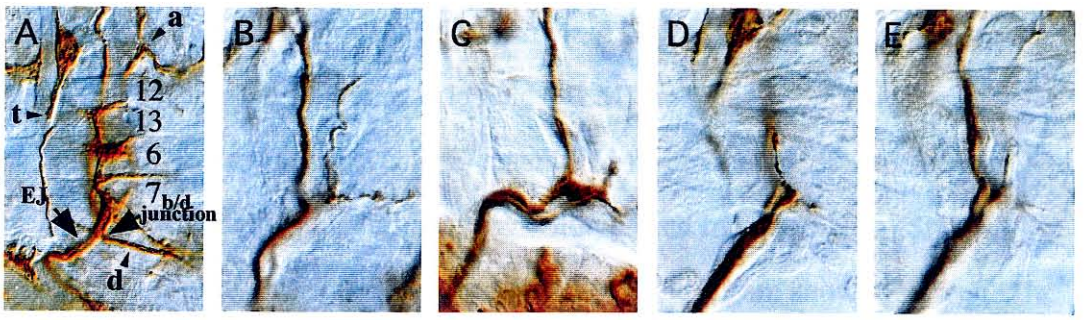
A
a
12
13
t
6
7
b/d junction
EJ
d
B
G
D
E

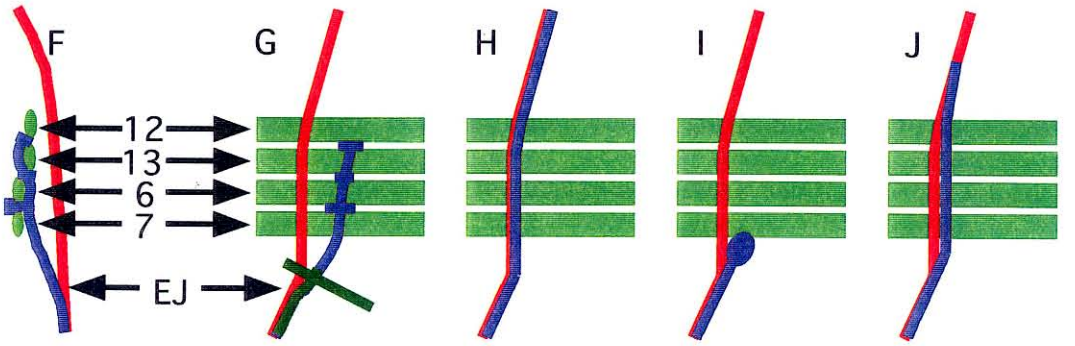
F
G
H
I
J
12
13
6
7
EJ

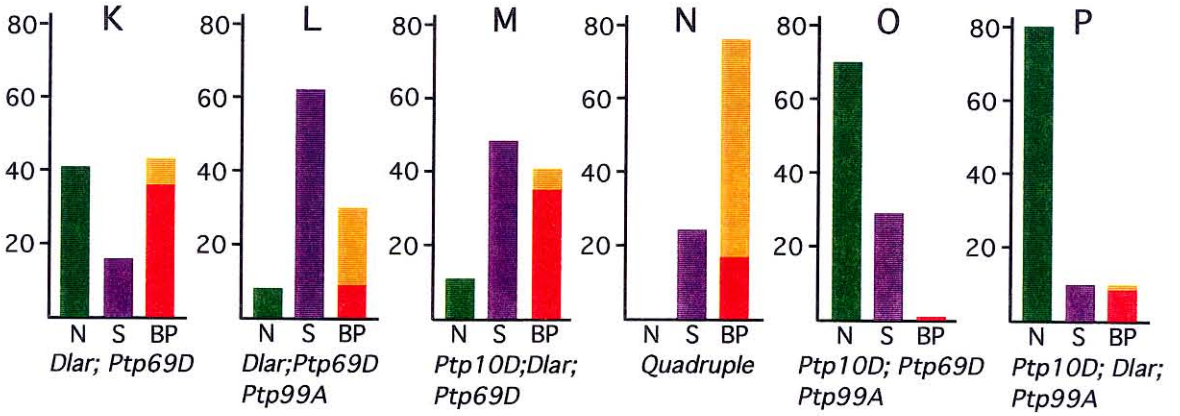
K
L
M
N
O
P
80
60
40
20
N S BP
Dlar; Ptp69D
Dlar;Ptp69D Ptp99A
Ptp10D;Dlar; Ptp69D
Quadruple
Ptp10D; Ptp69D Ptp99A
Ptp10D; Dlar; Ptp99A

Figure 5. ISNb phenotypes in *rptp* mutant embryos. (A) Wildtype ISNb stained with MAb 1D4. Four of the ISNb target muscles (6, 7, 12, 13), SNa (a), ISNd (d) and transverse nerve (t) are labeled. (B-E) Each panel shows an ISNb from a quadruple mutant embryo. (B) ISNb fuses with ISN. (C) ISNb stalls right after exit EJ. (D E) Two different focal planes of one quadruple mutant ISNb. D is interior. In wildtype embryos, ISNb enters the ventral muscle field (VLM) from the exterior side of muscles 6 and 7. The ISNb shown in (D) and (E) enters VLM from the interior side of muscles 6 and 7. (F-J) Schematic diagrams showing wildtype and mutant ISNbs. ISNb is shown in blue, ISN is shown in red. Muscles 6, 7, 12 and 13 are shown in green. The ISNb exit junction (EJ) is indicated. (F) (a cross section) and (G) are wildtypes. (H), (I) and (J) are fusion bypass, stall and parallel bypass respectively. (K-P) Bar graphs showing ISNb phenotypes of different mutants. The ordinates represent the penetrances (in %) of the various phenotypes. N (green bars): normal ISNb. S (purple bars): ISNb stalls. BP: parallel bypass (red bars) and fusion bypass (brown bars).

A. From first branch to second branch

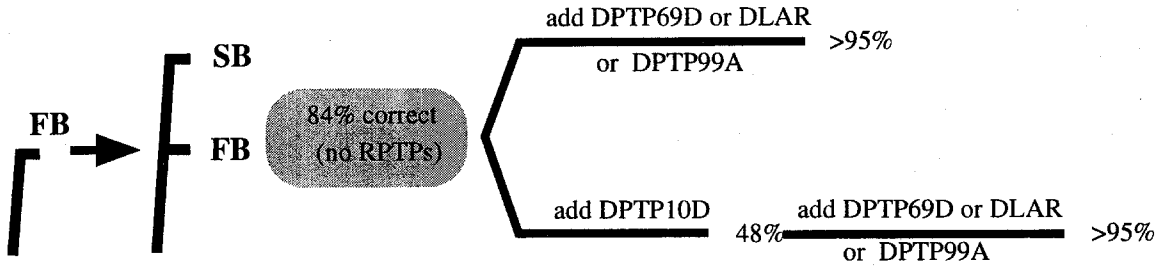

B. From second branch to terminal point

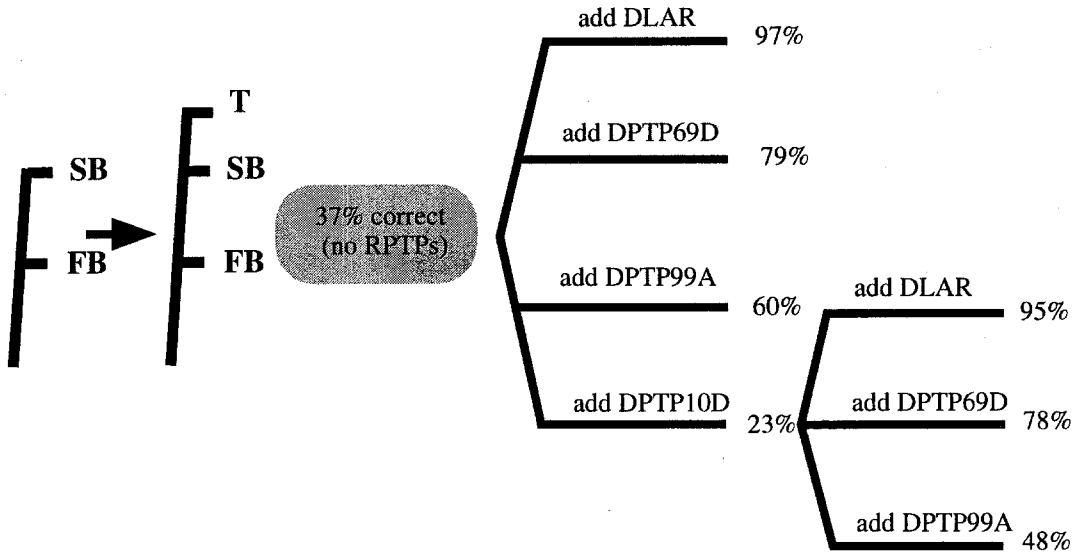

Figure 6 (part 1). Schematic diagrams showing contributions of each RPTP during ISN development. The two flowing charts depict the phenotypic changes with each RPTP added back into the mutants. They start with the quadruple mutants. Different RPTPs are added back sequentially as indicated. In chart A, the number for each genotype represents the percentage of ISN reaching the SB. It is calculated with the formula: [TB + (SB+) + SB] / n. Chart B shows RPTP function during ISN extending from SB to T. It is represented by the percentage of ISNs reach (TB) or partially reach (SB+) terminal arbor positions over the ISNs that have reached SBs. The formula for chart B: [TB + (SB+)] / [TB + (SB+) + SB]. (Data from Table 1)

C. Reaching the bifurcation point

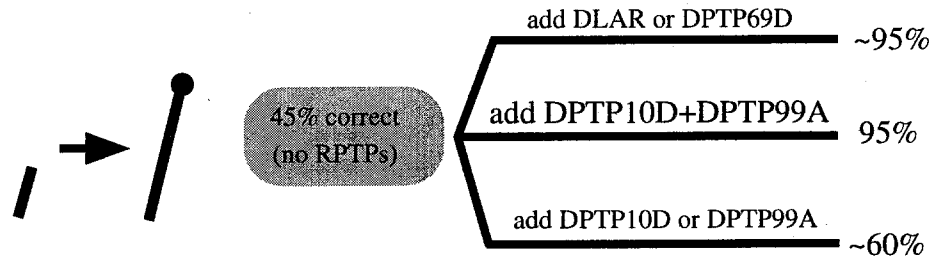

D. Bifurcating into anterior and posterior branches

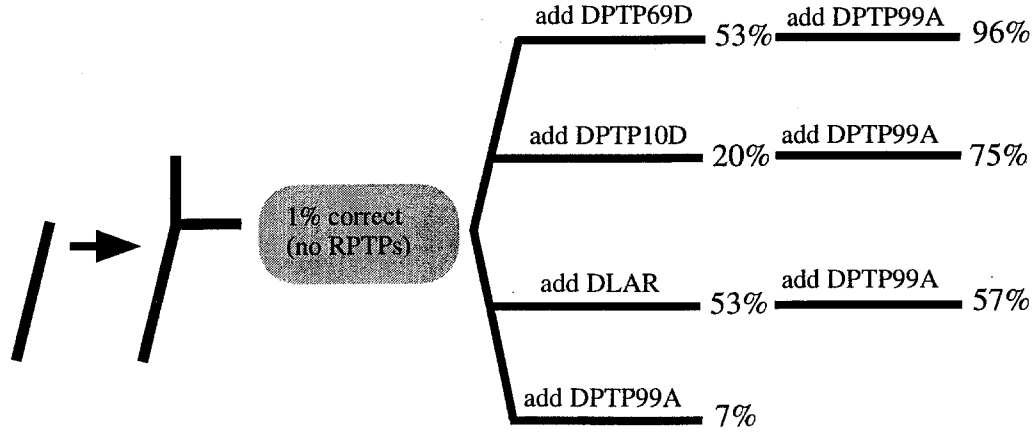

Figure 6 (part 2). Schematic diagrams showing contributions of each RPTP at different choice points of SNa. Chart C shows that percentage of SNa reaching the bifurcating points increases with each RPTP added back into the quadruple mutants. The formula for chart C: (N + B) / n. Chart D shows RPTP functions in SNa bifurcation. It is represented by the percentage of bifurcated SNas over the SNas that have reached the bifurcation point. The formula for chart D: N / (N+B). (Data from Table 2)

E. Defasciculation from the common ISN pathway

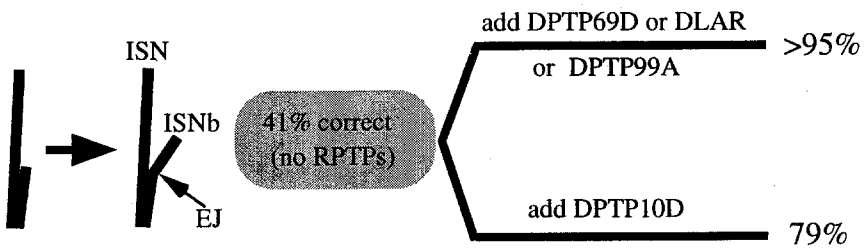

F. Passing ISNb/ISNd junction point

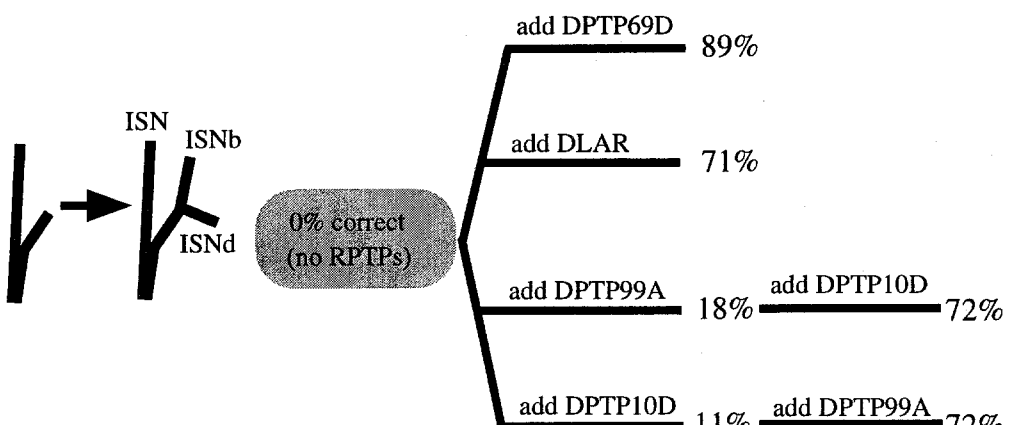

Figure 6 (part 3). Schematic diagrams showing contributions of each RPTP at different choice points of ISNb. Charts E and F represent two choice points of ISNb. (E) ISNb exits ISN common pathway at EJ. The formula for E: (N + S + PB) / n. (F) ISNb defasciculates from ISNd. It is represented by the percentage of stalls over ISNbs that have entered the VLM. The formula for F: N / (N+S) (Data from Table 3)

Table 1. ISN phenotypes in rptp mutant embryos

		Phenotype (%)			
Genotype	*n*	TB	SB+	SB	FB
ptp10D ; dlar ; ptp99a	105	48	30	21	1
ptp10D ; dlar ; ptp69D	107	20	38	38	4
ptp10D ; ptp69D ptp99A	118	91	6	3	0
dlar ; ptp69D ptp99A	118	1	10	37	52
quadruple	83	7	24	53	15
dlar; ptp69D	101	26	27	45	3
ptp10D ; dlar	96	48	37	15	0

n = Number of hemisegments (A2-A7) scored. TB: ISNs that reach the terminal arbor positions. SB+: ISNs stop between terminal positions and second branching points. SB: ISNs stop at the second branching points. FB: ISNs that fail to reach the SBs.

Table 2. SNa phenotypes in rptp mutant embryos

Genotype	Phenotypes (%)			
	n	N	B	ST
ptp10D ; dlar ; ptp99a	107	52	46	2
ptp10D ; dlar ; ptp69D	106	4	58	38
ptp10D ; ptp69D ptp99A	117	49	44	7
dlar ; ptp69D ptp99A	111	12	48	40
quadruple	71	1	44	55
ptp10D ; ptp69D	130	56	42	2
ptp69D ; dlar	118	75	25	0

n = Number of hemisegments (A2-A7) scored. N: Normal SNa. B: SNas that do not bifurcate after reaching the branching points. ST: very thin or very short SNas.

Table 3. ISNb phenotypes in *rptp* mutant embryos

Genotype	Phenotype (%)				
	n	N	S	PB	FB
dlar; ptp69D	119	41	16	36	7
dlar ; ptp69D ptp99A	119	8	62	9	21
ptp10D ; dlar ; ptp69D	106	11	48	35	6
quadruple	76	0	24	17	59
ptp10D ; ptp69D ptp99A	119	70	29	1	0
ptp10D ; dlar ; ptp99a	108	80	10	9	1

n = Number of hemisegments (A2-A7) scored. N: Normal ISNb. S: ISNbs stall before enteringVLMs. PB: parallel bypass, in which some or all ISNb axons separate from ISN but continue to grow adjacent to ISN. FB: fusion bypass, in which ISNb axons fail to defasciculate fro ISN at EJ, and continue to grow along ISN.

Chapter 4

A modular overexpression/misexpression screen for new genes involved in axon guidance

Qi Sun and Kai Zinn

Abstract

An overexpression/misexpression screen was carried out for genes involved in axon guidance and synaptogenesis. This screen allows the identification and rapid cloning of genes that cause axon guidance defects when they are overexpressed in all neurons or all muscle fibers. About 5000 EP-element insertions were screened. One known axon guidance gene and several novel genes with interesting phenotypes were identified.

Introduction

In the classic genetic approach to a biological process, the first step is to mutagenize the genome of a model organism and screen for mutations that specifically affect that process. This approach has been very successful in studying embryonic development of *Drosophila* (Nusslein-Volhard and Wieschaus, 1980). During the last ten years, fly neurobiologists have been using similar methods to search for molecular mediators of axon guidance. Extensive genetic screens were carried out for mutations that cause axon pathfinding errors (Seeger et al., 1993; Van Vactor et al., 1993); also Klaembt screen ref. Several important signaling pathways were characterized as a result of these screens. Still, the number of genes identified was much smaller than the number which one would expect to be involved in guidance, and some guidance processes did not seem to be affected by any of the isolated mutations. By contrast, the Nusslein-Vollhard/Wieschaus screens succeeded in identifying the majority of genes involved in embryonic patterning.

Several factors could account for the fact that many genes were not identified by direct phenotypic loss-of-function screens. The first is insufficient resolution of the screening methods, which employed antibodies that recognize many CNS axons and relied on examination of whole-mount embryos in dissecting microscopes (it would be impractical to dissect embryos from several thousand crosses and examine each of them under a compound microscope). Mutations that only affect a small subset of CNS axons, produce only subtle guidance defects, and/or cause low-penetrance phenotypes might not be recovered in such screens. Second, genetic redundancy or genetic compensation might prevent isolation of single mutations that affect many guidance processes. It has been estimated that 2/3 of all *Drosophila* genes will show no obvious loss-of-function phenotypes when mutated (Miklos and Rubin, 1996). Our studies of *Rptp* genes, and studies of *CAM* genes by other groups (see Introduction for details),

showed that mutations in individual genes often produce no detectable axon pathfinding defects. Severe CNS phenotypes were observed only when several *Rptp* or *CAM* genes were mutant (Desai et al., 1996; Desai et al., 1997). Third, many *Drosophila* genes carry out multiple functions at different stages of development. Null mutations in genes that also have early functions could cause embryos to exhibit severe phenotypes due to failures in developmental steps prior to axonogenesis.

A modular misexpression system developed by Rorth (1996) provides one promising approach to overcome these problems. With this system, one can identify genes that produce phenotypes when misexpressed or overexpressed at high levels in the desired cell types. In this chapter, I will describe a misexpression screen we carried out to isolate fly axon guidance genes. The screen was a logical choice for several reasons:

(1) As was mentioned in the previous chapters, growth cone behavior is determined by multiple environmental cues, including both attractive and repulsive signal. Overexpression of a gene in one signaling pathway, or misexpression of a gene on cells around those displaying an environmental cue, could perturb the balance among the competing forces, leading to axon pathfinding errors. In such situations, perturbation by gain-of-function can overcome the genetic redundancy or compensation barrier, causing more severe phenotypes than perturbation by loss-of-function. For example, the *Fas III* loss-of-function mutant displays no obvious nervous system defects, while overexpression of Fas III in the muscles around the target muscle 6/7 cleft causes ectopic innervation by RP3 axons (Chiba et al., 1995) (see Introduction for further discussion). Thus, a misexpression screen could uncover genes that could not be identified in a loss-of-function screen.

(2) One problem of loss-of-function screens is that early functions of a gene could mask its late functions. In the misexpression screen, the transcriptional activator GAL4 is

used to drive expression from a promoter within the P element that contains multiple GAL4 binding sites, known as UAS elements. Since many lines exist that express GAL4 is particular subsets of embryonic cells, we can use specific GAL4 sources to target gene expression to the correct cells at the correct time. Thus the phenotypes produced are specific to the targeted cells. In this screen, we used a pan-neuronal GAL4 driver expressed in postmitotic neurons, and a pan-muscle driver. The pan-neuronal driver should limit the observed defects to the nervous system. A pan-muscle driver was used to screen for genes involved in synaptic specificity.

(3) The misexpression screen allows the imposition of screening conditions that enrich for genes of interest. In an EMS loss-of-function screen, each chromosome carries multiple lethal mutations, and therefore one must directly examine embryos homozygous for each mutant chromosome without preselecting for lethality. In the misexpression screen, however, we prescreened for insertions that caused lethality or semilethality only when crossed to a specific driver. This prescreen meant that we only needed to stain and examine embryos from about 2% of the lines. As a result, we could dissect and visualize all of these embryos using a compound microscope. This meant that we could see subtle motor axon defects that would have escaped notice if embryos were only examined as whole-mounts under a dissecting microscope.

(4) Since this is a *P* screen, we can directly clone the genes involved in producing the phenotypes by isolating sequences flanking the insertion. We can also readily generate loss-of-function mutations by imprecise excision of the *P*. Finally, we can examine the consequences of expressing the same gene in a variety of tissues by using different GAL4 drivers.

Results

Misexpression screen strategy

The P-element does not jump randomly on the genome. Although not much is known about the molecular mechanisms underlying its distinctive transposition pattern, researchers have taken advantages of various properties of the P-element for genetic screens. One interesting aspect of the P-element is that it inserts preferentially into the 5' untranslated region (UTR) of a gene. The P-element construct used in this screen, designated EP, contains 14 GAL4 binding sites and a basic hsp70 promoter at its 3' end, so that an EP insertion can direct transcription of the downstream flanking gene in cells that express GAL4 (Figure 1).

Two different GAL4 sources were used in this screen, C155 and 24B. The C155 line has a GAL4 'enhancer trap' P element inserted near the ELAV gene, which is expressed in all post-mitotic neurons. We used C155 as a pan-neuronal GAL4 driver. 24B line is an enhancer trap line with GAL4 expression in all mesoderm cells and their progenies (Lin and Goodman, 1994; Luo et al., 1994). It was used as a pan-muscle GAL4 driver.

The screen was designed to isolate genes that perturb axon pathfinding or synapse specificity when misexpressed and/or overexpressed in all neurons or muscles. We presumed that a severe disruption of axon guidance would reduce adult viability. In our primary screen, we screened for EP lines that are lethal or semi-lethal after crossing to specific GAL4 drivers. In the secondary screen, we directly examined the mutants' axon pattern by staining with monoclonal antibody (mAb) 1D4, which recognizes Fasciclin II (Fas II), a cell adhesion molecule that is expressed in all motor axons and a subset of interneuronal axons.

An X-chromosome EP line, EP55, was used as the "jumpstarter" line. It was crossed to a P element transposase source, Δ2-3, on the third chromosome. Male flies with new EP insertions on the second or third chromosomes were selected, and crossed to either C155 or 24B. Any EP lines that are lethal or semi-lethal over C155 or 24B

were saved and balanced. Semi-lethal was arbitrarily defined as 20% viability (n>10). The cross strategy is illustrated in Figure 2.

EP lines that are lethal over C155 or 24B

About 5000 independent EP insertions were screened. Out of these, 131 lines are lethal over C155 or 24B (Table 1, 2, 3). Overall, about 2% of all EP lines are lethal over pan-neuronal driver C155. The precise frequency of lethality over 24B for this group is unknown, because not all 5000 EP lines were tested for lethality over 24B. The overall frequency of lethality over 24B, however, is likely to be in the same range as for C155.

Table 1. EP mutants that are lethal over C155 and 24B

	2nd Chromosome	3rd Chromosome
Lethal over C155 only	16	29
Lethal over 24B only	9	15
Lethal over C155 and 24B	22	40
Total	47	84

Abnormal CNS axonal pattern in EP lines crossed to the neuronal driver.

In the second phase of our screen, 131 selected EP lines were crossed to C155 and/or 24B, and their embryos were examined by staining with mAb 1D4. 18 lines display defects in CNS and/or motor axon patterns after crossing to C155 (Table 2, 3). These defects can be classified into four categories:

(1) Abnormal fasciculation of the CNS longitudinal axons.

These EP lines include T10, T31 and T63. In wildtype embryos, 1D4-positive axons are fasciculated into three major bundles at each side of longitudinal tracts. When these three lines are crossed to C155, the regular fasciculation pattern is disrupted in the progeny embryos.

T10: The three Fas II bundles do not separate well at segmental boundaries. The most outside bundles are not continuous (Figure 3A). SNa branches are usually short and thin (Figure 3C). Many ISNb branches show stall phenotypes (Figure 3B).

T31: There is a lot of defasciculation along the longitudinal tracts. Many CNS axons appear to stall in the neuropils at segmental boundaries (Figure 3D). ISNb branches are much thinner than in wildtype (Figure 3E).

T63: Disorganized CNS fasciculation pattern was observed in this mutant. ISNb and SNa development is also abnormal (Figure 4A).

(2) General CNS development is arrested at early embryonic stages.

Three EP lines belong to this category: T18, T42 and T71. Stage 16 embryos from a cross between these EP lines and C155 have axonal patterns that look like a stage 14 embryo (Figure 4B). All three lines turned out to have insertions in the same locus: a gene called *headcase* (*hdc*).

(3) CNS axons abnormally cross the midline.

There are four lines in this category: T32, T68, T96 and C44. When these lines are crossed to C155, extra axons are misrouted across the CNS midline.

T32: The longitudinal tracts also move closer to the midline, possibly due to extra midline crossing of the longitudinal axons (Figure 4C).

T68 and C44: These two lines have similar phenotypes. The inner bundles of Fas II longitudinal axons are fused in many segments. The longitudinal tracts are always broken (Figure 4E and 4F).

T96: The embryos from the cross between T96 and C155 look like *roundabout* mutants (*robo*) (Figure 4D). It was previously reported that overexpression of Commissureless (Comm) protein give rise to a *robo* like phenotype (Kidd et al., 1998). T96 is also a loss-of-function mutant; when homozygosed it has a *comm* like phenotype, and fails to complement *comm*, indicating that T96 is a *comm* allele.

(4) Motor axon pathfinding phenotypes.

Three second-chromosome EP lines C37, C53 and C56 exhibit ISNb pathfinding phenotypes after crossing to C155.

C37: In C155; C37 embryos, almost all ISNbs do not separate from ISN at the exit junctions. This phenotype is like the ISNb fusion bypass displayed by the quadruple *Rptp* mutants. These C155; C37 embryos also exhibit severe CNS phenotypes (Figure 5A and 5B). The two outside Fas II bundles are discontinuous, and defasciculated.

C53: C155; C53 embryos also exhibit high frequency of ISNb fusion bypass phenotype. However, these embryos have a relatively normall CNS (Figure 5C).

C56: C56 over C155 displays an ISNb stall phenotype. The most outside Fas II bundles are discontinuous even at late stage 16 (Figure 5D).

Genes identified in the misexpression screen

The EP element has a built-in rescue plasmid, enabling rapid cloning of the flanking genomic region. We have sequenced the flanking region of all the EP lines that show phenotypes after crossing to C155. Three of the identified EP lines have insertions in previously identified genes: *comm*, *hdc* and *bowl*.

Both loss-of-function and gain-of-function mutants of *comm* have been previously reported (Reviewed in Zinn, 1999). T96 loss-of-function and gain-of-function phenotypes resemble those of *comm*. The genetic complementation test showed that T96 is the same gene as *comm*.

The *hdc* gene was isolated three times in our screen. In mutant embryos that misexpress *hdc* in all post-mitotic neurons, the CNS development is arrested at around stage 14. *hdc* encodes a cytoplasmic protein with no homology with any of the known genes. In wildtype embryo, *hdc* is expressed by clusters of cells in the CNS, a subset of tracheal fusion cells, the primordia of the imaginal tissues and the imaginal tracheal cells of the spiracular branch. Detailed analysis of *hdc* expression in the imaginal tissues showed that its expression starts before cells entering mitotic divisions, while its inactivation correlates with the final cell division (Weaver and White, 1995). One model for how *hdc* expression in postmitotic neurons produces an arrest phenotype is that its normal function is to prevent precocious differentiation of cells during the proliferative phase of their development. If this were the case, then ectopic expression of *hdc* in differentiated neurons might reverse their differentiated status and cause an arrest of axon extension.

The C53 insertion is 5' to the gene *bowl*. *bowl* encodes a zinc finger transcription factor. It was previously identified as a terminal class gene and is involved in terminal system development. Transcripts of *bowl* are also present in a subset of CNS cells. Combination of C155 with C53 produces an ISNb fusion bypass phenotype, similar to the phenotype generated by overexpression of adhesion molecular Fas II. One possibility is that overexpression of *bowl* triggers the high-level expression of some homophilic adhesion molecules, so that ISNbs fail to separate from ISNs at the exit junctions.

T32 targets a novel gene that is a member of the AAA ATPase family

Overexpression of T32 with the C155 driver gives rise to a phenotype in which the Fas II positive axons move closer to the midline. Staining with another axonal marker, BP102, also shows that there is less space between the two longitudinal tracts in the gain-of-function mutants (Figure 6D). It has been shown two classes of mutation could cause this kind of phenotype. First, loss-of-function mutations in genes required for midline cell differentiation, such as *single-minded* (*sim*) (Nambu et al., 1993), could cause a midline collapsing phenotype. Second, mutations causing midline crossing of CNS axons, such as overexpression of *comm* or loss-of-function mutations in *robo* or *slit* cause the longitudinal tracts to move closer to the midline (Kidd et al., 1999). To distinguish between these two possibilities, we examined the C155; T32 embryos by staining with an antibody against the midline glial marker Wrapper. As shown in Figure 6F, the midline glia appear normal in the mutant embryos. This suggests that the phenotypes of C155; T32 are likely to be caused by abnormal midline crossing.

We wondered whether the mild crossing phenotype caused by T32; C155 might be due to the fact that the GAL4 amplification circuit introduces a delay in expression of about 1 hour (relative to expression of the *elav* gene into which the C155 element is inserted), so that some neurons might have begun to extend axons before they had begun to express T32 at high levels. Thus, we crossed T32 to a GAL4 driver that is expressed earlier than C155. *scabrous (sca)*-GAL4 drives expression in neurogenic cells prior to the last mitotic division. T32; sca-GAL4 embryos have a more severe phenotype in which many extra axons cross the midline. When we examined earlier embryos (stages 12-13) from these crosses, we found that the pCC and MP1 axons grow to the midline, as is observed in *robo* and *slit* mutants (N.T. Sherwood and Q.S., unpublished). Thus, T32 overexpression is likely to affect the midline repulsive

pathway in some manner (see Introduction and Chapter 2 for further discussion of this pathway).

We cloned a genomic fragment 3' to the T32 insertion. Sequence of this flanking region matches 3 overlapping ESTs in the Drosophila Genome Project database. We sequenced one of the EST clones, GH11184. There is a complete open reading frame (ORF) in GH11184. The putative translation start codon is 237 base pairs downstream from the T32 insertion. RNA *in situ* analysis showed that in C155; T32 embryos this ORF is expressed at much higher levels in the embryonic nervous system than in wildtype embryos, suggesting that the CNS phenotypes in these embryos are most likely caused by expression of this ORF in the CNS. In the remaining part of this chapter, we will refer to this ORF as T32.

T32 has a very dynamic expression pattern during embryonic development. From stage 15 to 17, however, T32 transcripts are restricted to the CNS (Figure 6E). Thus, the phenotypes we observe are not due to expression of T32 in a tissue in which it normally does not function. Rather, they are likely to be produced by ovexpression of T32 in cells that normally express it at low levels.

The deduced T32 protein has 758 amino acids (Figure 7). A 160 amino acid region in the N terminal half bears similarity with a region in the rod-like coiled-coil domain of myosin heavy chains (Figure 8). The C terminal 400 amino acids are most closely related to the ATPase domain of sea urchin Katanin (Hartman et al., 1998), which is a member of the large AAA ATPase family (ATPases associated with various cellular activities). The sequence alignment of ATPase domains of T32 and Katanin is shown in Figure 9. As Katanin has been shown to have microtubule-severing activity (Hartman et al., 1998), one interpretation of the T32 overexpression phenotype is that too much microtubule-severing activity could change the dynamics of cytoskeletal structure within axons and lead to abnormal axon growth.

There are many alternative hypotheses for T32 function, however, since the T32 AAA ATPase domain does not have features that uniquely identify it as a Katanin ortholog. Also, Katanin does not contain the coiled-coil motif. AAA ATPases function in many cellular processes, including vesicle transport, protein degradation, and protein folding. Thus, T32 overexpression could also influence growth cone repulsion by causing degradation or internalization of signaling proteins. Distinguishing among these models will require analysis of loss-of-function mutations, localization of T32 protein, and biochemical analyses of its activities and interactions with other proteins.

Discussion

During the development of fly embryonic CNS, axons follow highly stereotyped pathways to reach their targets. How to decode the genetic program that controls this process has been a prominent question faced by fly neurobiologists. Here we carried out a modular misexpression screen for fly axon guidance genes. About 5000 second and third chromosome EP insertions were generated, and 18 lines were isolated that show CNS axon defects after crossing to a neuronal driver. One of these lines targets a known axon guidance gene (*comm*), indicating that this screening method can identify genuine axon guidance genes. Two others identify genes (*hdc* and T32) for which overexpression produces interesting phenotypes (arrest of axon extension and ectopic midline crossing), and we are pursuing the analysis of these genes to identify their normal functions in CNS development.

Accumulating evidence from genetic studies of fly axon guidance suggests that there are multiple competing or collaborating signals at each choice point along axon pathways (Tessier-Lavigne and Goodman, 1996). Genetically removing or reinforcing one signal could perturb the balance among these competing forces and lead to axon guidance errors. Misexpression and loss-of-function screens are two complementing

ways to identify genes involved in these signaling pathways. In the past decade numerous genes have been identified in loss-of-function screens. But there are still many missing links. Most of the loci isolated in the misexpression screen described here were not previously associated with CNS development. We hope that this new screening method can help to fill some of the gaps in our understanding of neural development.

One disadvantage of the misexpression screen is that the screen relies on an unnatural condition: genes are forced to express at high levels in the targeted cell types. It is quite possible that in native conditions some of the genes isolated in the misexpression screen have no biological relevance to the process of interest. For example, high-level expression of a gene normally used for gut development in the CNS might produce nervous system phenotypes, but these would not be relevant to the normal processes of nervous system development. Thus, further characterization of mutants isolated in our screen is always necessary to establish their relevance. First, it is necessary to identify the EP-linked genes that are overexpressed and determine whether these genes are normally expressed in the CNS. This has been done for two of the genes whose characterization we describe here, *hdc* and T32. At present, gene identification and determination of expression patterns requires sequence analysis and *in situ* hybridization. However, as the fly genome project progresses it will be possible to address these questions by analyzing genomic and EST sequences (if the overexpressed gene corresponds to an EST from a brain library, for example, it is likely to be normally expressed in the CNS). Second, it is important to generate and analyze loss-of-function mutations and show that they produce CNS phenotypes, either alone or in combination with other mutations.

Another potential problem with our screen is that, in order to be able to screen thousands of insertions without dissecting embryos from all of these lines, we based our

primary screen on the assumption that mutants with axon guidance defects would have decreased viability. It is already known that mutations in some axon guidance genes that cause relatively severe phenotypes (such as *robo* and *comm*) are not 100% lethal (Seeger et al., 1993). Thus, there may be many genes for which misexpression causes interesting phenotypes but does not cause lethality. To address these problems, others in the group are now conducting EP screens for motor axon phenotypes in live larvae using green fluorescent protein (GFP) as a marker. This allows screening to be performed rapidly under a dissecting microscope, because larvae have large neuromuscular systems relative to those of embryos. It is thus possible to screen all insertions without imposing a selection for lethality.

In summary, the misexpression/overexpression screen I have conducted provides an alternative way to isolate genes that cannot be identified by classic loss-of-function screens. However, extra caution must be taken when interpreting phenotypes identified in this screen, and further experiments are required before any conclusions can be drawn about the functions of these genes during normal development of the nervous system.

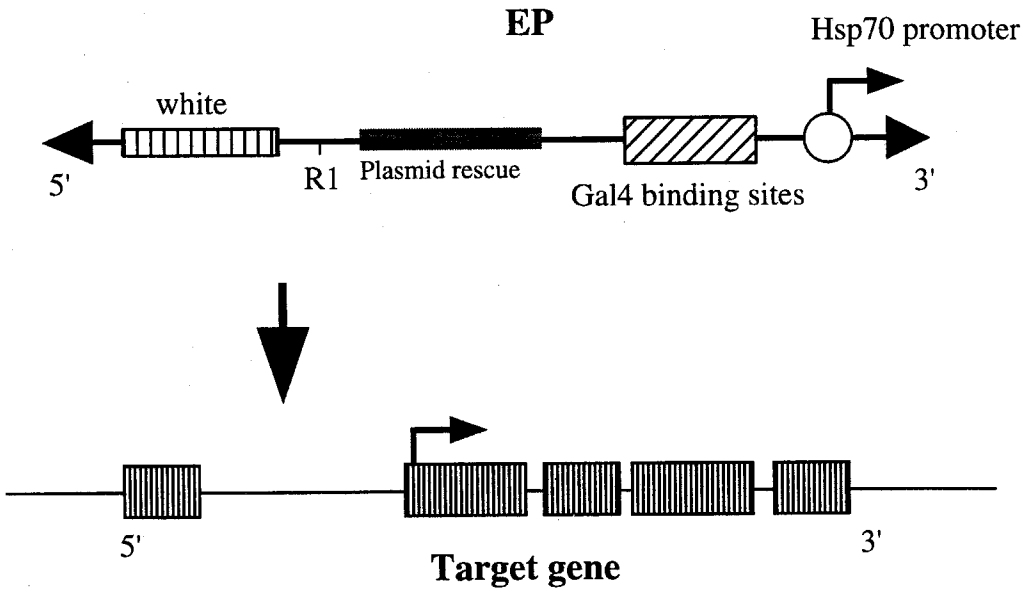

Figure 1. Molecular structure of the EP element. It contains a mini-white marker, a rescue plasmid, 14 GAL4 binding sites and an Hsp70 basic promoter. The EP element preferentially inserts into the 5'-UTP of a gene, and directs GAL4 dependent transcription of this downstream gene.

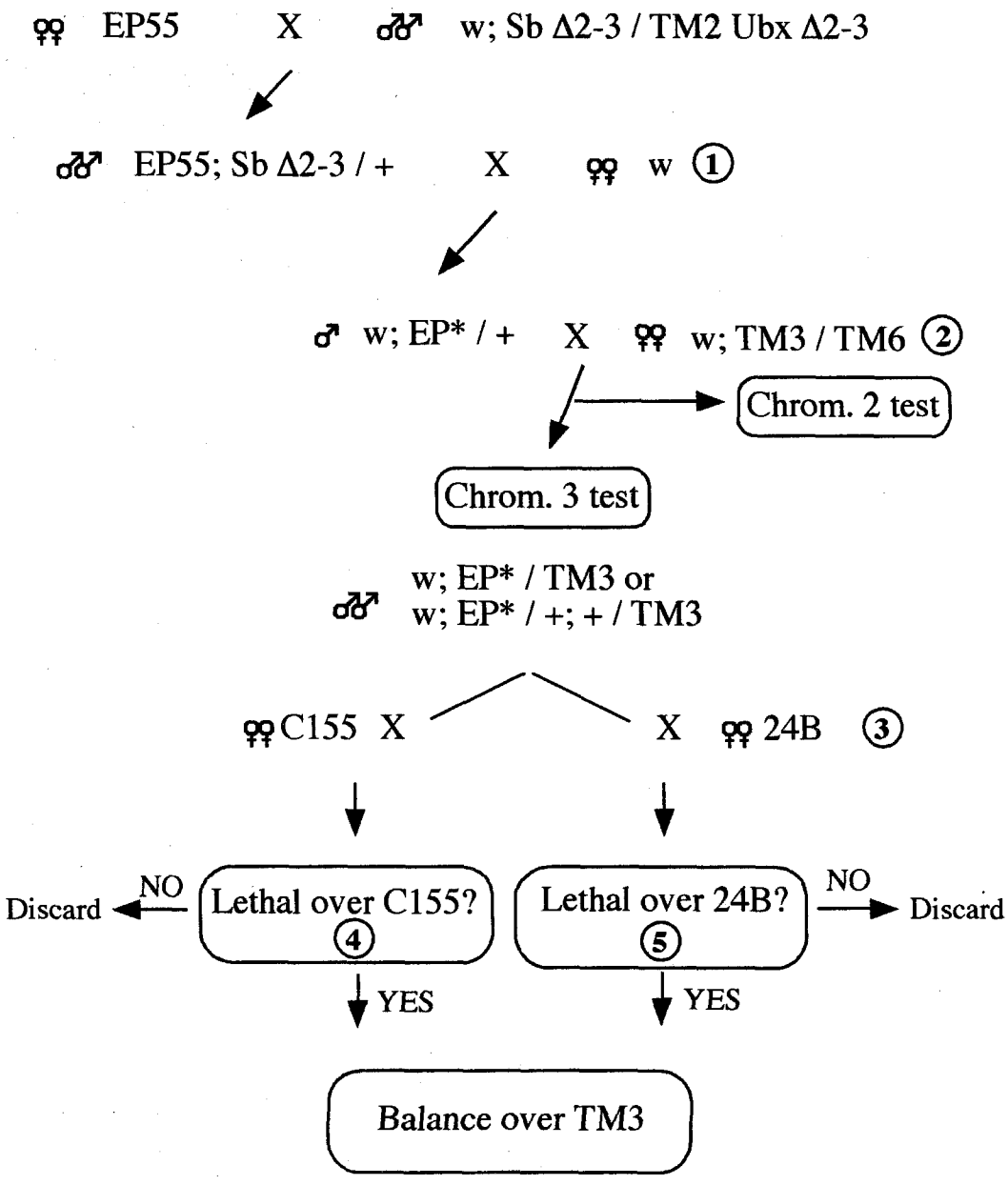

Figure 2. Cross strategy of the misexpression screen (Part 1).

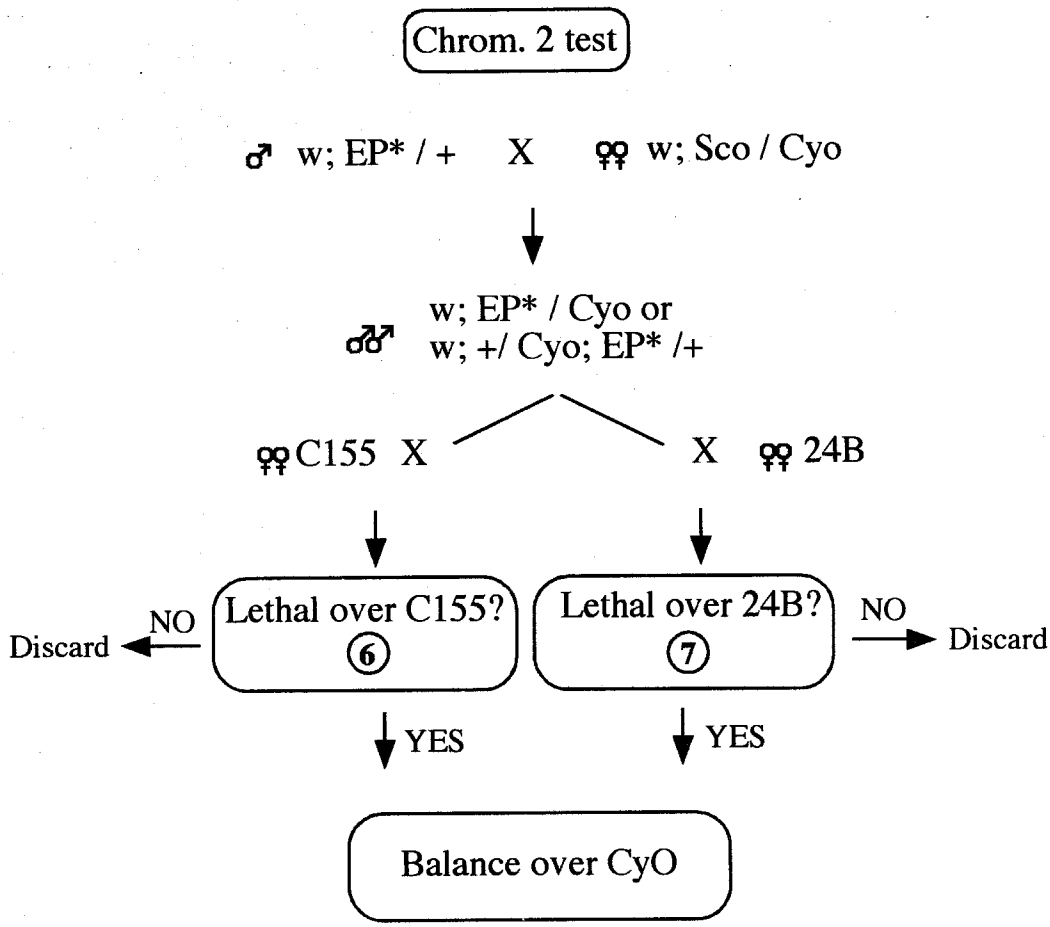

Figure 2. Cross strategy of the misexpression screen (Part 2).

(1) This cross was carried out in bottles. (20 female 20 male/bottle.)

(2) Maximum 20 new EP flies / bottle were isolated from previous cross. Individual lines were set up in vials for each new EP line.

(3) To test EP viablity with C155 or 24B, 2 famale and 2 male flies were used for each cross.

(4) and (5) If the EP line is lethal over C155 or 24B, only TM3 progenies are alive.

(6) and (7) If the EP line is lethal over C155 or 24B, only Cyo progenies are alive.

T10

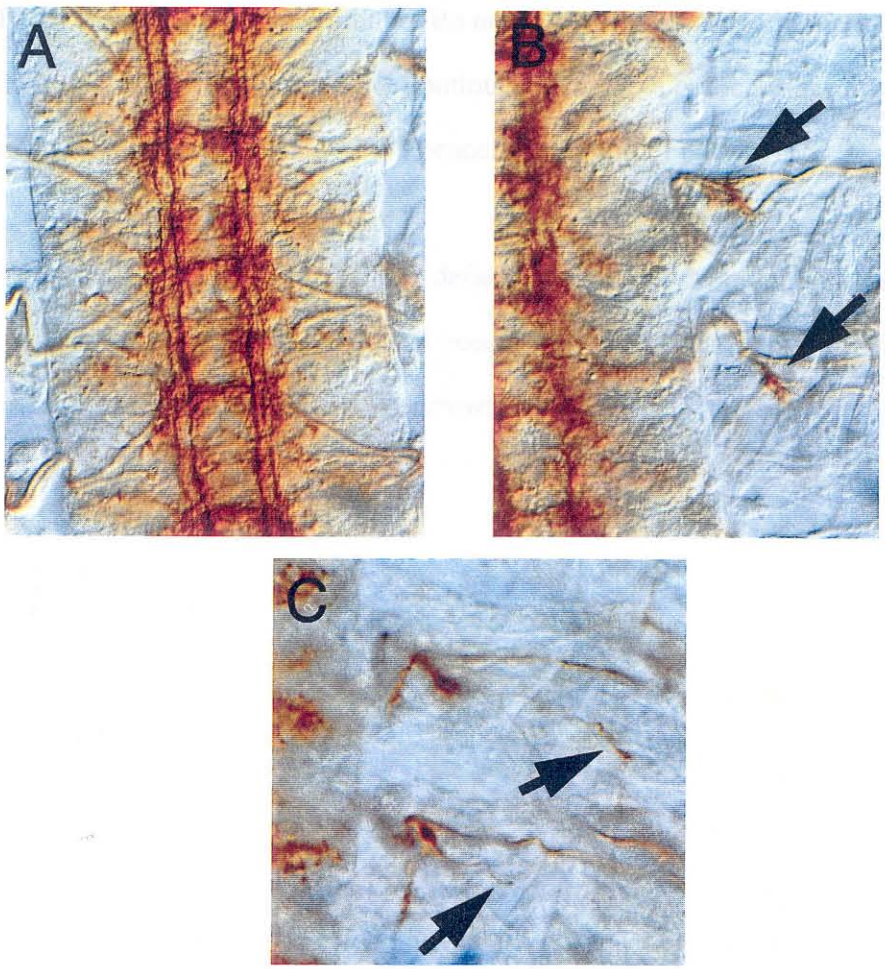

T31

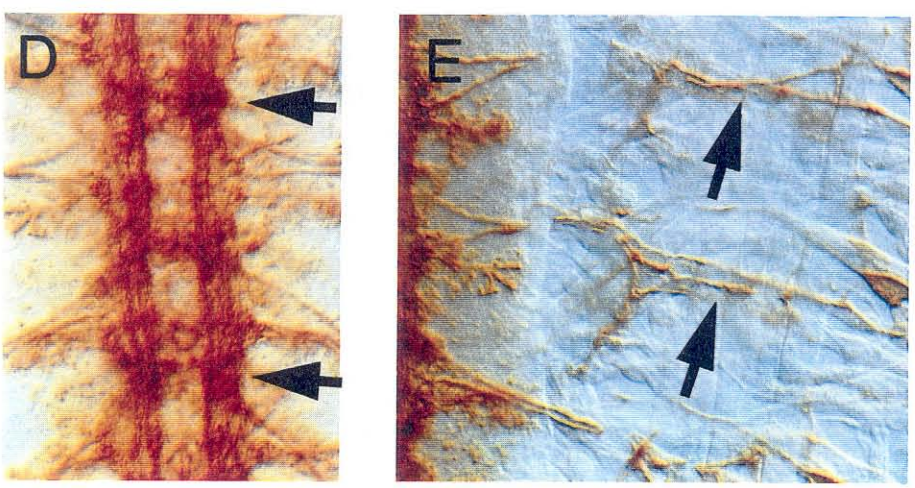

Figure 3. Phenotypes of EP lines (I).

(A-C) T10/C155: The three Fas II bundles do not separate well at segmental boundaries. The most outside bundles are not continuous (A). SNa branches are usually short and thin (C, arrows). Many ISNb branches show stall phenotypes (B, arrows).

(D-E) T31/C155: Fas II positive axons are defasciculated (D). Many CNS axons appear to stall in the neuropils at segmental boundaries (D, arrows). ISNb branches are much thinner than in wildtype (E, arrows).

T63

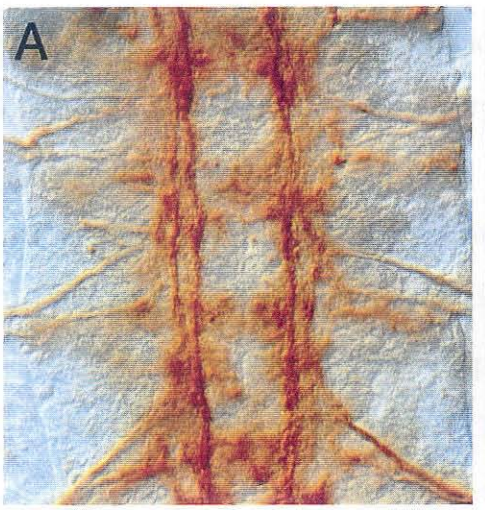

T18 (*headcase*)

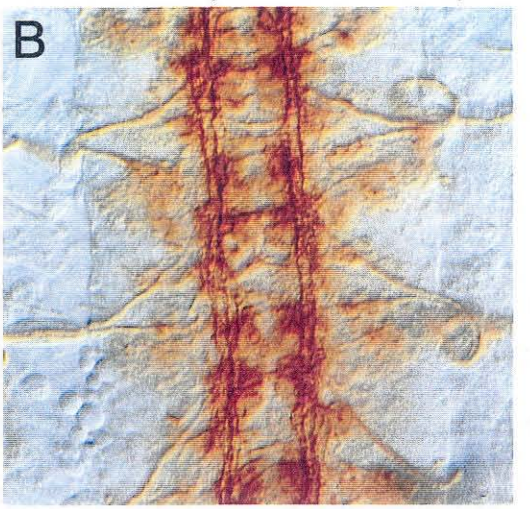

T32

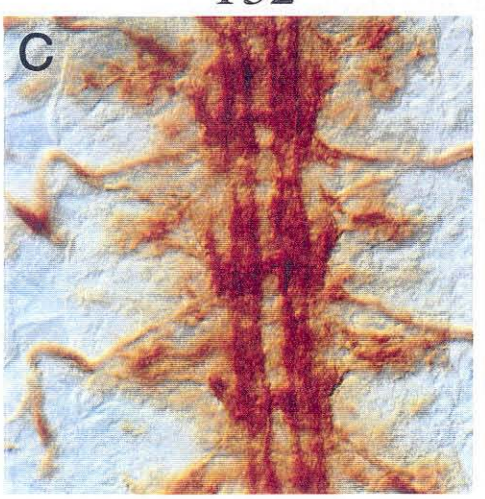

T96 (*commissureless*)

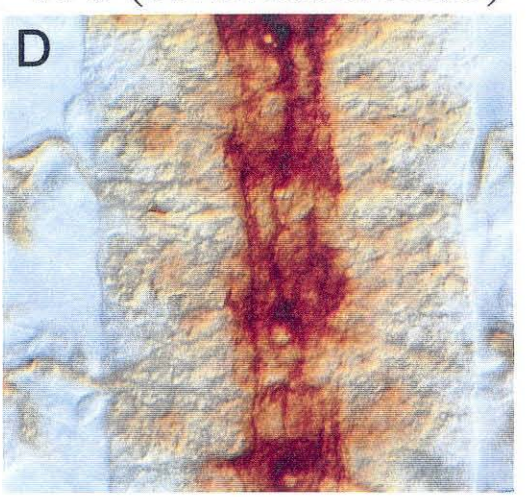

T68

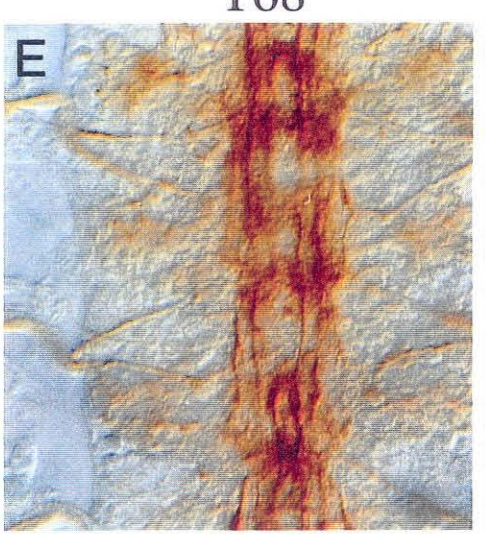

C44

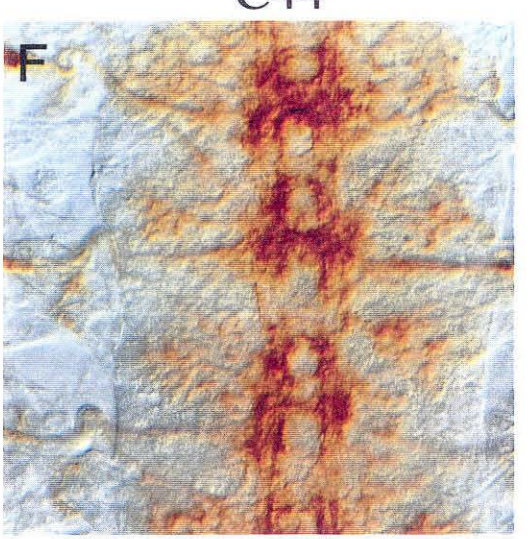

Figure 4. Phenotypes of EP lines (II).

(A) T63/C155: Disorganized CNS fasciculation pattern.

(B) T18/C155: A Stage 16 mutant embryo shows CNS axonal pattern like a stage 14 wild-type embryo.

(C) T32/C155: The longitudinal tracts of this embryo move closer to the midline.

(D) T96/C155: The inner axon bundle circles around the midline. This phenotype is similar to the *robo* mutant (see Chapter 2 of this thesis).

(E-F) T68/C155(E) and C44/C155(F): These two lines have similar phenotypes. The inner bundles of Fas II longitudinal axons are fused in many segments. The longitudinal tracts are always broken.

T37

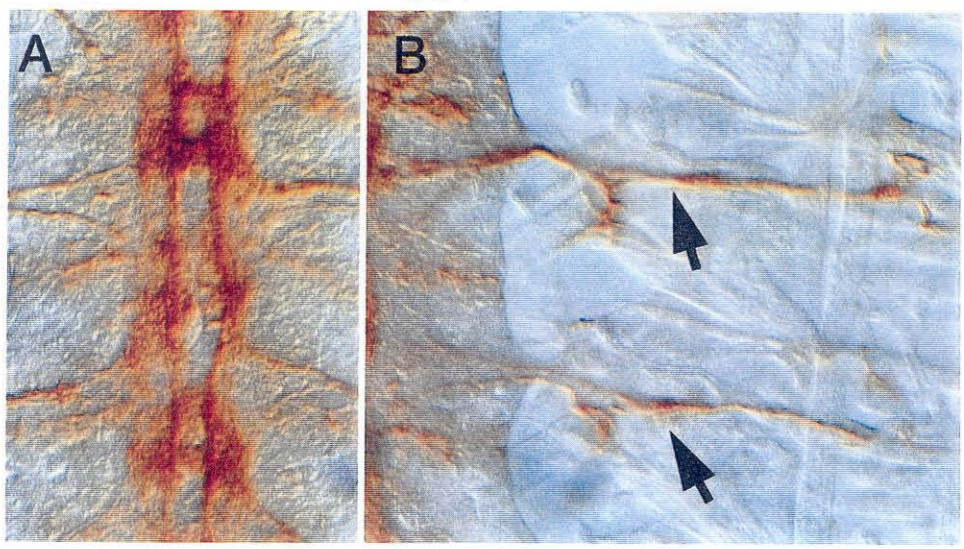

C53 (*bowl*)

C56

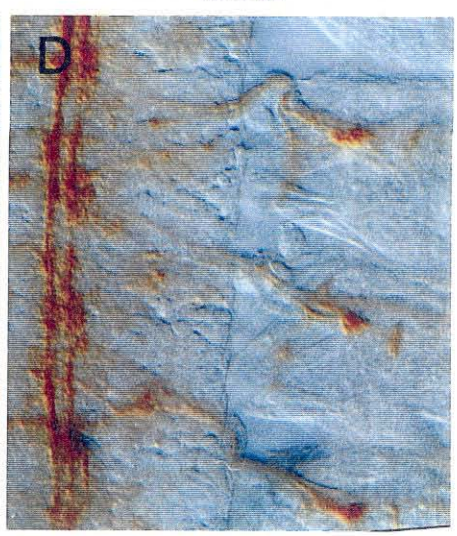

Figure 5. Phenotypes of EP lines (III).

(A-B) C37/C155: Almost all ISNbs do not separate from ISN at the exit junctions (B, arrows). These embryos also exhibit severe CNS phenotypes. The two outside Fas II bundles are discontinuous, and defasciculated (A).

(C) C53/C155: The mutant embryo exhibits high penetrance of ISNb fusion bypass phenotype. The CNS is relatively normal.

(D) C56/C155: ISNbs stall in most segments. The most outside Fas II bundles are discontinuous.

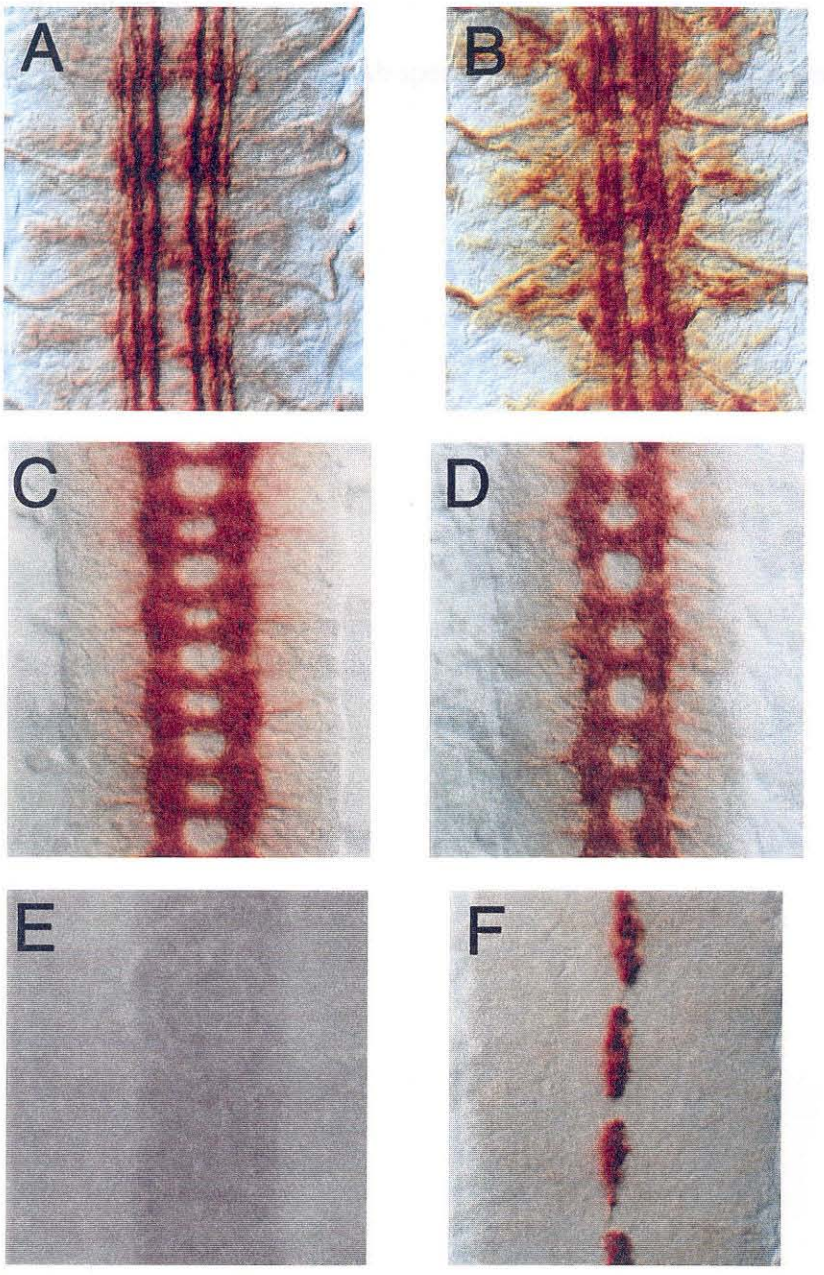
A
B
C
D
E
F

Figure 6. Expression pattern and mutant phenotypes of T32.

(A-D) Wild-type (A, C) or 155; T32 (B, D) embryos stained with mAb 1D4 (A, B) or mAb BP102 (C, D).

(E) RNA in situ pattern of T32.

(F) Wild-type embryo stained with a mAb specific for Wrapper, a midline-expressing protein.

```
        10         20         30         40         50         60         70         80
MVRTKNQSSS SSASSSSTKS PIKSSSGAGS SGGGLGGRQS THRSSSASNV AAVVAGGSSA AGGGSSSNRR SPGSSPDGDD

        90        100        110        120        130        140        150        160
DTTTTDDLTP TTCSPRSGHH HSYGGYSSSV HKQNLYVVSF PIIFLFNVLR SLIYQLFCIF RYLYGASTKV IYRPHRRDCN

       170        180        190        200        210        220        230        240
IEIVVQNSSK EQQQSLNHPS ELNREGDGQE QQLSNQPQRF RPIQPLEMAA NRPGGGYSPG PGDPLLAKQK HHHRRAFEYI

       250        260        270        280        290        300        310        320
SKALKIDEEN EGHKELAIEL YRKGIKELED GIAVDCWSGR GDVWDRAQRL HDKMQTNLSM ARDRLHFLAL REQDLQMQRL

       330        340        350        360        370        380        390        400
SLKEKQKEDA QSKPQKTREP MLAGMTNEPM KLRVRSSGYG PKATTSAQPT ASGRKLTIGS KRPVNLAVAN KSQTLPRNLG

       410        420        430        440        450        460        470        480
SKTSVGAVQR QPAXTAATPP AVRRQFSSGR NTPPQRSRTP INNNGPSGSG ASTPVVSVKG VEQKLVQLIL DEIVEGGAKV

       490        500        510        520        530        540        550        560
EWTDIAGQDV AKQALQEMVI LPSVRPELFT GLRAPAKGLL LFGPPGNGKT LLARAVATEC SATFLNISAA SLTSKYVGDG

       570        580        590        600        610        620        630        640
EKLVRALFAV ARHMQPSIIF IDEVDSLLSE RSSSEHEASR RLKTEFLVEF DGLPGNPDGD RIVVLAATNR PQELDEAALR

       650        660        670        680        690        700        710        720
RFTKRVYVSL PDEQTRELLL NRLLQKQGSP LDTEALRRLA KITDGYSGSD LTALAKDAAL EPIRELNVEQ VKCLDISAMR

       730        740        750
AITEQDFHSS LKRIRRSVAP QSLNSYEKWS QDYGDITI
```

Figure 7. Protein sequence of T32

```
T32 166   QNSSKEQQQSLNHPSELNREGDGQEQQLSNQPQRFRPIQPLEMAANRXXXXXXXXXXXXL 225
          + + +E   +  H  +L       EQ+  ++    R +Q  EMA
Myo 954   KKTDQELSDTKKHVQDLELSLRKAEQEKQSRDHNIRSLQD-EMANQDEAVAK-------- 1004

T32 226   LAKQKHHHRRAFEYISKALKIDEENEGHKELAIELYRKGIKELEDGIAVDCWSGRGDVWD 285
          L K+K H   +   +++ L+ +E+   H E       + + ELE+ I  +  S RGD+ +
Myo 1005  LNKEKKHQEESNRKLNEDLQSEEDKVNHLEKIRNKLEQQMDELEENIDREKRS-RGDI-E 1062

T32 286   RAQRLHDKMQTNLSMARDRLHFLALREQDLQMQRLSLKEKQKE 328
          +A+R   K++ +L +A++ +  +  ++ D++    +LK K+++
Myo 1063  KAKR---KVEGDLKVAQENIDEITKQKHDVE---TTLKRKEED 1099
```

Figure 8. Partial sequence alignment of T32 and *C. elegans* myosin heavy chain.

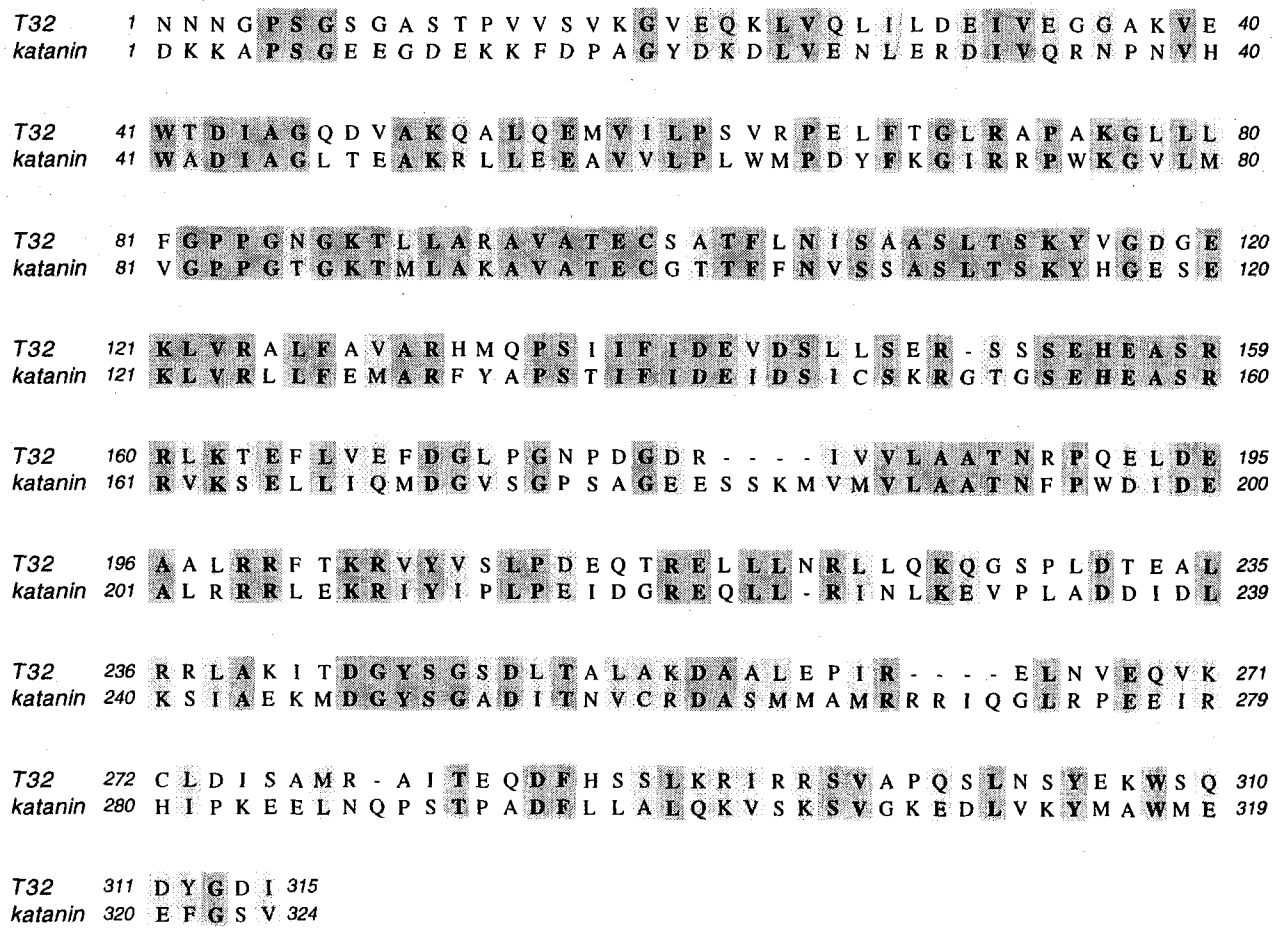

Figure 9. Sequence alignment of ATPase domain of T32 and Katanin.

Table 2. EP lines on 2nd Chromosome

LINE	Viability	X C155	X 24B	1D4 pattern (X C155)	1D4 pattern (X 24B)	Identified gene
C002	V	L	V	OK		
C003	L	L	L	OK		
C004	L	L	V	OK		
C010	V	L	L	OK		
C011	V	L	L	OK		
C012	L	L	L	OK		
C016	s	L	L	OK		
C017	V	L	V	OK		
C031	V	L	L	OK		
C032	V	L	V	OK		
C033	L	L	L	OK		
C034	V	s	V	OK		
C035	L	L	L	OK		
C036	V	L	L	OK		
C037	L	L	L	ISNb bypass, midline crossing		
C040	V	L	L	OK		
C041	V	L	V	OK		
C042	V	L	V	OK		
C043	L	L	L	OK		
C044	s	L	L	Midline crossing		
C045	V	L	L	OK		
C046	L	L	V	OK		
C049	L	L	V	OK		
C050	V	L	L	OK		
C051	L	L	L	OK		
C052	L	L	L	OK		
C053	V	L	L	ISNb bypass		*bowl*
C054	L	V	L		Abnormal Muscles and motoraxons	
C055	L	L	L	OK		
C056	L	s	V	ISNb stall (or delay)		
C057	L	L	s	OK		
C058	V	V	L		OK	
C059	V	V	L			
C061	V	L	V			
C062	L	V	L			
C063	s	L	L			
C064	L	V	L			
C065	V	L	L			
C066	V	L	V			
C067	V	V	L			

C068	L	V	L			
C069	V	s	V			
C070	L	L	V			
C072	V	V	L			
C100	V	L	V			
C101	V	V	L			
C103	s	s	V			

Table 3. EP lines on 3rd Chromosome

LINE	Viability	X C155	X 24B	1D4 pattern (X C155)	1D4 pattern (X 24B)	Identified gene
T003	L	L	V	OK		
T004	V	L	V	OK		
T006	L	s	s	OK		
T007	s	L	L	OK		
T010	L	L	V	Fasciculation error, ISNb stall		
T011	L	s	V	OK		
T012	L	L	L	OK		
T013	L	V	L	Abnormal		
T014	L	L	L	OK		
T015	V	L	L	OK		
T016	L	L	L	Abnormal		
T017	L	L	L	OK		
T018	V	L	V	Oveall CNS development stalled		*headcase*
T019	L	L	L	Defasciculatio n n=1		
T020	L	L	L	OK		
T021	L	L	L	OK		
T024	L	L	L	OK		
T025	L	L	L	OK		
T026	L	L	L	OK		
T027	V	L	L	OK		
T028	L	L	V	OK		
T029	V	L	V	OK		
T031	V	L	L	Fasciculation problems		
T032	V	L	L	Midline collapse		
T033	L	L	L	OK		
T034	L	L	L	OK		
T035	L	L	V	OK		
T036	L	L	V	OK		
T039	L	L	L	OK		
T040	s	L	V	OK		
T041	L	s	V	OK		
T042	V	L	s	Oveall CNS development stalled		*headcase*
T045	L	L	L	OK		
T046	V	L	L	OK		
T047	V	L	V	OK		

T050	L	L	L	OK		
T051	s	L	L	OK		
T052	L	L	L	OK		
T053	V	L	L	OK		
T055	L	L	L	OK		
T056	s	L	V	OK		
T058	V	L	L	OK		
T059	L	L	L	OK		
T060	L	L	L	OK		
T061	L	L	V	OK		
T063	L	L	V	*Fasciculation* problems		
T064	V	L	V	OK		
T065	L	L	L	OK		
T067	L	L	L	OK		
T068	L	L	L	Midline crossing		
T069	L	V	L		OK	
T071	L	L	V	Abnormal		*headcase*
T072	L	V	L		OK	
T073	s	L	V	OK		
T074	L	L	s	OK		
T075	L	V	L		OK	
T078	V	V	L		OK	
T080	L	V	L		OK	
T081	L	V	L		OK	
T082	L	L	L	OK		
T083	L	V	L		OK	
T084	V	V	L		OK	
T085	V	L	V	OK		
T086	L	L	V	Abnormal		
T087	L	V	L		OK	
T089	L	L	V	OK		
T090	V	L	V	OK		
T091	L	V	L		OK	
T092	L	L	L	OK		
T093	L	L	L	OK		
T094	L	V	L		OK	
T096	L	s	V	Midline crossing		*commissureless*
T097	L	L	s	OK		
T098	L	L	V	OK		
T099	L	L	V	OK		
T101		L	V			
T102	L	L	V	OK		
T103	L	L	L			
T104	L	V	L		OK	
T105	L	L	L	OK		

T106	V	L	V	OK		
T107	L	V	L		OK	
T108	L	L	V	OK		
T109	L	V	L		OK	

Appendix 1

Slit branches out: a secreted protein mediates both attractive and repulsive axon guidance

Kai Zinn and Qi Sun

Published in *Cell* **97**, 1-4, 1999

Slit is a large, modular extracellular matrix protein containing four arrays of leucine-rich repeat (LRR) sequences, followed by a string of epidermal growth factor-like (EGF) repeats (Rothberg et al., 1990). *slit* mutations were first identified in the famous Nüsslein-Volhard/Wieschaus patterning screen because they affect external midline structures in the *Drosophila* embryo (Nüsslein-Volhard, Wieschaus, and Kluding, 1984). *Drosophila* and *C. elegans* have a single *slit* gene, while humans and rats have three (Holmes et al., 1998; Itoh et al., 1998; Nakayama et al., 1998; Brose et al., 1999; Li et al., 1999).

Slit is expressed by midline glia in the fly embryo, and in *slit* mutants these glia are ventrally displaced and the ladder-like axon scaffold of the central nervous system (CNS) collapses down to a single tract at the midline (Figure 1B). Mutations that delete all midline glia produce similar phenotypes, so Slit was thought to be primarily involved in the control of midline cell fates. The collapse of the axon ladder was assumed to be a secondary consequence of these cell fate changes. A series of recent papers in *Cell* and *Neuron* (Kidd et al., 1999; Brose et al., 1999; Li et al., 1999; Wang et al., 1999; Nguyen Ba-Charvet et al., 1999), and a paper in press in *Development* (Battye et al., 1999), however, now show that Slit's major functions are likely to be in the direct control of axon guidance decisions. Remarkably, Slit has been shown to have at least two distinct guidance activities, discovered through complementary genetic and biochemical approaches.

Analysis of mutant phenotypes in *Drosophila* embryos showed that Slit is likely to represent a postulated activity at the midline that repels growth cones (Kidd et al., 1999). Vertebrate Slit proteins were shown to be capable of repulsion of axons in explant cultures (Brose et al., 1999; Li et al., 1999; Nguyen Ba-Charvet et al., 1999). The biochemical experiments that identified Slit were based on a different premise. Many vertebrate neurons extend collateral branches from their axon shafts after the

primary growth cone has already advanced far ahead. In some cases the main axon is later retracted, and the collateral branches become the connections to the major target area. In other cases both the collaterals and the primary axon are maintained, allowing the neuron to simultaneously communicate to multiple target areas. The factors that induce collateral branching far from the primary axon's target have not been molecularly characterized to date. Accordingly, an assay was devised to detect activities in brain extracts that could promote branch formation from axons of dissociated rat dorsal root ganglion (DRG) neurons. The purified branch-promoting activity turned out to be the N-terminal portion of the Slit protein (Wang et al., 1999).

Slit is required for repulsion of axons from the midline in *Drosophila*. In the fly CNS and the vertebrate spinal cord, axons grow to the midline because attractive molecules such as netrins are expressed there. Midline repulsive activities may also be necessary, however, to prevent longitudinal axons that express attractive netrin receptors from crossing the midline. Furthermore, repulsion is required to allow the growth cones of commissural neurons to leave the midline as they travel across the CNS, and to keep them from later returning to the midline. The transmembrane protein Roundabout (Robo), which is expressed on neuronal growth cones and axons, is a receptor for this midline repulsive signal in *Drosophila*. In *robo* mutants, some longitudinal axons fail to be repelled from the midline and cross over to the contralateral side of the CNS, while commissural axons follow looping paths around the midline, crossing it multiple times (Kidd et al., 1998a; Figure 1B).

Robo function is controlled by the Commissureless (Comm) protein. Comm is also a transmembrane protein, but it is expressed on midline glia and is transferred to commissural axons by an unknown mechanism (Tear et al., 1996). Comm causes degradation or downregulation of Robo in the commissures. After commissural axons

cross the midline, Robo protein inserted into the membrane at the growth cone may escape Comm-mediated downregulation, because the growth cone is no longer in the zone within which it can acquire Comm from the midline glia. Robo on the growth cone would now stimulate its growth, driving it away from the midline repellent. Repulsion can thus facilitate axonal growth as well as reduce it, allowing formation of axon tracts that cross over the repellent source (Figure 1A). In a *comm* mutant, Robo fails to be downregulated, so that all axons are repelled from the midline and no commissures form (Figure 1B; Kidd et al., 1998b).

A clue that secreted Slit might be the midline repellent for the Robo receptor came from experiments in which Comm was expressed on all neurons. Comm expression at moderate levels caused Robo to be downregulated on all axons and therefore generated a *robo*-like phenotype. High-level Comm expression, however, produced a phenotype like that of *slit*, in which all axons converged onto the midline (Kidd et al., 1999). Thus, Comm has additional targets involved in repulsion by the midline, and when all of these are eliminated axons grow to the midline and never leave. One such target might be a second Robo protein, Robo-2 (Kidd et al., 1998a).

The potential relationship between Slit as ligand and Robo as receptor suggested by these results was then tested by making double mutants, and it was found that *slit* and *robo* mutations interact in a dosage-sensitive manner (*i.e.*, *slit/+*, *robo/+* and *robo/robo* phenotypes are similar; Kidd et al., 1999). A dosage-sensitive relationship is usually taken as evidence that two mutations affect proteins in the same pathway. Slit was also demonstrated to be a repellent by overexpressing it either at the midline or in stripes across the CNS, resulting in phenotypes in which axons turned away from Slit-expressing regions (Battye et al., 1999).

Slit binds to Roundabout receptors.

To study the interactions of Slit and Robo *in vitro*, fly and vertebrate proteins were epitope-tagged and expressed in transfected mammalian cells. Slits bind to Robo-expressing cells, and *vice versa* . The two proteins can also be coprecipitated from a mixture of Slit and Robo-containing lysates. In cross-species binding experiments, the fly and mammalian Slits and Robos were able to interact with each other. The K_ds for binding of vertebrate Slits to Robos are in the low nanomolar range (Brose et al. 1999; Li et al., 1999).

Slit repels motor and olfactory bulb axons.

The mRNAs encoding the three mammalian Slits are localized in complex, overlapping patterns which are consistent with the involvement of Slit proteins in multiple guidance pathways. They are expressed, however, at two places and times where repulsion of axons apparently occurs. These are the floor plate in the spinal cord, and the septum in the forebrain, at E11-E13 (Itoh et al., 1998; Holmes et al., 1998; Brose et al., 1999; Li et al., 1999; Nguyen Ba-Charvet et al., 1999). Both regions have been shown to be capable of repelling axons in explant cultures (Pini, 1993; Guthrie and Pini, 1995).

To evaluate whether recombinant Slit could function as a repellent, Brose et al. (1999) co-cultured aggregates of Slit expressing cells with explants of ventral spinal cord. Spinal motor axons grow profusely out of these explants, and these axons are repelled by floor plate cells (Guthrie and Pini, 1995). It was observed that when an explant was placed adjacent to a Slit-expressing cell aggregate, axonal outgrowth was greatly reduced on the side of the explant that faced the aggregate (Figure 2B). Thus, Slit can repel motor axons. This repulsion might be mediated by Robo, since Robo mRNAs are expressed in the motor columns. Slit had no effect on spinal commissural axons, which by analogy to the fly system might be expected to be repelled by Slit after they cross the floor plate.

The axons of olfactory bulb projection neurons follow the lateral olfactory tract into the olfactory cortex, avoiding the septum. Septal tissue repels olfactory bulb axons in explant cultures (Pini, 1993). Slit-expressing cells were found to also be capable of repelling these axons when placed adjacent to olfactory bulb explants (Li et al., 1999; Nguyen Ba-Charvet et al., 1999). To examine the effects of Slit on axon outgrowth from the olfactory bulb in its normal context, an intact piece of tissue containing the olfactory bulb and telencephalon was cultured, and the telencephalon was covered with aggregates of Slit-expressing or control cells. Olfactory bulb projection axons turned away from regions covered with Slit cells, showing that Slit is capable of repelling these axons when they are growing along normal telencephalic pathways (Li et al., 1999; Figure 2C). Finally, Slit induced growth cone collapse when added to olfactory bulb cultures (Nguyen Ba-Charvet et al., 1999). Thus, Slits resemble semaphorins, the best characterized chemorepellents, in that they can both collapse growth cones in short-term assays and inhibit directional axon outgrowth in longer-term cultures.

Slit promotes axonal branching.

The identification of factor(s) that promote extension of collateral branches required the development of an assay in which branch formation could be easily quantitated. To do this, Wang et al. (1999) took advantage of certain properties of cultured DRG neurons. In the rat, DRG axons contact the spinal cord at the dorsal root entry zone, bifurcate and extend longitudinally in both rostral and caudal directions, and then branch and send collaterals into the dorsal spinal cord. Nerve growth factor (NGF)-responsive small-diameter DRG neurons begin to extend collateral branches into the spinal cord at E16. When E14 DRG neurons were cultured at low density in a collagen matrix in the presence of NGF, their development was slowed, so that they extended simple axons with few branches during the first four days. Later, however, the axons elaborated

more complex branches. This assay provided a way to search for activities that could promote the precocious formation of branches from E14 neurons.

E17 rat spinal cord extracts were found to stimulate axon outgrowth and increase branch number. Similar activities were found in extracts from calf brain membranes, providing an abundant source of material for purification. Calf brain extract was able to increase the number of branch points per axon by up to 5-fold (from about 0.5 to 2.5), while also increasing axonal length by up to 2.5-fold (Figure 2A). By fractionating the extract through several columns, it was determined that the presence of a 140 kD band correlated with activity. The sequences of tryptic peptides from the purified band identified it as bovine Slit-2.

Slit-1 and Slit-2 mRNAs are expressed in the dorsal spinal cord at the time when DRG neurons extend collateral branches (Wang et al., 1999), so Slits are in the right places to promote collateral formation *in vivo*. Some or all of the branch-promoting activity found in E17 rat spinal cord extracts is likely to be due to Slit proteins, since Slits are expressed at high levels in spinal cord at this time. We do not know, however, whether Slit can induce collateral branch formation in a system that more closely resembles the environment of the dorsal root entry zone in which DRG neurons branch into the spinal cord during embryogenesis. Thus, although Slit can promote branching in dissociated cultures, there is as yet no evidence that it actually does this *in vivo*.

Interestingly, all three Slit mRNAs are also present in the DRG itself, suggesting the possibility that the elaboration of axonal branches that occurs in the DRG cultures after several days is due to an autocrine effect of Slit produced by DRG neurons. It has not been determined whether Robo proteins, which are likely to be the receptors for the negative repulsive activities of vertebrate Slits, also mediate Slit's positive elongation and branch-promoting activities.

Slit expression and 3D axon guidance.

The complex geometry of Slit-expressing zones in the brain and spinal cord may be capable of sculpting the trajectories of many axon pathways in three dimensions. This is especially true since these zones may function as repellents for some axons and as attractants for others. For example, as proposed by Li et al. (1999), spinal commissural axons that have crossed the midline might be driven away from it by repulsion from Slit in the floor plate, then forced to turn longitudinally by avoidance of Slit in the motor columns. The detailed geometries of the Slit and Robo-expressing regions in the hippocampus (Nguyen Ba-Charvet, 1999) may be important in shaping its characteristic synaptic pathways and in determining its inputs from and outputs to other cortical regions.

Proteolytic processing of Slit.

The 140 kD protein that correlated with branching activity was smaller than full-length Slit, indicating that Slit is processed (Wang et al., 1999). When Slit-2 was expressed in mammalian cells, it was found to be cleaved into a 140 kD N-terminal fragment, Slit-2-N, and a smaller C-terminal fragment, Slit-2-C. Slit-2-N is tightly associated with the cell surface, while Slit-2-C partitions equally between the cell surface and the medium. *Drosophila* Slit is processed in a similar manner *in vivo* (Brose et al., 1999). The molecular mass of the N-terminal Slit fragment suggested that the bovine branch-promoting protein might be Slit-2-N, and recombinant human Slit-2-N was then found to be active in the branching and elongation assay. Full-length Slit-2 was inactive, however, and may actually inhibit the activity of Slit-2-N (Wang et al., 1999).

Slit as an organizer of guidance molecules.

Slit-2 was found to bind to netrin and laminin, and its affinity for netrin is similar to that for Robo (Brose et al., 1999). This result suggests that Slit, which is a large modular

protein with many different conserved binding domains, might be an extracellular 'organizer' which could simultaneously bind several different axon outgrowth and guidance factors and deliver them to Slit-responding neurons. The properties of Slit in directing guidance might thus vary depending on what other Slit-binding molecules are present in its vicinity. In this respect, Slit might be like an extracellular version of the large cytoplasmic insulin receptor substrate (IRS) proteins, which contain many distinct tyrosine motifs that are phosphorylated by different kinases and bind to different signaling adapters. IRS proteins organize different collections of signaling molecules (and thus stimulate or block specific transduction pathways) depending on which tyrosine kinases have been activated and which phosphotyrosine-binding adapters are available (White, 1998). Slit could perform conceptually similar functions in the extracellular milieu. In this regard, we note that since neither group has evaluated binding between purified proteins, it remains possible (though perhaps unlikely) that Slits and and Robos do not directly interact, but form a 'sandwich' complex with another protein expressed in the transfected cells that can bind to both Slit and Robo.

Concluding remarks.

The identification of Slit as a multifunctional axon guidance factor will undoubtedly soon lead to new findings concerning Slit signaling pathways, receptors for attractive Slit signals, and the phenotypes of *slit* knockout mice. Beyond these obvious experiments, many exciting problems for the future are suggested by the results presented in these papers. This work might eventually have clinical relevance if Slits can stimulate outgrowth and branch formation by regenerating spinal cord axons. Furthermore, activity-dependent collateral branch formation by cortical neurons might be mediated by Slits, since they are expressed in cortex after birth (Wang et al., 1999; Nguyen Ba-Charvet et al., 1999). For example, visual cortex neurons in an orientation

column have secondary collateral branches that selectively form connections within nearby columns with the same orientation specificity. These long-range horizontal connections are thought to be involved in perceiving the continuity of objects (Gilbert, 1992). Perhaps Slit function can be regulated by activity in order to promote formation of appropriate cortical connections such as these. Both positive and negative activities of Slit could be involved in plasticity, since branch formation would lead to creation of new synaptic connections and repulsion could prevent inappropriate connections from forming.

In summary, these papers identify Slit as a central player in repulsive and attractive axon guidance. Further work should clarify how and under what conditions Slit regulates formation and rearrangement of specific connections in the nervous system.

References.

Battye, R., Stevens, A., and Jacobs, J.R. (1999). Development, in press.

Brose, K., Bland, K. S., Wang, K. H., Arnott, D., Henzel, W., Goodman, C. S., Tessier-Lavigne, M., and Kidd, T. (1999). Cell, in press.

Gilbert, C. D. (1992). Neuron *9*, 1-13.

Guthrie, S., and Pini, A. (1995). Neuron *14*, 1117-30.

Holmes, G. P., Negus, K., Burridge, L., Raman, S., Algar, E., Yamada, T., and Little, M. H. (1998). Mech Dev *79*, 57-72.

Itoh, A., Miyabayashi, T., Ohno, M., and Sakano, S. (1998). Mol Brain Res *62*, 175-86.

Kidd, T., Brose, K., Mitchell, K. J., Fetter, R. D., Tessier-Lavigne, M., Goodman, C. S., and Tear, G. (1998a). Cell *92*, 205-15.

Kidd, T., Russell, C., Goodman, C. S., and Tear, G. (1998b). Neuron *20*, 25-33.

Kidd, T., Bland, K. S., and Goodman, C. S. (1999). Cell, in press.

Li, H. S., Chen, J. H., Wu, W., Fagaly, T., Zhou, L. J., Yuan, W. L., Dupuis, S., Jiang, Z. H., Nash, W., Gick, C., Ornitz, D. M., Wu, J. Y., and Rao, Y. (1999). Cell, in press.

Nakayama, M., Nakajima, D., Nagase, T., Nomura, N., Seki, N., and Ohara, O. (1998). Genomics *51*, 27-34.

Nguyen Ba-Charvet, K. T., Brose, K., Marillat, V., Kidd, T., Goodman, C. S., Tessier-Lavigne, M., Sotelo, C., and Chedotal, A. (1999). Neuron, in press.

Nusslein-Volhard, C., Wieschaus, E., and Kluding, H. (1984). Roux's Arch Dev Biol *193*, 267-282.

Pini, A. (1993). Science *261*, 95-8.

Rothberg, J. M., Jacobs, J. R., Goodman, C. S., and Artavanis-Tsakonas, S. (1990). Genes Dev *4*, 2169-87.

Tear, G., Harris, R., Sutaria, S., Kilomanski, K., Goodman, C. S., and Seeger, M. A. (1996). Neuron *16*, 501-14.

Wang, K. H:, Brose, K., Arnott, D., Kidd, T., Goodman, C. S., Henzel, C., and Tessier-Lavigne, M. (1999). Cell, in press.

White, M. F. (1998). Mol Cell Biochem *182*, 3-11.

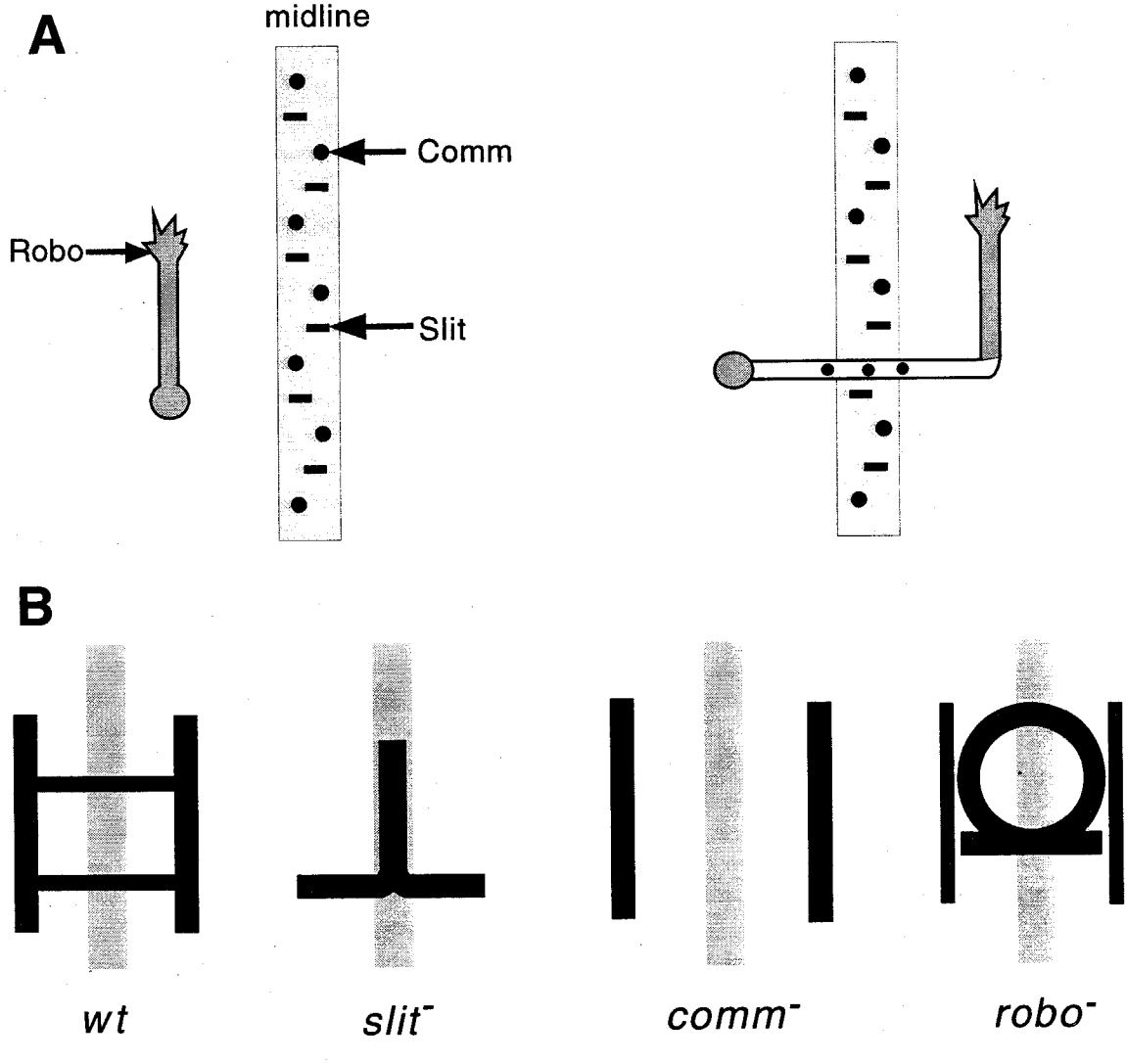
A
midline
Comm
Robo
Slit
B
wt
slit-
comm-
robo-

Figure 1. Mutations affecting growth cone behavior at the midline.

A. Normal behavior of longitudinal and commissural axons. Comm and Slit are expressed by midline glia, while Robo is on CNS growth cones. Comm is transferred to commissural axons and Robo is downregulated when commissural growth cones contact the midline.

B. Wild-type and mutant CNS axon arrays. In the wild-type embryo, two longitudinal axon bundles extend along the length of the embryo. In each segment, there are two commissures crossing the midline. The *robo* and *slit* cartoons represent a subset of axons that are strongly affected by the *robo* mutation.

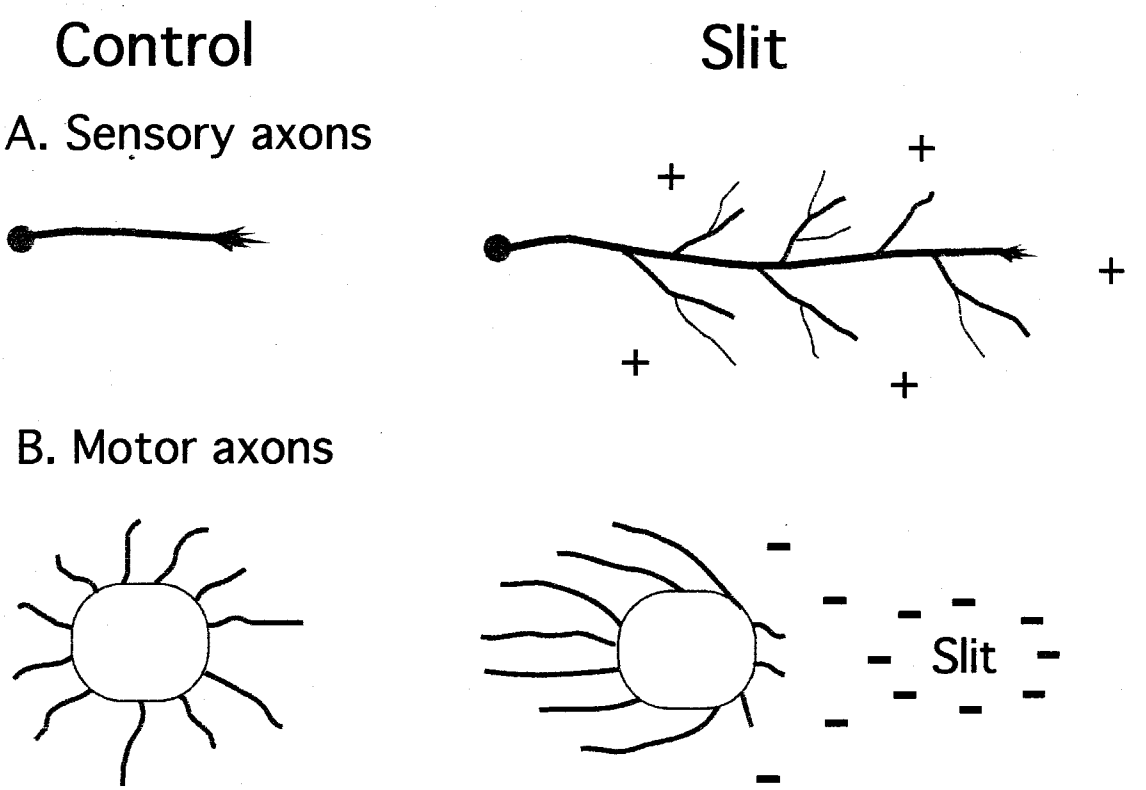
Control
Slit
A. Sensory axons
B. Motor axons
Slit
C. Olfactory bulb axons
Slit

Figure 2. Slit activities.

A. Slit promotes branching of cultured NGF-responsive DRG axons.

B. Slit repels motor axons extending from a spinal cord explant.

C. Olfactory bulb projection axons turn away from Slit-expressing cells covering the telencephalon.

Appendix 2

Tyrosine phosphorylation and axon guidance: of mice and flies

Chand J Desai, Qi Sun and Kai Zinn

Published in *Current opinion in Neurobiology* **7**, 70-74, 1997

Tyrosine phosphorylation and axon guidance: of mice and flies

Chand J Desai[1], Qi Sun[2] and Kai Zinn[3]

Recent genetic evidence suggests that tyrosine kinases and tyrosine phosphatases can control the guidance of specific growth cones. Within a family of related phosphatases or kinases, individual members can have partially redundant functions. Receptor phosphatases can work together at one guidance choice point, but in opposition at another. The specific combination of kinases and phosphatases active in a growth cone may be an important determinant of pathway choice. One mechanism by which these proteins could control guidance decisions is through regulation of adhesion between growth cones and axons.

Addresses
Division of Biology 216-76, California Institute of Technology, Pasadena, California 91125, USA
[1]e-mail: desai@seqaxp.caltech.edu
[2]e-mail: sunq@starbase1.caltech.edu
[3]e-mail: zinnk@starbase1.caltech.edu

Abbreviations

CAM	cell adhesion molecule
DLAR	*Drosophila* homolog of LAR
DPTP	*Drosophila* PTP
Drl	Derailed
FGF	fibroblast growth factor
FGFR	FGF receptor
ISN	intersegmental nerve
LAR	leukocyte common antigen related
NCAM	neural cell adhesion molecule
PTP	protein tyrosine phosphatase
RPTP	receptor PTP
RTK	receptor tyrosine kinase
SNb	segmental nerve b
TK	tyrosine kinase

Current Opinion in Neurobiology 1997, 7:70–74

Electronic identifier: 0959-4388-007-00070

Introduction

A wealth of biochemical and cell biological data indicate that the regulation of tyrosine phosphorylation is essential for neuronal process outgrowth and guidance. Recent genetic analyses have implicated both receptor protein tyrosine phosphatases (RPTPs) and tyrosine kinases (TKs) in the guidance of specific axons. In *Drosophila* embryos, three RPTPs (DLAR, DPTP69D and DPTP99A) and Derailed (Drl), a receptor tyrosine kinase (RTK), are required for guidance of specific axons [1•–3•]. In the mouse, the RTK Nuk is required for anterior commissure formation in the brain [4•]. In addition, studies of mouse mutants have implicated the Src and Fyn TKs in the regulation of neurite outgrowth [5,6].

These genetic results, together with other data on RTK function in vertebrate systems, have led to several basic conclusions about the roles of protein tyrosine phosphatase (PTP) and TK families in controlling outgrowth and guidance. First, members of RPTP and TK families can often have partially redundant functions, so that the absence of one member does not produce strong phenotypes. Second, among the members of a family, there is sometimes a pathway-specific hierarchy of functional importance. Third, RPTP family members can have antagonistic relationships. Fourth, neurite outgrowth on specific substrates may differentially require TK or PTP activity. Finally, RPTP and TK activities may affect guidance by regulating growth cone adhesiveness. In this review, we focus on genetic and reverse genetic studies of RPTPs and TKs that support these conclusions.

Redundancy and compensation among RPTPs and TKs

The genetic analysis of axon guidance has been hampered by a shortage of mutations producing strong and reproducible phenotypes. In *Drosophila*, mutants lacking various neuronal surface proteins whose expression patterns and structures suggest that they are involved in guidance along specific axon pathways have remarkably normal axonal architecture [7–12]. Researchers have postulated that these molecules are important for axon guidance, but functionally redundant pathways could compensate for their loss. Such redundancy would ensure proper nervous system connectivity. Until recently, however, genetic studies have provided little experimental support for this postulate, and it was considered in some quarters to be a 'charitable' explanation at best.

In *Drosophila*, four of the five identified RPTPs are selectively localized to CNS axons in late-stage embryos, suggesting that the primary role of this family of proteins is enacted during neuronal development [13–16]. Mutations have been generated in the genes encoding all four axonal RPTPs, facilitating analyses of function and redundancy within the family. Mutants lacking the RPTPs DPTP99A or DPTP10D are viable, fertile, and have no detectable defects in the embryonic CNS ([12]; S Bahri, Q Sun, K Zinn, W Chia, unpublished results), and the axonal abnormalities observed in mutants lacking DLAR or DPTP69D are incompletely penetrant [1•,2•]. Furthermore, these abnormalities are dramatically enhanced in certain double- and triple-mutant combinations, strongly suggesting that these RPTPs have overlapping functions during development.

The cytoplasmic TKs structurally related to Src (Src-family TKs) also display redundancy of function. Src,

Figure 1

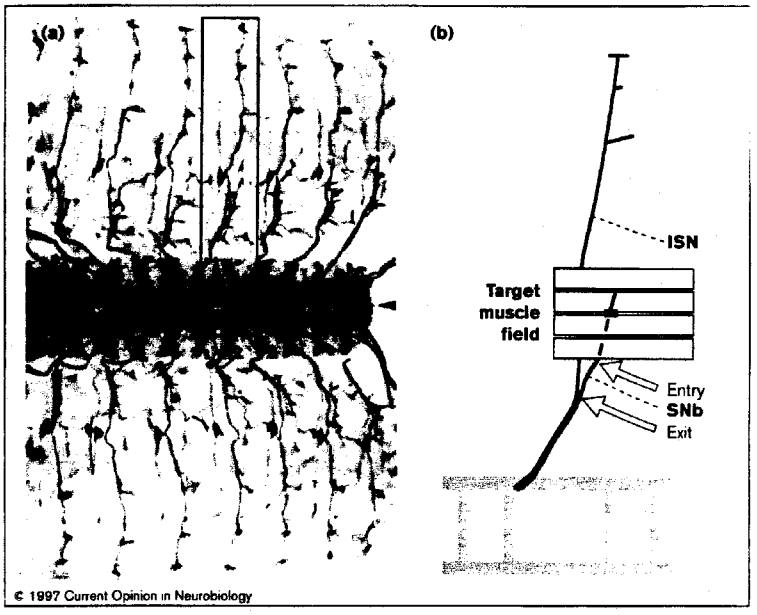

Abdominal motor axon pathways in the *Drosophila* embryo. **(a)** A stage 17 embryo stained with an anti-fasciclin II monoclonal antibody that stains all motor axons. The stereotyped pattern of innervation shared by these hemisegments makes the abdominal neuromuscular system ideal for analyzing axon guidance. Three pairs of axon bundles in the CNS (black arrow) are also stained by this monoclonal antibody. One hemisegment is boxed and shown schematically in the cartoon on the right. **(b)** The only motor nerves shown are the ISN and the SNb. Two choice points along the SNb pathway are indicated (white arrows): Exit, the point at which SNb axons defasciculate from the common pathway; and Entry, the point at which SNb axons enter their target muscle field.

Fyn, Yes and Lyn are expressed in the developing vertebrate CNS, and Src, Fyn and Yes are enriched in growth cone membrane fractions [17–19], suggesting that these TKs are important for neurite outgrowth. Mouse knock-out mutants of all four have been made (reviewed in [20•]; see also [21–26]); however, only *fyn*⁻ mice display any obvious neuronal defects [22]. *fyn*⁻ hippocampi contain extra granule and pyramidal neurons and appear slightly disorganized. *fyn*⁻ mice also perform poorly in certain learning tests, but this learning disability appears to be independent of the anatomical defects [20•]. Although aberrant axonal guidance is not apparent in any of the knock-outs, the complexity of the mouse brain may prevent detection of subtle, incompletely penetrant guidance defects similar to those observed in the *Drosophila* RPTP mutants [1•,2•].

Compensatory interactions among Src-family TKs may ameliorate the phenotypic consequences of single gene knock-outs. *In vitro* experiments show elevated Src activity in both *fyn*⁻ and *yes*⁻ brains, and the activities of Fyn and Yes are increased in *src*⁻ brains [27•]. In contrast, the activities of Yes in *fyn*⁻ brains and Fyn in *yes*⁻ brains are unchanged. The alterations in TK activity in knock-out mice suggest that Src and Fyn act together in one process, whereas Src and Yes cooperate in another. *src*⁻;*fyn*⁻ and *src*⁻;*yes*⁻, but not *fyn*⁻;*yes*⁻, double mutants die at birth [24], suggesting that the compensation seen in single mutants is functionally important for viability. However, synergistic neuronal defects in double mutants have not yet been documented.

Hierarchies among RPTPs and TKs are dependent upon developmental context

Although they share responsibilities for certain guidance decisions, a detailed analysis of two motor nerves has revealed that RPTPs also have unique functions (C Desai, NX Krueger, H Saito, K Zinn, unpublished data). For axons in the segmented nerve b (SNb) (Figure 1), DPTP69D plays the major role in an early guidance decision to exit a common nerve pathway, because this decision rarely fails in RPTP mutant combinations unless Ptp69D function is absent. Navigation of SNb growth cones among the muscle fibers also involves DPTP69D function. By contrast, DLAR is most important for early guidance along the intersegmental nerve (ISN) (Figure 1), whereas DPTP69D is a minor player in these decisions. The loss of DPTP69D and/or DPTP99A leads to premature termination of ISN axons, but only in a *Dlar*⁻ background. Along both pathways, DLAR appears to be required for maturation of growth cones into synapses. From these observations emerges a picture of RPTP foremen and assistants, with the identity of the foreman being dependent on the job to be performed.

The hierarchical relationships among Src-family TKs also depend upon developmental context (reviewed in [20•]). Several of these TKs are widely expressed in the brain and other tissues. In the brain, however, Fyn is first among equals, because only in *fyn*⁻ mice are anatomical defects and reduced tyrosine phosphorylation of proteins in the brain observed [22]. By contrast, osteoclast defects are only observed in *src* mutants [21], and B cell defects

are unique to *lyn* mutants [25,26]. *yes* mutants have no detectable defects in any tissue [24]. These phenotypes suggest that individual Src-family TKs can have primary responsibilities in one developmental process, but defer to another family member in another.

Cooperation and competition among RPTPs

In the SNb pathway, the relationship between DPTP69D and DPTP99A is similar to that between Batman and Robin. When Batman (DPTP69D) is on the scene, no one cares if Robin (DPTP99A) shows up. When DPTP69D is mutant, however, DPTP99A function becomes important for many guidance decisions. In *Ptp69D*;*Ptp99A* double mutants, errors in SNb axon guidance increase by 5- to 10-fold relative to mutants lacking DPTP69D alone [1•]. Along the ISN pathway, DPTP99A can also assist DLAR: *Ptp99A* mutations synergize with *Dlar* mutations to produce more severe defects. By contrast, DLAR and DPTP99A have an antagonistic relationship at one decision point along the SNb pathway. In *Dlar* mutants, the SNb nerve sometimes turns away from its muscle targets after leaving the common nerve pathway, resulting in a failure of muscle innervation (C Desai, NX Krueger, H Saito, K Zinn, unpublished data). The concomitant loss of DPTP99A suppresses this 'parallel bypass' phenotype, indicating that it is a consequence of inappropriate DPTP99A activity. These results suggest that DLAR downregulates or counteracts DPTP99A activity at the muscle entry point

It is interesting to compare this parallel bypass phenotype to the behavior of *Xenopus* retinal axons when the function of the fibroblast growth factor receptor (FGFR) is perturbed. In brains bathed in exogenous fibroblast growth factor (FGF), retinal axons often fail to enter their normal synaptic target, the optic tectum [28•]. Surprisingly, similar errors are made by axons expressing a dominant-negative FGFR construct [29•]. The finding that either constitutively activating or inhibiting the FGFR produces similar phenotypes suggests that a change in FGFR activity is crucial for recognition of the tectum. This supposition is supported by the presence of endogenous FGF in the optic tract and its absence in the tectum.

One intriguing speculation is that common processes are involved in target recognition in *Drosophila* and *Xenopus*. In *Drosophila*, inhibition of DPTP99A signaling at the muscle entry point may change the balance between TK and PTP activities in the SNb growth cones. Such a change may be required for recognition of these muscles by the SNb growth cones, just as a change in FGFR activity appears to signal recognition of the tectum by retinal axons in *Xenopus*.

Axon pathways are differentially dependent upon RPTP function

One of the paradoxes of the genetic analysis of RPTP function is that although most or all axons express DLAR, DPTP69D and DPTP99A, only specific pathways are abnormal in mutants. In particular, certain CNS pathways appear relatively normal even in triple mutants (C Desai, NX Krueger, H Saito, K Zinn, unpublished data). Among the mixed nerves, motor axon extension along established sensory axon bundles also proceeds relatively normally in triple mutants, suggesting that RPTP activity may be more important for axons pioneering trails into virgin territory.

RTK activity, however, does appear to be required for normal axonal growth within nerve bundles [29•]. In *Xenopus*, the FGFR appears to be important for retinal axons as they extend along other axons in the optic tract. Both the rate and the extent of growth within the optic tract is reduced for axons expressing dominant-negative FGFR [30]. *In vitro* experiments suggest that these effects result from the inability of dominant-negative FGFR-expressing retinal cells to respond to endogenous FGF in the optic tract. By contrast, the FGFR appears dispensable for targeting within the FGF-free tectum, in which retinal growth cones are solo navigators.

Tyrosine phosphorylation may regulate interaxonal adhesion

Some of the phenotypes of RPTP mutants are consistent with the idea that RPTP activity promotes defasciculation of axons. In particular, the decision by SNb growth cones to leave the common pathway often fails in triple mutants. This 'fusion bypass' phenotype could occur if the affinity of the SNb axons for other axons in the common pathway were too high. Similarly, increased adhesion among SNb axons may lead to growth cones clumping together and failing to extend individually. Such a 'stall' phenotype is often observed in RPTP mutants [1•].

Remarkably, stall and fusion bypass phenotypes are also observed in mutants overexpressing fasciclin II on all axons [31]. Fasciclin II is a homophilic adhesion molecule [32] and is homologous to the vertebrate neural cell adhesion molecule (NCAM). These results suggest that motor axons and growth cones expressing too much fasciclin II or having too little RPTP activity may be more adhesive. Perhaps RPTP signaling reduces interaxonal adhesion mediated by NCAM or its relatives, allowing growth cones to leave bundles and explore new territory (Figure 2).

Conversely, TK activity may be required for adhesion among axons within bundles or between axons and substrates. For example, activation of the REK7 RTK is required for the bundling of cortical axons extending

Figure 2

Structures of several RPTPs, the cytoplasmic TKs Src and Fyn, and the neural CAMs L1 and NCAM. Studies of *src*⁻ and *fyn*⁻ mutant mice suggest that Src helps mediate the NCAM neurite outgrowth promoting signal, whereas Fyn mediates the L1 signal. LAR, leukocyte common antigen related. The SH1 domain is the tyrosine kinase catalytic region. The SH2 domain is the phosphotyrosine binding site. The SH3 domain binds to proline-rich sequences.

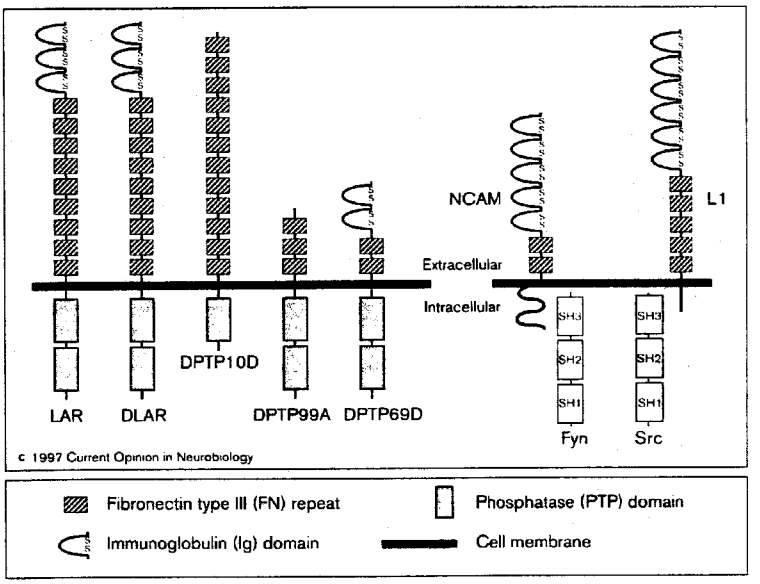

on astrocytes [33•]. As the ligand for REK7 is on the astrocytes, it is likely that REK7 signaling promotes axon fasciculation indirectly, perhaps by upregulating or activating neural cell adhesion molecules (CAMs). Furthermore, cultured cerebellar granule cell neurons from *src*⁻ mice are defective in responding to the neural CAM L1 as a neurite outgrowth promoting substrate [6]. Similarly, cultured granule cell neurons from *fyn*⁻ mice are completely refractory to the neurite-promoting effect of NCAM [5]. L1, NCAM and other neural CAMs are thought to be important axon guidance molecules *in vivo*, and neurite outgrowth promotion is considered a surrogate for this activity *in vitro*. The defective response of *src*⁻ and *fyn*⁻ neurons to L1 and NCAM suggests that the adhesive and guidance signals initiated by these CAMs result in increased tyrosine phosphorylation of growth cone proteins mediated by activation of Src-family TKs (Figure 2).

Conclusions

In summary, TKs and PTPs appear to work in tandem to control different aspects of growth cone guidance. The presence of multiple members of both families in growth cones may reflect the complexity involved in correctly wiring the nervous system. Growth cone guidance along one pathway could employ a specific subset of PTP and TK family members, whereas guidance along another pathway may exploit a different but overlapping subset. Functional redundancy among family members may thus be a by-product of the large number of TKs and PTPs required to guide growth cones along distinct pathways. The activity of TKs may be highest when axons are traveling together in groups, as in the optic tract. In this context, high interaxonal adhesion mediated through neural CAMs and TKs may keep retinal axons on track. High PTP activity may induce defasciculation, allowing individual axons to seek their synaptic targets. The level of tyrosine phosphorylation in growth cones may be regulated by the differential expression of PTP and TK ligands along axonal pathways. In this way, changing levels of tyrosine phosphorylation could steer growth cones.

Acknowledgements

Funding in the authors' laboratory is from a National Institutes of Health (NIH) ROI grant to K Zinn.

References and recommended reading

Papers of particular interest, published within the annual period of review, have been highlighted as:

- • of special interest

1. • Desai CJ, Gindhart JG, Goldstein LSB, Zinn K: **Receptor tyrosine phosphatases are required for motor axon guidance in the *Drosophila* embryo.** *Cell* 1996, **84**:599–609.
See annotation [2•].

2. • Krueger NX, Van Vactor D, Wan HI, Gelbart WM, Goodman CS, Saito H: **The transmembrane tyrosine phosphatase DLAR controls motor axon guidance in *Drosophila*.** *Cell* 1996, **84**:611–622.
These papers [1•,2•] are the first demonstration of RPTP function in nervous system development. They show that the RPTPs DLAR, DPTP69D and DPTP99A are important for the guidance of certain motor axons. Desai *et al.* [1•] also provide an example of functional redundancy between molecules (DPTP69D and DPTP99A) involved in specific axon guidance.

3. • Callahan CA, Muralidhar MG, Lundgren SE, Scully AL, Thomas JB: **Control of neuronal pathway selection by a *Drosophila* receptor protein tyrosine kinase family member.** *Nature* 1995, **376**:171–174.

Identifies a RTK required for specific axon guidance in *Drosophila*. The axons of interneurons that normally express Derailed (Drl) grow along aberrant pathways in *Drl* mutants.

4. • Henkemeyer M, Orioli D, Henderson JT, Saxton TM, Roder J, Pawson T, Klein R: **Nuk controls pathfinding of commissural axons in the mammalian central nervous system.** *Cell* 1996, **86**:35–46.

The authors provide the first genetic evidence in vertebrates that an RTK is required for the formation of a specific axon tract. Interestingly, Nuk (an Eph family RTK) is not expressed by the commissural axons affected in the mutant. Rather, the neurons over which these axons grow express Nuk, whereas the commissural axons themselves express Lerk2, a ligand of Nuk. Furthermore, the Nuk kinase domain is not required for commissure formation, indicating that, in this case, Nuk may be the ligand and Lerk2 the receptor.

5. Beggs HE, Soriano P, Maness PF: **NCAM-dependent neurite outgrowth is inhibited in neurons from *fyn*-minus mice.** *J Cell Biol* 1994, **127**:825–833.

6. Ignelzi MA, Miller DR, Soriano P, Maness PF: **Impaired neurite outgrowth of *src*-minus cerebellar neurons on the cell-adhesion molecule L1.** *Neuron* 1994, **12**:873–884.

7. Elkins T, Zinn K, McAllister L, Hoffmann FM, Goodman CS: **Genetic analysis of a *Drosophila* neural cell adhesion molecule: interaction of *fasciclin I* and Abelson tyrosine kinase mutations.** *Cell* 1990, **60**:565–575.

8. Grenningloh G, Rehn EJ, Goodman CS: **Genetic analysis of growth cone guidance in *Drosophila*: fasciclin II functions as a neuronal recognition molecule.** *Cell* 1991, **67**:45–57.

9. Kolodkin AL, Matthes DJ, Goodman CS: **The *semaphorin* genes encode a family of transmembrane and secreted growth cone guidance molecules.** *Cell* 1993, **75**:1389–1399.

10. Nose A, Takeichi M, Goodman CS: **Ectopic expression of connectin reveals a repulsive function during growth cone guidance and synaptogenesis.** *Neuron* 1994, **13**:525–539.

11. Chiba A, Snow P, Keshishian H, Hotta Y: **Fasciclin III as a synaptic target recognition molecule in *Drosophila*.** *Nature* 1995, **374**:166–168.

12. Hamilton BA, Ho A, Zinn K: **Targeted mutagenesis and genetic analysis of a *Drosophila* receptor-linked protein tyrosine phosphatase gene.** *Rouxs Arch Dev Biol* 1995, **204**:187–192.

13. Tian S-S, Tsoulfas P, Zinn K: **Three receptor-linked protein-tyrosine phosphatases are selectively expressed on central nervous system axons in the *Drosophila* embryo.** *Cell* 1991, **67**:675–685.

14. Yang X, Seow KT, Bahri SM, Oon SH, Chia W: **Two *Drosophila* receptor-like tyrosine phosphatase genes are expressed in a subset of developing axons and pioneer neurons in the embryonic CNS.** *Cell* 1991, **67**:661–673.

15. Hariharan I, Chuang P-T, Rubin GM: **Cloning and characterization of a receptor-class phosphotyrosine phosphatase gene expressed on central nervous system axons in *Drosophila melanogaster*.** *Proc Natl Acad Sci USA* 1991, **88**:11266–11270.

16. Desai CJ, Popova E, Zinn K: **A *Drosophila* receptor tyrosine phosphatase expressed in the embryonic CNS and larval optic lobes is a member of the set of proteins bearing the 'HRP' carbohydrate epitope.** *J Neurosci* 1994, **14**:7272–7283.

17. Bare DJ, Lauder JM, Wilkie MB, Maness PF: **p59*fyn* in rat brain is localized in developing axon tracts and subpopulations of adult neurons and glia.** *Oncogene* 1993, **8**:1429–1436.

18. Maness PF, Aubury M, Shores CG, Frame L, Pfenninger KH: ***c-src* gene product in developing rat brain is enriched in nerve growth cone membranes.** *Proc Natl Acad Sci USA* 1988, **85**:5001–5005.

19. Bixby JL, Jhabvala P: **Tyrosine phosphorylation in early embryonic growth cones.** *J Neurosci* 1993, **13**:3421-3432.

20. • Lowell CA, Soriano P: **Knockouts of Src-family kinases: stiff bones, wimpy T cells, and bad memories.** *Genes Dev* 1996, **10**:1845–1857.

A comprehensive, well written review of genetic studies of Src-family kinases.

21. Soriano P, Montgomery C, Geske R, Bradley A: **Targeted disruption of the c-src proto-oncogene leads to osteopetrosis in mice.** *Cell* 1991, **64**:693–702.

22. Grant SG, O'Dell TJ, Karl KA, Stein PL, Soriano P, Kandel ER: **Impaired long-term potentiation, spatial learning, and hippocampal development in Fyn mutant mice.** *Science* 1992, **258**:1903–1910.

23. Yagi T, Aizawa S, Tokunaga T, Shigetani Y, Takeda N, Ikawa Y: **A role for Fyn tyrosine kinase in the suckling behaviour of neonatal mice.** *Nature* 1993, **366**:742–745.

24. Stein PL, Vogel H, Soriano P: **Combined deficiencies of Src, Fyn, and Yes tyrosine kinases in mutant mice.** *Genes Dev* 1994, **8**:1999–2007.

25. Hibbs ML, Tarlinton DM, Armes J, Grail D, Hodgson G, Maglitto R, Stacker SA, Dunn AR: **Multiple defects in the immune system of Lyn-deficient mice, culminating in autoimmune disease.** *Cell* 1995, **83**:301–311.

26. Nishizumi H, Taniuchi I, Yamanashi Y, Kitamura D, Ilic D, Mori S, Watanabe T, Yamamoto T: **Impaired proliferation of peripheral B cells and indication of autoimmune disease in lyn-deficient mice.** *Immunity* 1995, **3**:549–560.

27. • Grant SGN, Karl KA, Kandel ER: **Focal adhesion kinase in the brain: novel subcellular localization and specific regulation by Fyn tyrosine kinase in mutant mice.** *Genes Dev* 1995, **9**:1909–1921.

Shows compensatory regulation among Src-family kinases in knock-out mice. Src activity is higher in *fyn*$^-$ and *yes*$^-$ mutants than in wild-type mice, whereas Fyn and Yes activity is increased in *src*$^-$ mutants.

28. • McFarlane S, McNeill L, Holt CE: **FGF signaling and target recognition in the developing *Xenopus* visual system.** *Neuron* 1995, **15**:1017–1028.

See annotation [29•].

29. • McFarlane S, Cornel E, Amaya E, Holt CE: **Inhibition of FGF receptor activity in retinal ganglion cell axons causes errors in target recognition.** *Neuron* 1996, **17**:245–254.

These two papers [28•,29•] show that constitutive activation or inactivation of the FGFR similarly disrupt the guidance of retinal ganglion cell axons at the tectum. This results suggest that a change in FGFR activity may be important for target recognition.

30. Amaya E, Musci TJ, Kirschner MW: **Expression of a dominant negative mutant of the FGF receptor disrupts mesoderm formation in *Xenopus* embryos.** *Cell* 1991, **66**:257–270.

31. Lin DM, Goodman CS: **Ectopic and increased expression of fasciclin II alters motoneuron growth cone guidance.** *Neuron* 1994, **13**:507–523.

32. Grenningloh G, Bieber AJ, Rehm EJ, Snow PM, Traquina Z, Hortsch M, Patel NH, Goodman CS: **Molecular genetics of neuronal recognition in *Drosophila*: evolution and function of immunoglobulin superfamily cell adhesion molecules.** *Cold Spring Harb Symp Quant Biol* 1990, **55**:327–340.

33. • Winslow JW, Moran P, Valverde J, Shih A, Yuan JQ, Wong SC, Tsai SP, Goddard A, Henzel WJ, Hefti F: **Cloning of AL-1, a ligand for an Eph-related tyrosine kinase receptor involved in axon bundle formation.** *Neuron* 1995, **14**:973–981.

The authors show that REK7, an Eph RTK, is involved in bundling of cortical neuron axons *in vitro*. The REK ligand AL1 is expressed by the astrocytes over which the cortical axons extend. Interestingly, soluble AL1 blocks bundling, suggesting that proper presentation of the ligand is essential for REK7 signaling.

Appendix 3

Genetic analysis of gp150

Qi Sun and Kai Zinn

Introduction

Genetic studies of the RPTP genes showed that they control specific growth cone guidance decisions at multiple choice points during embryonic CNS development (Desai et al., 1996; Desai et al., 1997; Krueger et al., 1996), but very little is known about the signaling pathways of these RPTP genes. Tian (1994) and Fashena (1997) showed that a transmembrane glycoprotein gp150 specifically binds to the cytoplasmic domain of DPTP10D. DPTP10D and DPTP99A can mediate dephosphorylation of gp150 both *in vitro* and in S2 cells, suggesting that gp150 might be a substrate of these two RPTPs.

gp150 is a transmembrane protein. Its extracellular domain contains 18 leucine-rich repeat (LRR) sequences, which are present in many of the adhesion/signaling molecules. The short cytoplasmic domain of gp150 contains four tyrosine residues arranged in motifs similar to vertebrate immunoreceptor family tyrosine-based activation motifs (ITAMs) (Tian and Zinn, 1994).

In this study, we isolated P element mutations of the gp150. We show that gp150 is not essential for fly embryonic CNS development.

Results and Discussion

Isolation of gp150 mutants

The gp150 gene is located at the polytene chromosomal band 58D1-D2 (Tian and Zinn, 1994). No previously known mutants have ever been mapped to this region. We decided to carry out P-element targeted mutagenesis of the gp150 locus.

of gp150; in the second step the "local jumping" method was used to isolate P insertions in the gp150 gene; in the third step, imprecise excisions were generated that delete the gp150 coding region.

Step 1:

Two overlapping P1 clones, DS00566 and DS03886, were mapped to 58D1-D2. gp150 coding sequence is contained within DS03886 but not DS00566 (FlyBase, 1998). In step 1, we screened for P insertions in the genomic region covered by these two P1 clones.

Cross strategy for step one is shown in Figure 2. The jump start line we used for this screen was C(1)RM, 4 P {lacW}/Y, which has 4 P{lacW} insertions on each arm of its compound X chromosome. About 1500 P-element insertions in the 2nd and 3rd chromosomes were generated. Individual lines were established for each new insertion. These P-element lines were then grouped into pools with 50 lines in each pool. The P-element flanking regions were amplified by inverse PCR (see Experimental Procedures). ^{32}P labeled PCR products were then used to probe the two P1 clones DS00566 and DS03886. P-element line *C7* was isolated with an insertion in DS00566.

Step 2:

C7 was used as the jump start line for the local jumping screen. The cross strategy of step 2 is shown in Figure 3. After screening 500 lines with new P element insertions, *P46* was isolated with a P element insertion in the intron 5' to the gp150 coding sequence (Figure 1).

Step 3:

Deletion lines were generated by mobilizing the P element in *P46*. Two of the deletion lines *Df(2R)46-24* and *Df(2R)46-5* are shown in Figure 1. In *Df(2R)46-24*, about 6 kb of a gp150 intron is deleted, but the gp150 coding sequence remains intact.

insertions, *P46* was isolated with a P element insertion in the intron 5' to the gp150 coding sequence (Figure 1).

Step 3:

Deletion lines were generated by mobilizing the P element in *P46*. Two of the deletion lines *Df(2R)46-24* and *Df(2R)46-5* are shown in Figure 1. In *Df(2R)46-24*, about 6 kb of a gp150 intron is deleted, but the gp150 coding sequence remains intact. *Df(2R)46-5* delete all the gp150 coding sequence. We have not been able to map the distal breaking point of *Df(2R)46-5*.

No abnormality was observed in the embryonic CNS of gp150 mutant

gp150 is ubiquitously expressed in the fly embryo. After stage 13, gp150 RNA is highly expressed in the muscle attachment sites on the epidermis. We did not detect any gp150 RNA expression in the P insertion line *P46*. However, *P46* is viable, and its embryonic neuromuscular systems develop normally.

Because *P46* does not disrupt the gp150 coding sequence, we cannot rule out the possibility that there is residual amount of gp150 expressed in P46 that is beyond the sensitivity of the *in situ* analysis.

Both deletion lines *Df(2R)46-24* and *Df(2R)46-5* are lethal. *Df(2R)46-24* does not have any phenotypes in the embryonic muscle and nervous system. *Df(2R)46-5*, on the other hand, has defects in the muscle and central nervous system. But the phenotypes of *Df(2R)46-5* is not due to lacking of gp150. Zhi-chun Lai's group at Pennsylvania State University independently generated a *gp150* allele *defu*^{4}, which is

produce a strong synergistic phenotype when combined with mutations in*Ptp69D* (Chapter 2). We reasoned that if gp150 is downstream of DPTP10D and is required for its signaling functions, a double mutant lacking both gp150 and DPTP69D might have a phenotype like that of a *Ptp10D Ptp69D* mutant. Accordingly, we constructed the double mutant combinations *Ptp10D*; *gp150* and *gp150*; *Ptp69D*. Embryos lacking both *Ptp10D* and *gp150* develop normally, and embryos that are double mutants for *gp150* and *Ptp69D* exhibit the same phenotypes as *Ptp69D* single mutant.

Our results show that gp150 is not essential for development of the CNS axon array, and we have no evidence at present that it is involved in axon guidance at all. We have not been able to demonstrate any genetic interactions between *gp150* and *Ptp10D* or *gp150* and *Ptp69D*. However, as described in the previous chapters, the signaling pathways through the RPTPs are complex and redundant. At this point, we cannot determine if gp150 has a role in RPTP downstream signaling. Two possibilities for its function are: 1) gp150 is an in vivo substrate and signaling protein downstream of the DPTP4E RPTP. DPTP4E is closely related to DPTP10D, so it might be expected to also bind to gp150 (80% identity in the cytoplasmic domain). Unlike DPTP10D, however, DPTP4E is widely expressed. Thus, its expression pattern is similar to that of gp150. 2) gp150 is in fact downstream of DPTP10D, but it is redundant with other signaling molecules, at least for embryonic nervous system development.

Experimental procedures:

Inverse PCR screen

The inverse PCR screen protocol was modified from (Yeo et al., 1995). From each 50-line pool, we collected 100 flies (2 flies/line). Fly genomic DNA preparation was performed as described (Hamilton and Zinn, 1994). Normally we got 1 μg DNA per fly. Digest 2 μg of DNA with either Mbo I or Hpa II in 20 μl volume. Heat-inactivate

the restriction enzyme at 65 C for 15 minutes. Ligate 2 µl of the digest (no purification needed) in a total volume of 20 µl for at least 4 hours at 16 C. Heat-inactivate the restriction enzyme at 65 C for 15 minutes. PCR amplify 2.5 µl of ligation (no purification needed) in 25 µl volume using primer set 1. PCR amplify again with primer set 2 (2 µl from the first round of PCR product in 25 µl volume). Mix the PCR products from both the Mbo I and Hpa II sets. Label 4 µl of PCR products by random priming. Probe the blots of P1 DNA. Normally, 8 hours or overnight exposure is enough to give the signals.

Primer set 1: AAATG CGTCG TTTAG AGCAG; TCCAGTCACA GCTTT GCAGC

Primer set 2: AAGTG TATAC TTCGG TAAGC; AGAGCAACTA CGAAACGTGG

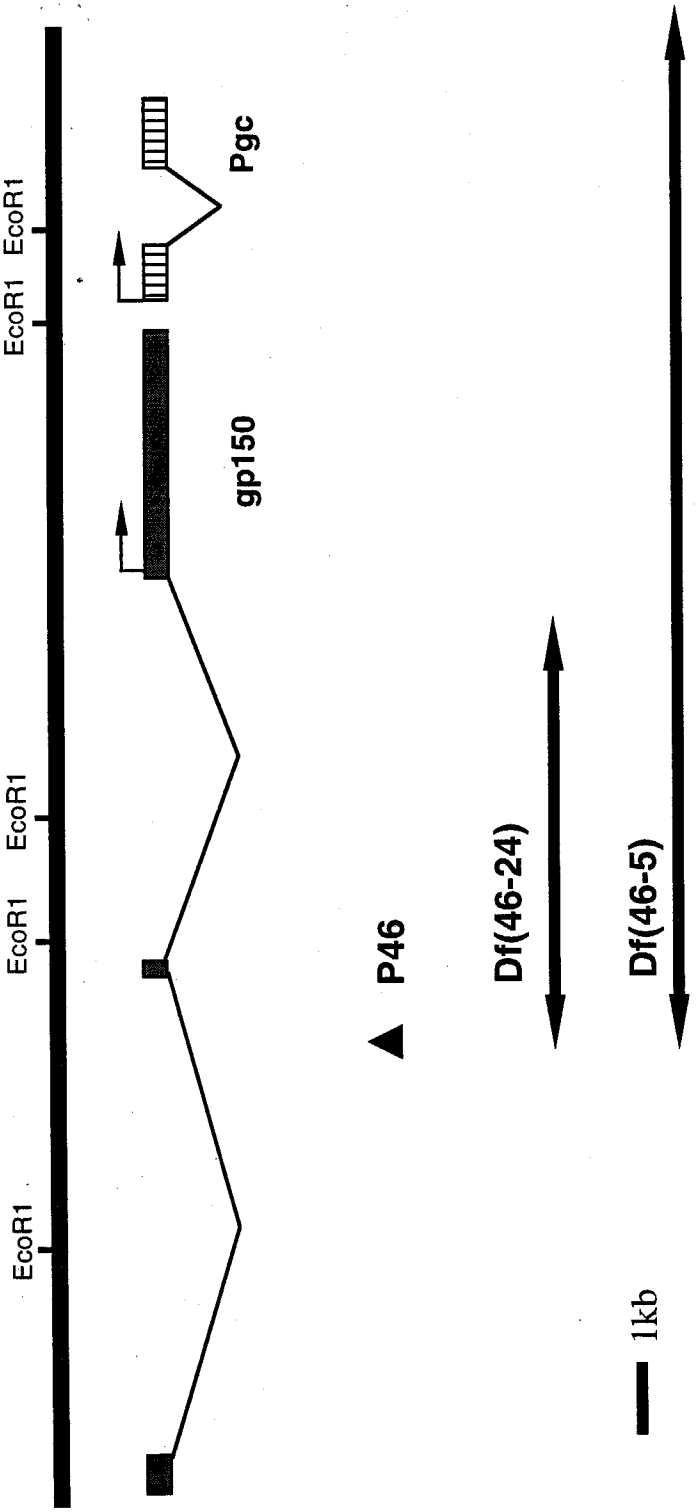

Figure 1. Genomic region of gp150

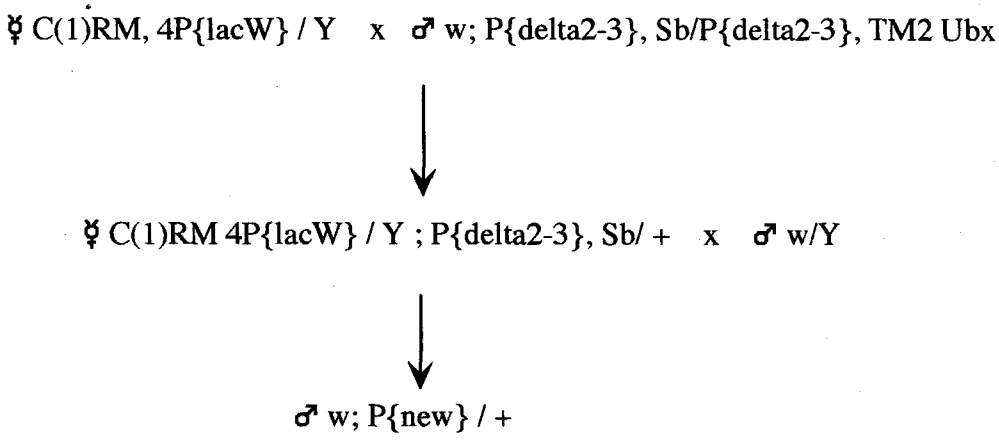

Figure 2. Cross strategy of step 1.

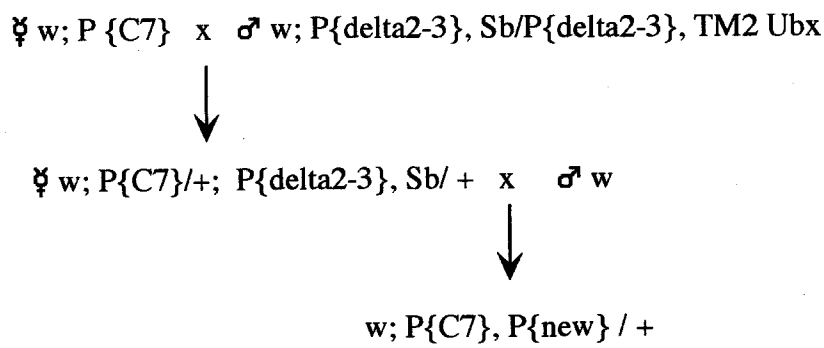

Figure 3. Cross strategy of step 2.

References

Bahri, S. M., Yang, X., and Chia, W. (1997). The Drosophila bifocal gene encodes a novel protein which colocalizes with actin and is necessary for photoreceptor morphogenesis. Mol Cell Biol *17*, 5521-9.

Battye, R., Stevens, A., and Jacobs, J. R. (1999). Axon repulsion from the midline of the drosophila CNS requires slit function [In Process Citation]. Development *126*, 2475-81.

Bazan, J. F., and Goodman, C. S. (1997). Modular structure of the Drosophila Beat protein [letter]. Curr Biol *7*, R338-9.

Bentley, D., and O'Connor, T. P. (1992). The nerve growth cone, P. C. Letourneau, S. B. Kater and E. R. Macagno, eds. (New York: Raven).

Bilwes, A. M., den Hertog, J., Hunter, T., and Noel, J. P. (1996). Structural basis for inhibition of receptor protein-tyrosine phosphatase-alpha by dimerization. Nature *382*, 555-9.

Brose, K., Bland, K. S., Wang, K. H., Arnott, D., Henzel, W., Goodman, C. S., Tessier-Lavigne, M., and Kidd, T. (1999). Slit proteins bind Robo receptors and have an evolutionarily conserved role in repulsive axon guidance. Cell *96*, 795-806.

Callahan, C. A., Muralidhar, M. G., Lundgren, S. E., Scully, A. L., and Thomas, J. B. (1995). Control of neuronal pathway selection by a Drosophila receptor protein-tyrosine kinase family member. Nature *376*, 171-4.

Cash, S., Chiba, A., and Keshishian, H. (1992). Alternate neuromuscular target selection following the loss of single muscle fibers in Drosophila. J Neurosci *12*, 2051-64.

Chiba, A., Hing, H., Cash, S., and Keshishian, H. (1993). Growth cone choices of Drosophila motoneurons in response to muscle fiber mismatch. J Neurosci *13*, 714-32.

Chiba, A., Snow, P., Keshishian, H., and Hotta, Y. (1995). Fasciclin III as a synaptic target recognition molecule in Drosophila. Nature *374*, 166-8.

Chien, C. B. (1998). Why does the growth cone cross the road? Neuron *20*, 3-6.

Davis, G. W., Schuster, C. M., and Goodman, C. S. (1997). Genetic analysis of the mechanisms controlling target selection: target- derived Fasciclin II regulates the pattern of synapse formation. Neuron *19*, 561-73.

Desai, C. J., Garrity, P. A., Keshishian, H., Zipursky, S. L., and Zinn, K. (1999). The Drosophila SH2-SH3 adapter protein Dock is expressed in embryonic axons and facilitates synapse formation by the RP3 motoneuron. Development *126*, 1527-35.

Desai, C. J., Gindhart, J. G., Jr., Goldstein, L. S., and Zinn, K. (1996). Receptor tyrosine phosphatases are required for motor axon guidance in the Drosophila embryo. Cell *84*, 599-609.

Desai, C. J., Krueger, N. X., Saito, H., and Zinn, K. (1997a). Competition and cooperation among receptor tyrosine phosphatases control motoneuron growth cone guidance in Drosophila. Development *124*, 1941-52.

Desai, C. J., Popova, E., and Zinn, K. (1994). A Drosophila receptor tyrosine phosphatase expressed in the embryonic CNS and larval optic lobes is a member of the set of proteins bearing the "HRP" carbohydrate epitope. J Neurosci *14*, 7272-83.

Desai, C. J., Sun, Q., and Zinn, K. (1997b). Tyrosine phosphorylation and axon guidance: of mice and flies. Curr Opin Neurobiol *7*, 70-4.

Doherty, P., and Walsh, F. S. (1994). Signal transduction events underlying neurite outgrowth stimulated by cell adhesion molecules. Curr Opin Neurobiol *4*, 49-55.

Elkins, T., Zinn, K., McAllister, L., Hoffmann, F. M., and Goodman, C. S. (1990). Genetic analysis of a Drosophila neural cell adhesion molecule: interaction of fasciclin I and Abelson tyrosine kinase mutations. Cell *60*, 565-75.

Fambrough, D., and Goodman, C. S. (1996). The Drosophila beaten path gene encodes a novel secreted protein that regulates defasciculation at motor axon choice points. Cell *87*, 1049-58.

Fashena, S. J., and Zinn, K. (1995). Cell-cell signaling: The ins and outs of receptor tyrosine phosphatases. Curr Biol *5*, 1367-9.

Fashena, S. J., and Zinn, K. (1997). Transmembrane glycoprotein gp150 is a substrate for receptor tyrosine phosphatase DPTP10D in Drosophila cells. Mol Cell Biol *17*, 6859-67.

FlyBase (1998). FlyBase: a Drosophila database. Nucleic Acids Res *26*, 85-8.

Garrity, P. A., Lee, C. H., Salecker, I., Robertson, H. C., Desai, C. J., Zinn, K., and Zipursky, S. L. (1999). Retinal axon target selection in Drosophila is regulated by a receptor protein tyrosine phosphatase. Neuron *22*, 707-17.

Gilbert, C. D. (1992). Horizontal integration and cortical dynamics. Neuron *9*, 1-13.

Gloor, G. B., Preston, C. R., Johnson-Schlitz, D. M., Nassif, N. A., Phillis, R. W., Benz, W. K., Robertson, H. M., and Engels, W. R. (1993). Type I repressors of P element mobility. Genetics *135*, 81-95.

Goodman, C. S., and Doe, C. Q. (1993). Embryonic development of the *Drosophila* central nervous system. In The Development of *Drosophila melanogaster*, M. Bate and A. M. Arias, eds.: Cold Spring Habor Laboratory Press), pp. 1131-1206.

Grenningloh, G., Rehm, E. J., and Goodman, C. S. (1991). Genetic analysis of growth cone guidance in Drosophila: fasciclin II functions as a neuronal recognition molecule. Cell *67*, 45-57.

Guthrie, S., and Pini, A. (1995). Chemorepulsion of developing motor axons by the floor plate. Neuron *14*, 1117-30.

Hall, S. G., and Bieber, A. J. (1997). Mutations in the Drosophila neuroglian cell adhesion molecule affect motor neuron pathfinding and peripheral nervous system patterning. J Neurobiol *32*, 325-40.

Hamilton, B. A., Ho, A., and Zinn, K. (1995). Targeted mutagenesis and genetic analysis of a Drosophila receptor-linked protein tyrosine phosphatase gene. Roux's Arch. Dev. Biol. *204*, 187-192.

Hamilton, B. A., and Zinn, K. (1994). From clone to mutant gene. Methods Cell Biol *44*, 81-94.

Hariharan, I. K., Chuang, P. T., and Rubin, G. M. (1991). Cloning and characterization of a receptor-class phosphotyrosine phosphatase gene expressed on central nervous system axons in Drosophila melanogaster. Proc Natl Acad Sci U S A *88*, 11266-70.

Harris, R., Sabatelli, L. M., and Seeger, M. A. (1996). Guidance cues at the Drosophila CNS midline: identification and characterization of two Drosophila Netrin/UNC-6 homologs. Neuron *17*, 217-28.

Hartman, J. J., Mahr, J., McNally, K., Okawa, K., Iwamatsu, A., Thomas, S., Cheesman, S., Heuser, J., Vale, R. D., and McNally, F. J. (1998). Katanin, a microtubule-severing protein, is a novel AAA ATPase that targets to the centrosome using a WD40-containing subunit. Cell *93*, 277-87.

Hidalgo, A., and Brand, A. H. (1997). Targeted neuronal ablation: the role of pioneer neurons in guidance and fasciculation in the CNS of Drosophila [published erratum appears in Development 1997 Nov;124(22):3258-60]. Development *124*, 3253-62.

Hidalgo, A., Urban, J., and Brand, A. H. (1995). Targeted ablation of glia disrupts axon tract formation in the Drosophila CNS. Development *121*, 3703-12.

Iwai, Y., Usui, T., Hirano, S., Steward, R., Takeichi, M., and Uemura, T. (1997). Axon patterning requires DN-cadherin, a novel neuronal adhesion receptor, in the Drosophila embryonic CNS. Neuron *19*, 77-89.

Kania, A., Han, P. L., Kim, Y. T., and Bellen, H. (1993). Neuromusculin, a Drosophila gene expressed in peripheral neuronal precursors and muscles, encodes a cell adhesion molecule. Neuron *11*, 673-87.

Keshishian, H., Broadie, K., Chiba, A., and Bate, M. (1996). The drosophila neuromuscular junction: a model system for studying synaptic development and function. Annu Rev Neurosci *19*, 545-75.

Kidd, T., Bland, K. S., and Goodman, C. S. (1999). Slit is the midline repellent for the robo receptor in Drosophila. Cell *96*, 785-94.

Kidd, T., Brose, K., Mitchell, K. J., Fetter, R. D., Tessier-Lavigne, M., Goodman, C. S., and Tear, G. (1998a). Roundabout controls axon crossing of the CNS midline and defines a novel subfamily of evolutionarily conserved guidance receptors. Cell *92*, 205-15.

Kidd, T., Russell, C., Goodman, C. S., and Tear, G. (1998b). Dosage-sensitive and complementary functions of roundabout and commissureless control axon crossing of the CNS midline. Neuron *20*, 25-33.

Kolodkin, A. L., Matthes, D. J., and Goodman, C. S. (1993). The semaphorin genes encode a family of transmembrane and secreted growth cone guidance molecules. Cell *75*, 1389-99.

Kolodziej, P. A., Timpe, L. C., Mitchell, K. J., Fried, S. R., Goodman, C. S., Jan, L. Y., and Jan, Y. N. (1996). frazzled encodes a Drosophila member of the DCC immunoglobulin subfamily and is required for CNS and motor axon guidance. Cell *87*, 197-204.

Kose, H., Rose, D., Zhu, X., and Chiba, A. (1997). Homophilic synaptic target recognition mediated by immunoglobulin-like cell adhesion molecule Fasciclin III. Development *124*, 4143-52.

Krueger, N. X., Van Vactor, D., Wan, H. I., Gelbart, W. M., Goodman, C. S., and Saito, H. (1996). The transmembrane tyrosine phosphatase DLAR controls motor axon guidance in Drosophila. Cell *84*, 611-22.

Ledig, M. M., McKinnell, I. W., Mrsic-Flogel, T., Wang, J., Alvares, C., Mason, I., Bixby, J. L., Mueller, B. K., and Stoker, A. W. (1999). Expression of receptor tyrosine phosphatases during development of the retinotectal projection of the chick [In Process Citation]. J Neurobiol *39*, 81-96.

Li, H. S., Chen, J. H., Wu, W., Fagaly, T., Zhou, L., Yuan, W., Dupuis, S., Jiang, Z. H., Nash, W., Gick, C., Ornitz, D. M., Wu, J. Y., and Rao, Y. (1999). Vertebrate slit, a secreted ligand for the transmembrane protein roundabout, is a repellent for olfactory bulb axons. Cell *96*, 807-18.

Lim, K. L., Kolatkar, P. R., Ng, K. P., Ng, C. H., and Pallen, C. J. (1998). Interconversion of the kinetic identities of the tandem catalytic domains of receptor-like protein-tyrosine phosphatase PTPalpha by two point mutations is synergistic and substrate-dependent. J Biol Chem *273*, 28986-93.

Lin, D. M., Auld, V. J., and Goodman, C. S. (1995). Targeted neuronal cell ablation in the Drosophila embryo: pathfinding by follower growth cones in the absence of pioneers. Neuron *14*, 707-15.

Lin, D. M., Fetter, R. D., Kopczynski, C., Grenningloh, G., and Goodman, C. S. (1994). Genetic analysis of Fasciclin II in Drosophila: defasciculation, refasciculation, and altered fasciculation. Neuron *13*, 1055-69.

Lin, D. M., and Goodman, C. S. (1994). Ectopic and increased expression of Fasciclin II alters motoneuron growth cone guidance. Neuron *13*, 507-23.

Luo, L., Liao, Y. J., Jan, L. Y., and Jan, Y. N. (1994). Distinct morphogenetic functions of similar small GTPases: Drosophila Drac1 is involved in axonal outgrowth and myoblast fusion. Genes Dev *8*, 1787-802.

Majeti, R., Bilwes, A. M., Noel, J. P., Hunter, T., and Weiss, A. (1998). Dimerization-induced inhibition of receptor protein tyrosine phosphatase function through an inhibitory wedge. Science *279*, 88-91.

Matthes, D. J., Sink, H., Kolodkin, A. L., and Goodman, C. S. (1995). Semaphorin II can function as a selective inhibitor of specific synaptic arborizations. Cell *81*, 631-9.

Meadows, L. A., Gell, D., Broadie, K., Gould, A. P., and White, R. A. (1994). The cell adhesion molecule, connectin, and the development of the Drosophila neuromuscular system. J Cell Sci *107*, 321-8.

Menon, K. P., and Zinn, K. (1998). Tyrosine kinase inhibition produces specific alterations in axon guidance in the grasshopper embryo. Development *125*, 4121-31.

Miklos, G. L., and Rubin, G. M. (1996). The role of the genome project in determining gene function: insights from model organisms. Cell *86*, 521-9.

Mitchell, K. J., Doyle, J. L., Serafini, T., Kennedy, T. E., Tessier-Lavigne, M., Goodman, C. S., and Dickson, B. J. (1996). Genetic analysis of Netrin genes in Drosophila: Netrins guide CNS commissural axons and peripheral motor axons. Neuron *17*, 203-15.

Mushegian, A. R. (1997). The Drosophila Beat protein is related to adhesion proteins that contain immunoglobulin domains [letter]. Curr Biol *7*, R336-8.

Nambu, J. R., Lewis, J. O., and Crews, S. T. (1993). The development and function of the Drosophila CNS midline cells. Comp Biochem Physiol Comp Physiol *104*, 399-409.

Nose, A., Mahajan, V. B., and Goodman, C. S. (1992a). Connectin: a homophilic cell adhesion molecule expressed on a subset of muscles and the motoneurons that innervate them in Drosophila. Cell *70*, 553-67.

Nose, A., Takeichi, M., and Goodman, C. S. (1994). Ectopic expression of connectin reveals a repulsive function during growth cone guidance and synapse formation. Neuron *13*, 525-39.

Nose, A., Umeda, T., and Takeichi, M. (1997). Neuromuscular target recognition by a homophilic interaction of connectin cell adhesion molecules in Drosophila. Development *124*, 1433-41.

Nose, A., Van Vactor, D., Auld, V., and Goodman, C. S. (1992b). Development of neuromuscular specificity in Drosophila. Cold Spring Harb Symp Quant Biol *57*, 441-9.

Nusslein-Volhard, C., and Wieschaus, E. (1980). Mutations affecting segment number and polarity in Drosophila. Nature *287*, 795-801.

O'Grady, P., Thai, T. C., and Saito, H. (1998). The laminin-nidogen complex is a ligand for a specific splice isoform of the transmembrane protein tyrosine phosphatase LAR. J Cell Biol *141*, 1675-84.

Patel, N. H. (1994). Imaging neuronal subsets and other cell types in whole-mount Drosophila embryos and larvae using antibody probes. Methods Cell Biol *44*, 445-87.

Peles, E., Nativ, M., Campbell, P. L., Sakurai, T., Martinez, R., Lev, S., Clary, D. O., Schilling, J., Barnea, G., Plowman, G. D., and et al. (1995). The carbonic anhydrase domain of receptor tyrosine phosphatase beta is a functional ligand for the axonal cell recognition molecule contactin. Cell *82*, 251-60.

Ramos, R. G., Igloi, G. L., Lichte, B., Baumann, U., Maier, D., Schneider, T., Brandstatter, J. H., Frohlich, A., and Fischbach, K. F. (1993). The irregular chiasm C-roughest locus of Drosophila, which affects axonal projections and programmed cell death, encodes a novel immunoglobulin-like protein. Genes Dev *7*, 2533-47.

Rorth, P. (1996). A modular misexpression screen in Drosophila detecting tissue-specific phenotypes. Proc Natl Acad Sci U S A *93*, 12418-22.

Rorth, P., Szabo, K., Bailey, A., Laverty, T., Rehm, J., Rubin, G. M., Weigmann, K., Milan, M., Benes, V., Ansorge, W., and Cohen, S. M. (1998). Systematic gain-of-function genetics in Drosophila. Development *125*, 1049-57.

Rose, D., and Chiba, A. (1999). A single growth cone is capable of integrating simultaneously presented and functionally distinct molecular cues during target recognition. J Neurosci *19*, 4899-4906.

Rose, D., Zhu, X., Kose, H., Hoang, B., Cho, J., and Chiba, A. (1997). Toll, a muscle cell surface molecule, locally inhibits synaptic initiation of the RP3 motoneuron growth cone in Drosophila. Development *124*, 1561-71.

Rothberg, J. M., Jacobs, J. R., Goodman, C. S., and Artavanis-Tsakonas, S. (1990). slit: an extracellular protein necessary for development of midline glia and commissural axon pathways contains both EGF and LRR domains. Genes Dev *4*, 2169-87.

Rutishauser, U. (1993). Adhesion molecules of the nervous system. Curr Opin Neurobiol *3*, 709-15.

Schmid, A., Chiba, A., and Doe, C. Q. (1999). The lineages of *Drosophila* neuroblasts: lineage-specific characteristics reveal early patterning events. Development *in press*.

Seeger, M., Tear, G., Ferres-Marco, D., and Goodman, C. S. (1993). Mutations affecting growth cone guidance in Drosophila: genes necessary for guidance toward or away from the midline. Neuron *10*, 409-26.

Shishido, E., Takeichi, M., and Nose, A. (1998). Drosophila synapse formation: regulation by transmembrane protein with Leu-rich repeats, CAPRICIOUS. Science *280*, 2118-21.

Sonnenfeld, M. J., and Jacobs, J. R. (1995). Apoptosis of the midline glia during Drosophila embryogenesis: a correlation with axon contact. Development *121*, 569-78.

Speicher, S., Garcia-Alonso, L., Carmena, A., Martin-Bermudo, M. D., de la Escalera, S., and Jimenez, F. (1998). Neurotactin functions in concert with other identified CAMs in growth cone guidance in Drosophila. Neuron *20*, 221-33.

Stoker, A., and Dutta, R. (1998). Protein tyrosine phosphatases and neural development. Bioessays *20*, 463-72.

Tang, J., Landmesser, L., and Rutishauser, U. (1992). Polysialic acid influences specific pathfinding by avian motoneurons. Neuron *8*, 1031-44.

Tang, J., Rutishauser, U., and Landmesser, L. (1994). Polysialic acid regulates growth cone behavior during sorting of motor axons in the plexus region. Neuron *13*, 405-14.

Tear, G., Harris, R., Sutaria, S., Kilomanski, K., Goodman, C. S., and Seeger, M. A. (1996). commissureless controls growth cone guidance across the CNS midline in Drosophila and encodes a novel membrane protein. Neuron *16*, 501-14.

Tessier-Lavigne, M., and Goodman, C. S. (1996). The molecular biology of axon guidance. Science *274*, 1123-33.

Thomas, J. B. (1998). Axon guidance: crossing the midline. Curr Biol *8*, R102-4.

Tian, S. S., Tsoulfas, P., and Zinn, K. (1991). Three receptor-linked protein-tyrosine phosphatases are selectively expressed on central nervous system axons in the Drosophila embryo. Cell *67*, 675-80.

Tian, S. S., and Zinn, K. (1994). An adhesion molecule-like protein that interacts with and is a substrate for a Drosophila receptor-linked protein tyrosine phosphatase. J Biol Chem *269*, 28478-86.

Van Vactor, D. (1998). Adhesion and signaling in axonal fasciculation. Curr Opin Neurobiol *8*, 80-6.

Van Vactor, D., Sink, H., Fambrough, D., Tsoo, R., and Goodman, C. S. (1993). Genes that control neuromuscular specificity in Drosophila. Cell *73*, 1137-53.

Van Vactor, D. L., Jr., Cagan, R. L., Kramer, H., and Zipursky, S. L. (1991). Induction in the developing compound eye of Drosophila: multiple mechanisms restrict R7 induction to a single retinal precursor cell. Cell *67*, 1145-55.

Weaver, T. A., and White, R. A. (1995). headcase, an imaginal specific gene required for adult morphogenesis in Drosophila melanogaster. Development *121*, 4149-60.

Weiss, A., and Littman, D. R. (1994). Signal transduction by lymphocyte antigen receptors. Cell *76*, 263-74.

Wills, Z., Bateman, J., Korey, C. A., Comer, A., and Van Vactor, D. (1999a). The tyrosine kinase Abl and its substrate enabled collaborate with the receptor phosphatase Dlar to control motor axon guidance. Neuron *22*, 301-12.

Wills, Z., Marr, L., Zinn, K., Goodman, C. S., and Van Vactor, D. (1999b). Profilin and the Abl tyrosine kinase are required for motor axon outgrowth in the Drosophila embryo. Neuron *22*, 291-9.

Winberg, M. L., Mitchell, K. J., and Goodman, C. S. (1998a). Genetic analysis of the mechanisms controlling target selection: complementary and combinatorial functions of netrins, semaphorins, and IgCAMs. Cell *93*, 581-91.

Winberg, M. L., Noordermeer, J. N., Tamagnone, L., Comoglio, P. M., Spriggs, M. K., Tessier-Lavigne, M., and Goodman, C. S. (1998b). Plexin A is a neuronal semaphorin receptor that controls axon guidance. Cell *95*, 903-16.

Wolf, B., Seeger, M. A., and Chiba, A. (1998). Commissureless endocytosis is correlated with initiation of neuromuscular synaptogenesis. Development *125*, 3853-63.

Worley, T., and Holt, C. (1996). Inhibition of protein tyrosine kinases impairs axon extension in the embryonic optic tract. J Neurosci *16*, 2294-306.

Wu, D. Y., and Goldberg, D. J. (1993). Regulated tyrosine phosphorylation at the tips of growth cone filopodia. J Cell Biol *123*, 653-64.

Wu, Q., and Maniatis, T. (1999). A Striking Organization of a Large Family of Human Neural Cadherin-like Cell Adhesion Genes. Cell *97*, 779-790.

Yang, P., Yin, X., and Rutishauser, U. (1992). Intercellular space is affected by the polysialic acid content of NCAM. J Cell Biol *116*, 1487-96.

Yang, X. H., Seow, K. T., Bahri, S. M., Oon, S. H., and Chia, W. (1991). Two Drosophila receptor-like tyrosine phosphatase genes are expressed in a subset of developing axons and pioneer neurons in the embryonic CNS. Cell *67*, 661-73.

Yeo, S. L., Lloyd, A., Kozak, K., Dinh, A., Dick, T., Yang, X., Sakonju, S., and Chia, W. (1995). On the functional overlap between two Drosophila POU homeo domain genes and the cell fate specification of a CNS neural precursor. Genes Dev *9*, 1223-36.

Zallen, J. A., Yi, B. A., and Bargmann, C. I. (1998). The conserved immunoglobulin superfamily member SAX-3/Robo directs multiple aspects of axon guidance in C. elegans. Cell *92*, 217-27.

Zinn, K., and Sun, Q. (1999). Slit branches out: a secreted protein mediates both attractive and repulsive axon guidance. Cell *97*, 1-4.

Zipursky, S. L., Venkatesh, T. R., Teplow, D. B., and Benzer, S. (1984). Neuronal development in the Drosophila retina: monoclonal antibodies as molecular probes. Cell *36*, 15-26.